SILVER NANOWIRE-DECORATED GLASS FIBER FILTERS FOR BACTERIA
REMOVAL FROM WATER

A THESIS SUBMITTED TO
THE GRADUATE SCHOOL OF NATURAL AND APPLIED SCIENCES
OF
MIDDLE EAST TECHNICAL UNIVERSITY

BY

ECEM BAHÇELIOĞLU

IN PARTIAL FULFILLMENT OF THE REQUIREMENTS
FOR
THE DEGREE OF MASTER OF SCIENCE
IN
ENVIRONMENTAL ENGINEERING

SEPTEMBER 2019

Approval of the thesis:

SILVER NANOWIRE-DECORATED GLASS FIBER FILTERS FOR BACTERIA REMOVAL FROM WATER

submitted by **ECEM BAHÇELIOĞLU** in partial fulfillment of the requirements for the degree of **Master of Science in Environmental Engineering Department, Middle East Technical University** by,

Prof. Dr. Halil Kalıpçılar
Dean, Graduate School of **Natural and Applied Sciences**   _____

Prof. Dr. Bülent İçgen
Head of Department, **Environmental Eng.**   _____

Assoc. Prof. Dr. Tuba Hande Ergüder Bayramoğlu
Supervisor, **Environmental Eng., METU**   _____

Prof. Dr. Hüsnü Emrah Ünalan
Co-Supervisor, **Metallurgical and Materials Eng.**   _____

Examining Committee Members:

Prof. Dr. Ayşegül Aksoy
Environmental Engineering, METU   _____

Assoc. Prof. Dr. Tuba Hande Ergüder Bayramoğlu
Environmental Eng., METU   _____

Prof. Dr. Hüsnü Emrah Ünalan
Metallurgical and Materials Engineering, METU   _____

Assoc. Prof. Dr. Yeşim Soyer
Food Engineering, METU   _____

Assoc. Prof. Dr. Selim Sanin
Environmental Engineering, Hacettepe University   _____

Date: 05.09.2019

I hereby declare that all information in this document has been obtained and presented in accordance with academic rules and ethical conduct. I also declare that, as required by these rules and conduct, I have fully cited and referenced all material and results that are not original to this work.

Name, Surname: Ecem Bahçelioğlu

Signature:

ABSTRACT

**SILVER NANOWIRE-DECORATED GLASS FIBER FILTERS FOR
BACTERIA REMOVAL FROM WATER**

Bahçelioğlu, Ecem
Master of Science, Environmental Engineering
Supervisor: Assoc. Prof. Dr. Tuba Hande Ergüder Bayramoğlu
Co-Supervisor: Prof. Dr. Hüsnü Emrah Ünalan

September 2019, 137 pages

Investigation of a new, low-cost, safe and highly efficient water disinfection alternative to conventional methods has prime importance. This study aims to develop silver nanowire decorated glass fiber (AgNW-GF) filters for the removal of *E. coli* from water. This study is one of the first studies to fabricate a novel AgNW-GF filter and to investigate its use for point-of-use (POU) water disinfection. To this purpose, effect of flow rate, AgNW loading and influent *E. coli* concentration on the removal efficiency of *E. coli* and Ag release from AgNW-GF filters were investigated. In addition, effect of volume of filtrate on Ag release was also analyzed. Disk diffusion tests revealed that AgNW-GF filters having different AgNW loadings had antibacterial effects against *E. coli* at concentration range of $10^3 - 10^8$ CFU/ml. In order to investigate optimal conditions at which AgNW-GF filters achieved the highest removal efficiencies, flow tests were conducted with different flow rates (1, 2.5, 5 ml/min), AgNW loadings (0.95, 4.8, 9.9 mg/g) and *E. coli* concentrations (10^3, 10^5, 10^8 CFU/ml). Optimal flow rate, AgNW loading and influent *E. coli* concentration were found out as 1 ml/min, 9.9 mg/g, and 10^3 CFU/ml, respectively. The highest removal efficiency was obtained as 2.12 log after two-stage serial filtration application applied under optimal conditions. The released Ag amounts were all below the limit

value of 100 ppb for potable water. Under determined optimal conditions, AgNW-GF filter was found as a promising alternative for POU water disinfection method to be used in contaminated natural water ($<10^3$ CFU/ml). In order to achieve higher removal efficiencies for more contaminated water and improve POU water disinfection with AgNW-GF filters, low-voltage can be applied to the developed AgNW-GF POU disinfection system.

Keywords: Silver nanowires, glass fiber filter, antibacterial, point-of-use, water disinfection, E. coli

ÖZ

SULARDAN BAKTERİ GİDERİMİ İÇİN GÜMÜŞ NANOTELLER İLE GELİŞTİRİLEN CAM FİBER FİLTRELER

Bahçelioğlu, Ecem
Yüksek Lisans, Çevre Mühendisliği
Tez Danışmanı: Doç. Dr. Tuba Hande Ergüder Bayramoğlu
Ortak Tez Danışmanı: Prof. Dr. Hüsnü Emrah Ünalan

Eylül 2019, 137 sayfa

Geleneksel dezenfeksiyon yöntemlerinin yan etkilerini azaltmak amacıyla alternative olarak yeni, düşük maliyetli, güvenilir ve yüksek verimli bir dezenfeksiyon yönteminin araştırılması büyük önem taşımaktadır. Bu çalışma, *E. coli*'nin içme sularından giderimi için gümüş nanoteller ile geliştirilen cam fiber (AgNT-CF) filtreleri üretmeyi amaçlamaktadır. Bu çalışma, AgNT-CF filtrelerin üretilmesini ve kullanım noktası (POU) su dezenfeksiyonu için kullanılmasını araştıran ilk çalışmalardan biridir. Bu kapsamda, akış hızının, AgNT miktarının ve *E. coli* konsantrasyonunun *E. coli* giderim verimine ve filtrelerden Ag salınımına etkisi araştırılmıştır. Ayrıca, filtrelenen su hacminin Ag salınımına etkisi de analiz edilmiştir. Disk difüzyon testleri farklı AgNT yüklerine sahip AgNT-CF filtrelerinin 10^3-10^8 KOB/ml aralığındaki *E. coli* konsantrasyonuna karşı antibakteriyel etkilerini ortaya koymuştur. AgNT-CF filtrelerin en yüksek verime ulaştığı optimum koşulları araştırmak için farklı akış hızlarında (1, 2,5 ve 5 ml/dk), AgNT yükleriyle (0,95, 4,8, ve 9,9 mg/g) ve *E. coli* konsantrasyonlarıyla (10^3, 10^5 ve 10^8 KOB/ml) akış testleri yapılmıştır. Optimum akış hızı, AgNT yükü ve *E. coli* konsantrasyonu sırasıyla 1 ml/dk, 9,9 mg/g ve 10^3 KOB/ml olarak bulunmuştur. Optimum koşullar altında uygulanan iki aşamalı seri filtrasyon uygulamasından sonra en yüksek giderim verimi

2,12 log olarak elde edilmiştir. Ag salınımı miktarları içme suları için önerilen 100 ppb sınır değerinin altındadır. Belirlenen uygun koşullar altında, geliştirilen AgNT-CF filtrelerin kontamine olmuş ($<10^3$ KOB/ml) doğal sularda kullanılabilecek alternatif bir POU su dezenfeksiyonu methodu için umut verici olduğu bulunmuştur. Daha fazla kontamine olmuş sularda daha yüksek giderim verimlerine ulaşmak ve AgNT-CF filtreler ile POU su dezenfeksiyonunu geliştirmek için üretilen AgNT-CF dezenfeksiyon sistemine düşük voltaj uygulanabilir.

Anahtar Kelimeler: Gümüş nanotel, cam fiber filtre, antibakteriyel, kullanım noktasında su dezenfeksiyonu, E. coli

To my dearest family…

ACKNOWLEDGEMENTS

So many great friends in my life! I must say to thank my friends from SAT Ezgi Selin Kaya, İlknur Abakbigan, Mahmut Şahin, Yunus Emre Gök, Görkem Varol, Çağatay Önder and Ali Aygün for their friendship, trusts and energies during my stressful times. I am also thankful to my friends Kumru Kocaman, Cem Ataman, Mehtap Demir Karanfil and our new and the cutest member Uzi for our lovely meetings. I would like to thank my office-mates and my dear friends Nazlı Barçın Doğan, Beyza Özel and Numan Burak Barkış for all the enjoyful times and great lunches. B-07 will always be in my memories. Thank you my colleagues Hazal Aksu Bahçeci, Ece Arı and Umut Yıldız for their supports and for the times shared together. I would like to express my thanks to my dear close friends Tuğkan Tanır, Pelin Yılmaz, Sevde Karayılan, Serkan Küçükünsal, Onur Fatih Bulut and Şükrü Uzun for great memories that we have shared together since our undergraduate times. Distances between us never matter. I am grateful to have a friend like Özgür Taylan Turan. Thank you for all support, contributions, and lifelong friendship. I am also thankful to my besties İrem Küçüknarin and Nilay Seçgin. Thank you all for always being there whenever I need you. You all provide such valuable friendship. Finally, I would like to express my special thanks to Erhan Ersoy. Thank you for all your endless support, trust, patience, percipience and love❤. Thank you for being a part of my life.

Most importantly, I would like to express my biggest appreciation to my family for always supporting me during my whole life. I owe my special thanks to my dear dad Serdar Bahçelioğlu, my dear mom Gülden Bahçelioğlu, and my lovely sister İrem Bahcelioğlu for their unconditional and endless love, support, percipience and patience throughout my life. I feel very lucky to have such a wonderful family.

TABLE OF CONTENTS

xiii

LIST OF TABLES

TABLES

LIST OF FIGURES

FIGURES

LIST OF ABBREVIATIONS

ABBREVIATIONS

AgCl	Silver Chloride
AgNCs	Silver Nanocubes
$AgNO_3$	Silver Nitrate
AgNPs	Silver Nanoparticles
AgNWs	Silver Nanowires
AgNWs-CC	Silver Nanowires – carbon fiber cloth
AgNWs-GF	Silver nanowire decorated glass fiber
CFU	Coliform Forming Unit
CNTs	Carbon Nanotubes
DBPs	Disinfection by-products
EG	Ethylene Glycol
GF	Glass fiber filter
GO	Graphene Oxide
HAAs	Haloacetic Acids
ICP-MS	Inductively Coupled Plasma Mass Spectrometry
LB	Luria-Bertani
MBC	Minimum Bactericidal Concentration
MGO	Magnetic Graphene Oxide
MH	Mueller-Hinton
MHC	Magnetic Hybrid Colloids
MIC	Minimum Inhibitory Concentration
NOMs	Natural Organic Matters
OD	Optical Density
PAN	Polyacrylonitrile
PANI	Polyaniline

PBS	Phosphate Buffered Saline
POU	Point-of-use
PTFE	Polytetrafluorethylene
PVP	Polyvinylpyrrolidone
ROS	Reactive Oxygen Species
SEM	Scanning Electron Microscopy
THM	Primarily Trihalomethanes
TOC	Total Organic Carbon
TPU	Thermoplastic Polyurethane
TTC	Thermotolerant Coliforms
USEPA	United States Environmental Protection Agency
UV	Ultraviolet
WHO	World Health Organization
WWTP	Wastewater Treatment Plant

CHAPTER 1

INTRODUCTION

Today, there are many problems in supplying clean water in many parts of the world. This situation has fatal consequences for human health. Increasing drought and human population makes it more difficult to supply clean and safe water (Tiwari, Behari, & Sen, 2008). According to World Health Organization (WHO) (2018a), it is estimated that about 842 000 people, most of which are children aged under 5 years, die each year from diarrheal diseases resulting from unsafe drinking water, hand hygiene and inadequate sanitation. Everyone has the right to access safe and reliable water for personal and domestic use. However, it is a great challenge to supply clean water in undeveloped or developing regions, especially in rural areas. By 2025, half of the world's population will be living in water-stressed areas (WHO, 2016).

Several methods, such as chlorination, ozonation and ultraviolet treatment, have been proven for their high disinfection efficiencies against pathogens. However, these conventional methods have several drawbacks in today's standards. Although chlorination is one of the most preferred disinfection method, it produces carcinogenic disinfection by-products (DBPs) (Mukherji, Mukherji, & Mukherji, 2017; Tan et al., 2018). Besides chlorination, high-energy use and cost of ultraviolet (UV) and ozone disinfection limit the widespread use of these methods. Reverse osmosis membrane is another method used for water disinfection, which is very costly and prone to fouling (Biswas and Bandyopadhyaya, 2016). Therefore, investigation of a new, low-cost, safe and highly-efficient disinfection route as an alternative to conventional methods to overcome aforementioned drawbacks has prime importance (Lin et al., 2013).

With the developments in nanotechnology, the use of nanomaterials is being investigated in the field of environmental engineering for various purposes such as the removal of pesticides, chemical and biological substances and salt to obtain fresh water (Hossain, Perales-Perez, Hwang, & Román, 2014; Tiwari et al., 2008). Silver and silver compounds are the most effective bactericides known since ancient times (Fewtrell, 2014; Song et al., 2016). Nanosilver shows higher antibacterial effect compared to the conventional silver bactericides (Song et al., 2016). The number of studies conducted using silver nanoparticles (AgNPs) and silver nanowires (AgNWs) have increased in the last 10 years and have shown positive results in the point-of-use (POU) disinfection of water (Hossain et al., 2014; Q. Li et al., 2008). POU disinfection systems, which are efficient due to low energy consumption, easy to use and portable, are units installed at specific water supply points such as at tap/faucet or bottling from river (Praveena and Aris, 2015).

Nanosilver is found to be effective against both gram-positive bacteria (*Bacillus, Clostridium, Enterococcus, Listeria, Staphylococcus* and *Streptococcus* etc.) and gram-negative bacteria (*Acinetobacter, Escherichia, Pseudomonas, Salmonella* and *Vibrio* etc.) (Fewtrell, 2014). Besides, several studies show that nanosilver has an antiviral effect on bacteriophage MS2 (Fewtrell, 2014; Hong et al., 2016a; Rao et al., 2016) and antifungal effect (S*pergillus niger, Candida albicans* and *Saccharomyces cerevisiae* etc.) (Fewtrell, 2014). They are non-toxic at minute concentrations. The report published by WHO specifies allowable silver concentration in water as 0.1 mg/l (100 ppb) (WHO, 2011). Compared to conventional disinfection methods, the use of AgNPs and AgNWs are promising since they do not lead to formation of carcinogenic DBPs, require less energy, free of clogging problem and show high efficiency on a wide range of organisms (Lalley et al., 2014; Schoen et al., 2010).

Despite of many reported advantages of silver/nanosilver use in water disinfection and especially its potential use in POU water disinfection, the research on the topic is still in the development stage. Among reviewed 120 studies related to the silver/nanosilver research, only 36 of them are found to be conducted with the aim of POU water disinfection. In addition, the number of research studies conducted with AgNWs for water disinfection is very limited (Basheer and Abu-thabit, 2014; Hong et al., 2016a; Liu et al., 2013; Schoen et al., 2010; Tan et al., 2018; Wen et al., 2017). Only two studies use coated glass fibers in literature for this purpose. One was conducted using AgNPs-impregnated fiberglass (Nangmenyi, Xao, Mehrabi, Mintz, & Economy, 2009) while the other one with silver-modified iron oxide nanoparticle impregnated fiberglass (Nangmenyi, Li, Mehrabi, Mintz, & Economy, 2011). In Turkey, studies on the antibacterial effect of nanosilver are currently very limited (Cicek et al., 2015; Doganay et al., 2019; Dogru et al., 2017; Eltugral and Simsir, 2016; Erdem and Akal, 2015; Koizhaiganova et al., 2016; Lkhagvajav et al., 2015; Toker and Kahraman, 2013; Atay et al., 2014). Most importantly, it has not been encountered any studies on the investigation of nanosilver-containing materials used for water disinfection in Turkey.

This thesis aims to develop AgNW-decorated glass fiber (AgNW-GF) filters for the removal of *Escherichia coli* (i.e. *E. coli)* from water. This work is one of the first studies to fabricate a novel AgNW-GF filter and to investigate its use for POU water disinfection. In this scope, the specific objectives of this thesis are given as follows:

- To investigate the antibacterial effect of AgNW-GF filters against gram-negative *E. coli,*

- To investigate the effect of flow rate, Ag concentration and *E. coli* concentration on the removal efficiency of *E. coli* from water via AgNW-GF filters,

- To investigate the effect of flow rate, volume of the filtrate, Ag concentration and *E. coli* concentration on Ag release from AgNW-GF filters.

This thesis is organized into five major chapters. Chapter 1 highlights the current problems about the water supply and disinfection, and gives the aim and specific objectives of the study. A background and literature review on the nanosilver and their mechanisms, antibacterial effects, applications, and properties are discussed in Chapter 2. Key contributions to POU water disinfection field are discussed and evaluated. Chapter 3 provides materials and methods of this study in detail. The results obtained from the study are discussed in Chapter 4 as three main parts: Characterization of the AgNW-GF filters, antibacterial testing and Ag release analyses. In Chapter 5, main findings and results of this study are highlighted. Finally, future recommendations are provided in Chapter 6.

CHAPTER 2

LITERATURE REVIEW

2.1. Microbial Contamination of Waters and Disinfection

Water is a crucial need for not only metabolic activities for survival; but also, domestic use for humans, irrigation purposes or recreational activities. Since all living things are in contact with water, water safety in terms of pollution is essential. Different authorities can use different parameters to define water pollution, including biological oxygen demand, dissolved oxygen or chemical constituents (Okafor, 2011). Feces introduction into water is the most dangerous form of microbial pollution of water (Tortora et al., 2013) due to the presence of pathogenic organisms. Surface water and groundwater are susceptible to microbial contamination from agricultural lands, treatment plants or the other diffuse and point sources (Percival et al., 2013). Microbial water pollution is verified based on the presence of indicator microorganisms, which are generally nonpathogenic bacteria (Pepper et al., 2015). Basically, indicator organisms should be useful for all types of water, have some direct relationship to the degree of fecal pollution, naturally be a member of intestinal microflora of warm-blooded animals, and be easy to detect and cultivate (Pepper et al., 2015; WHO, 2011). Organisms used for indicators of fecal contamination could be *E. coli, Streptococcus fecalis, Bifidobacteria* or *C.perfringens* (Okafor, 2011). Among those, *E. coli* (2.0-6.0 μm in length and 1.1-1.5 μm in wide) which are defined as gram-negative, non-spore forming rods capable of fermenting lactose aerobically or facultatively with the production of acid and gas, is the most widely used indicator organism (Okafor, 2011; Percival et al., 2013).

Figure 2-1 shows an *E. coli* image (Madigan et al., 2012). The presence of such organisms certainly indicates fecal pollution of water (Okafor, 2011) while the absence of indicator coliforms or *E. coli* may not ensure safety, since viruses and protozoa are more resistant to be still present (Okafor, 2011; WHO, 2011).
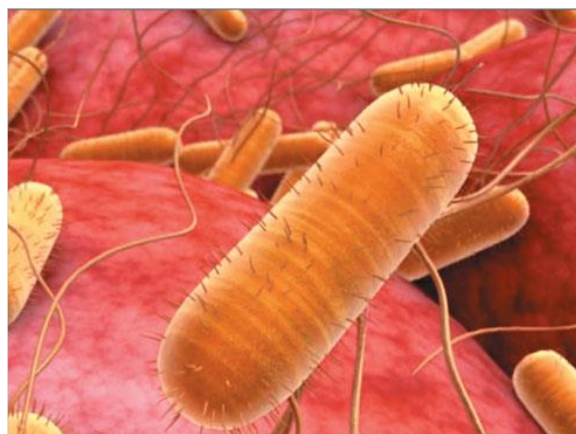
Figure 2-1. E. coli image (Madigan et al., 2012).

For a century, the coliform group has been used as a standard for assessing fecal contamination of waters. An approximate number of occurrences of fecal coliforms are represented in Table 2-1. The table indicates that the number of indicator organisms varies between $10^2 - 10^5$ Coliform Forming Unit (CFU) per 100 ml in raw/contaminated water; $10^6 - 10^{10}$ CFU per 100 ml in untreated wastewater and approximately 10^7 CFU per gram of feces. Clasen and Bastable (2003) examined fecal contamination of drinking water during collection and storage in the Kailahun District of Sierra Leone. It has been found that 92.9% of the samples taken from the household collection were contaminated with 244 Thermotolerant Coliforms (TTC) per 100 ml of the arithmetic mean. Another study shows high levels of fecal contamination in the Kokolo Canal, the Democratic Republic of the Congo (Kayembe et al., 2018). In this work, the number of *E. coli* of samples was found to change between $10^4 - 10^5$ CFU per 100 ml from the Canal, indicating potential human health risk associated with the exposure to water contamination. Likewise, a study conducted in India through

collecting water samples from 27 different villages estimates the amount of total coliform in the region as 10^4 - 10^5 CFU per 100 ml. Such contamination would lead to an increase in the number of waterborne diseases in the rural areas (Suthar, Chhimpa, & Singh, 2008).

Table 2-1. *Approximate amount of total coliforms or E. coli in different contaminated sources.*

	Number (CFU[a])	Reference
Fecal coliforms per gram of feces	10^7	WHO (2011)
Fecal coliforms per liter in untreated wastewater	$10^6 – 10^{10}$	WHO (2011)
Fecal coliforms per liter in raw water	$10^2 – 10^5$	WHO (2011)
E. coli per 100 ml raw sewage	$10^6 – 10^7$	Pepper et al. (2015)
Total coliform per 100 ml contaminated natural water[b]	10^4 - 10^5	Suthar et al. (2008)
Total coliform per ml contaminated natural water[b]	1200 - 2000	El-Aassar et al. (2013)
TTC per 100 ml contaminated natural water[b]	244	Clasen and Bastable (2003)
Number of *E. coli* per 100 ml contaminated natural water[b]	5000-665000	Dankovich et al. (2016)
Number of *E. coli* per 100 ml contaminated natural water[b]	10^4 - 10^5	Kayembe et al. (2018)
Number of *E. coli* per 100 ml contaminated natural water[b]	224	Kallman et al. (2009)

[a]CFU = colony forming unit
[b]Case study

According to the water quality standards of U.S. EPA and European Union, safe drinking water should contain no detectable coliforms in 100 ml (Pepper et al., 2015; WHO, 2011). Otherwise, it could lead to potential fresh outbreaks due to spreading of waterborne diseases. Waterborne diseases are caused by pathogens such as cholera,

Salmonella and *Shigella* that originate in fecal substances and are transmitted by ingestion through contaminated water (Okafor, 2011; Pepper et al., 2015). Frequently encountered waterborne diseases include cholera, typhoid fever (Pepper et al., 2015), dysentery, hepatitis A and diarrhea (WHO, 2018a). Diarrheal diseases are among the top 10 global causes of deaths in 2016 as indicated by WHO (2018b). Diarrheal diseases are mostly caused by pathogenic *E. coli* introduced from contaminated water following a 10-72 hr incubation period (Pepper et al., 2015). The type and incidence of waterborne diseases change according to the economic situation of the regions. It is based on providing a safe and clean water capacity of the countries to their citizens (Okafor, 2011). Inadequate, inappropriately managed or absent water and sanitation services increase the individual's preventable health risks. Today, globally 159 million people consume untreated surface water from lakes, ponds, rivers and streams and at least 2 billion people use drinking water contaminated with feces (WHO, 2018a).

To eliminate pathogens and to prevent waterborne diseases, disinfection is the most crucial process in water treatment (Lee et al., 2015). Disinfection is a term to indicate the removal of harmful microorganisms in order to obtain safe water free from waterborne diseases (Backer, 2019). Disinfection, however, is not designed to sterilize water, instead it inactivates the pathogens to reduce the risk of infection via normal consumption (Percival et al., 2013). Water disinfection could be applied either in a central water treatment plant or at the point of use (POU) treatment (household treatment) (WHO, 2011). Where lack of adequate and safe water infrastructure, contaminated water source or contaminated water storage, especially in rural and urban regions, POU water disinfection technologies provide safe and rapid solutions (Clasen and Bastable, 2003; Lilje and Mosler, 2018; WHO, 2011). Not only lack of safe water supply but also in case of any natural disaster such as floods, hurricanes and earthquakes, usage of POU water disinfection is advised. Such technology can also be used by travelers, where they have no reliable water sources. Conventionally, chemical disinfection, filtration techniques, solar disinfection, UV treatment,

coagulation/flocculation and thermal technologies are available for POU treatment (Backer, 2019; WHO, 2011). Not all POU treatment technologies are highly effective against all classes of waterborne pathogens. In fact, each technology has some drawbacks. Of all conventional disinfection methods, the oldest and most reliable one is thermal treatment (Backer, 2019), which destroys microorganisms by raising the temperature of water to 60-70°C through heating (WHO, 2011). However, heat source can be expensive or unavailable and it does not prevent recontamination during storage (Backer, 2019). Chlorination as a chemical disinfectant is a widely used technique, which is extremely effective against most pathogens, is the least expensive method providing residual protection. Besides the advantages, chlorination is not sufficient for *Cryptosporidium* and other waterborne protozoan and it may cause taste and odor problem depending on the applied dosage. Most importantly, during chlorination, free chlorine reacts with natural organic matters (NOMs) in water to form carcinogenic disinfection by-products (DBPs), primarily trihalomethanes (THM) and haloacetic acids (HAAs). Ozone treatment, unlike chlorination, does not produce carcinogenic DBPs and effective against even *Cryptosporidium.* However*,* it is more expensive, more complicated, and does not maintain residual disinfectant for further protection (Okafor, 2011; The Environmental Protection Agency, 2011). Another conventional disinfection method is UV treatment. UV treatment is also effective against resistant organisms. However, it is less effective in turbid water (Okafor, 2011). Additionally, UV treatment has limited use due to the need for a power supply, is costly and require maintenance (WHO, 2011). Solar disinfection, on the other hand, is independent of water turbidity is more effective and economical alternative compared to UV treatment (O. M. Lee et al., 2015). However, it requires strong, direct and abundant sunlight with prolonged exposure (Backer, 2019). Finally, yet importantly, filtration systems can be used to eliminate waterborne pathogens. Filters can be classified based on their pore sizes. This method can be more expensive than chemical methods since the small pore sizes require higher pressures for filtration. The effectiveness is not solely based on the pore size. Filtration may not be also reliable for a high level of removal of viruses. Additionally, it may require maintenance due

to clogging of the filters (Backer, 2019). Considering the aforementioned disadvantages of each conventional disinfection method, robust, inexpensive, self-sustained and free of DBPs POU water disinfection methods should be developed.

2.2. Nanosilver

Since the first mention of nanotechnology in 1974 (Khodashenas and Ghorbani, 2015), nanotechnology and nanoparticles were used in numerous applications such as material science, electronics, biotechnology, environmental, medical and pharmaceutical fields. Nanoparticles are zero-dimensional structures with diameters in the range of 1-100 nm (Ahamed et al., 2010; Khodashenas and Ghorbani, 2015). In the past decades, nanostructures of silver received great deal of interest due to their promising electrical and thermal conductivity (Coskun et al., 2011; P. Zhang et al., 2017), well-known antibacterial activity (Khodashenas and Ghorbani, 2015) making use of unique structures with high aspect ratio (Martinez-Gutierrez et al., 2010) and excellent optical properties (Nateghi and Shateri-Khalilabad, 2015; P. Zhang et al., 2017). Nanoscale electrochemical sensors with fast response time and low detection limits were demonstrated with nanosilver (Kholoud et al., 2010). Unique optical scattering properties of nanosilver allowed its use in bio-sensing and imaging applications (Ahamed et al., 2010; Kholoud et al., 2010) such as solar cells, medical imaging and, Raman spectroscopy (Nateghi and Shateri-Khalilabad, 2015; Tolaymat et al., 2010). Moreover, as discussed in Zhang et al.'s review (2017), the strong electrical and thermal conductivity of nanosilver enabled its demonstration in potential applications in the field of electronics to fabricate conductive films, laser diodes and conductive fillers.

Apart from these applications, Ag has been known as a robust antimicrobial agent (El-Aassar et al., 2013; Wong and Liu, 2010) since the ancient times to prevent infections using in water containers and putrefaction (Rai et al., 2009; Silvestry-Rodriques et al.,

2007). Before the introduction of nanotechnology, Ag was also used clinically (Wong and Liu, 2010) for wound management and ulcers treatment (Durán et al., 2016). For preventing infections, Ag has been applied to newborns' eyes as well as used in burn wound care in the Western world as an antiseptic. Not only in medical field; but also in the production of antimicrobial surfaces of public phones, toilets and toys, Ag has been used for decades (Silvestry-Rodriques et al., 2007). Further investigations showed excellent antibacterial properties of Ag and it started to be extensively used in nanoforms in the disinfection of medical devices, food packaging, clothing, fabrics, water and air (El-Aassar et al., 2013; Kholoud et al., 2010; Maillard and Hartemann, 2013; Tolaymat et al., 2010). The bactericidal action of nanosilver is effective on a wide range of organisms such as gram-positive (e.g. *Streptococcus*) and gram-negative (e.g. *E. coli*) bacteria, viruses (e.g. *hepatitis B, HIV-1*) and fungi (e.g. *Candida albicans*) (Fewtrell, 2014). In fact, recent studies show that nanosilver as a disinfectant is very promising to replace or enhance the conventional water disinfection methods (El-Aassar et al., 2013).

The different synthesis methods produce nanosilver with different sizes, shapes and characteristics (Khodashenas and Ghorbani, 2015). Cubic, plates, belts, beams, tubes, rods and wires are the typical Ag nanostructures as discussed in Zhang et al.'s (2017) and Khodashenas and Ghorbani's (2018) reviews. Figure 2-2 shows the typical scanning electron microscopy (SEM) images for silver nanoparticles (AgNPs), silver nanowires (AgNWs), and silver nanocubes (AgNCs). Morphology of nanosilver plays a vital role in the antibacterial performance of Ag as it depends on the surface area (P. Zhang et al., 2017). As indicated by Morones et al. (2005), size of nanosilver has an impact on its bactericidal effect as bacteria has a direct interaction with the nanoparticles with diameters of 1-10 nm . One study on gram-negative *E. coli* revealed that the shape of nanosilver also changes the antibacterial performance (Pal et al., 2007). It has been found that triangular nanosilver have the highest performance following the spherical nanosilver. The weakest performance against *E. coli* belongs

to rod-shaped nanosilver. In contrast, Gao et al. (2013) suggested better antibacterial performance for spherical nanosilver against *E. coli* compared to triangular nanosilver. Another study (Hong et al., 2016b) conducted with Ag nanocubes, nanospheres and nanowires supported inferences of Pal et al. (2007). Results revealed weaker performance of nanowires than nanocubes and nanospheres. On the other hand, Schoen et al. (2010) suggested that AgNWs provide an advantage over AgNPs by having multiple binding points with the supporting media. Likewise, Feng et al. (2018) reported that the antibacterial activity of AgNWs is higher than that of sphere-like AgNPs for both gram-negative and gram-positive bacteria. The shape dependent results were attributed to effective contact areas and facet reactivity. The better antibacterial performance of the nanosilver was attributed to the larger specific surface area that is in contact with cells. Likewise, the size of nanosilver was found to be important as discussed by Rizzello and Pompa (2014). Smaller nanoparticles showed stronger inhibition effect on microorganisms' growth compared to the bigger ones. On the other hand, a recent study (Gorka et al., 2015), indicated that the shape of nanostructures also affect the environmental toxicity. It has been shown that AgNWs have insignificant environmental toxicity toward the roots and shoots compared to AgNPs and AgNCs. Similarly, another study conducted with *Daphnia magna* (Scanlan et al., 2013), which is an indicator of freshwater ecology and toxicity, revealed that the toxicity of AgNWs is significantly less than that of silver nitrate ($AgNO_3$) and silver nanoparticles.
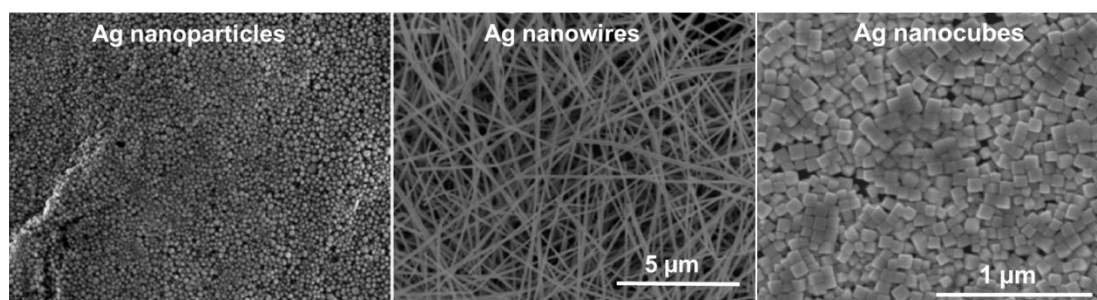
Figure 2-2. Typical SEM images for AgNPs, AgNWs (Coskun et al., 2011), and AgNCs (Zhao et al., 2011).

AgNWs are defined as one-dimensional structures with diameters and lengths typically in the range of 10-200 nm and 5-100 μm, respectively. An important characteristic of AgNWs is their aspect ratio (length/diameter), which is greater than 10. Otherwise, the structure is called as a nanorod. However, it is not easy to control the morphology of wires (P. Zhang et al., 2017). To date, several methods have been introduced to fabricate AgNWs, including chemical synthesis methods, electrochemical methods, hard-template method and polyol method (Coskun et al., 2011; Khodashenas and Ghorbani, 2015; Wei et al., 2015; P. Zhang et al., 2017). Of AgNW synthesis methods, solution based polyol method and its derivatives are the most promising ones in terms of cost, yield, simplicity and uniformity (Coskun et al., 2011; P. Zhang et al., 2017). The polyol process is conducted under elevated temperatures via the reduction of $AgNO_3$ as a metal salt by a polyol. In this method, ethylene glycol acts as both solvent and reducing agent, polyvinylpyrrolidone (PVP) act as a stabilizing agent and $AgNO_3$ act as the silver source (Coskun et al., 2011).

2.3. Silver as an Antimicrobial Agent

2.3.1. Mechanism of antimicrobial action

Although microbial inactivation of Ag had been proven for centuries, its mechanism has not been fully understood. Researchers still study on possible mechanisms. It has been proved that the structural and morphology of the bacteria changes due to Ag ions. To date, the major mechanisms of action of Ag generally reported in the literature are:

(1) Reaction with thiol groups (Nangmenyi and Economy, 2009; Rai et al., 2009) such as NADH-dehydrogenase II (Hossain et al., 2014) to inhibit enzymatic activity (Lalley et al., 2014), which eventually interrupt the DNA replication process (Hossain et al., 2014) and to produce Reactive Oxygen Species (ROS) (El-Aassar et al., 2013) resulting in the generation of oxidative stress

13

(Quinteros et al., 2016) and to increase permeability in the membrane (Durán et al., 2016),

(2) Binding the bacterial cell wall and cell membrane (Nangmenyi and Economy, 2009; Silvestry-Rodriques et al., 2007; Tartanson et al., 2014) to inhibit cellular respiratory chain (Rai et al., 2009) and electron transfer (Silvestry-Rodriques et al., 2007) or interfere with membrane permeability (Duran et al., 2010) resulting in cell death (Maillard and Hartemann, 2013),

(3) Binding to DNA displacing the hydrogen bonds between purine and pyrimidine base pairs to denature DNA molecule as well as replication of DNA (Lalley et al., 2014; Silvestry-Rodriques et al., 2007).

Figure 2-3 represents some mechanisms of antimicrobial action of Ag nanomaterials.
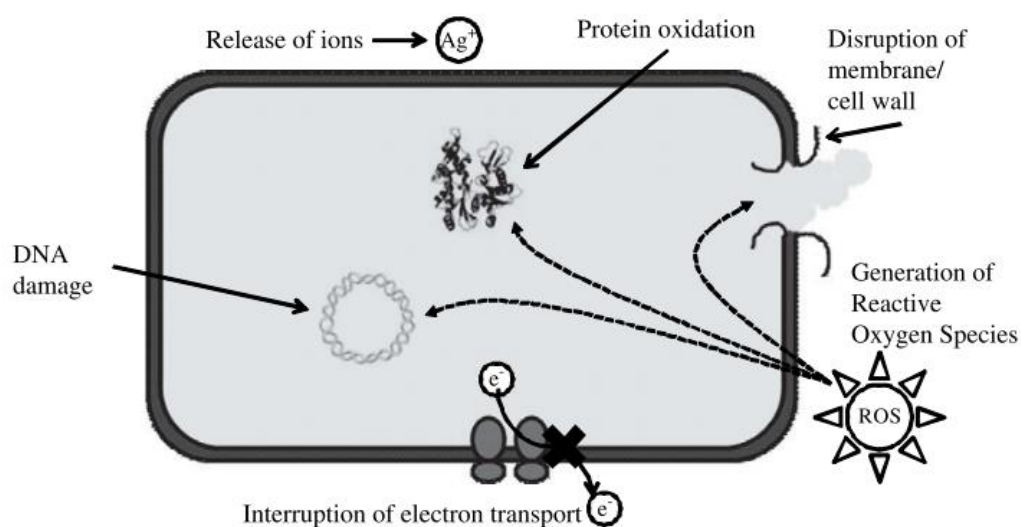
Figure 2-3. Various antibacterial mechanisms of Ag nanomaterials (Q. Li et al., 2008).

It is still under debate whether the antimicrobial action of nanosilver is the same as that of Ag ions or not. Compared with Ag compounds, larger surface area to volume ratio of nanosilver results in much better antimicrobial efficacy (Wong and Liu, 2010). Several experiments revealed that nanosilver had higher antimicrobial efficiency than ionic Ag at the same concentration (Zhang et al., 2016). This effect of nanosilver was observed at a concentration with a 10-fold lower magnitude than those of Ag compounds (Durán et al., 2016). Choi et al. (2008) provided two contradictory results of the same concentrations of AgNPs, Ag ions and silver chloride (AgCl) on autotrophic bacteria and heterotrophic *E. coli*. AgNPs showed stronger inhibition on bacterial growth than Ag ions and AgCl colloids on autotrophic nitrifying bacteria at the same concentrations while they showed weaker inhibition performance on heterotrophic *E. coli*. Another study demonstrated that although the antibacterial activity of AgNPs was higher than that of Ag ions related to the large surface area of NPs, increasing AgNP loading did not improve the antibacterial performance (Shameli et al., 2012). These studies bring the debate to whether the antimicrobial effect of nanosilver is particle-specific or not (Zhang et al., 2016). Although there could be various mechanisms (Park et al., 2017), it is generally accepted that Ag ion release from nanosilver is the major antimicrobial mechanism (Dankovich, 2012; Zhang et al., 2016). Therefore, the mechanisms of nanosilver are similar to those of Ag ions (Wong and Liu, 2010) resulting from Ag^+ release from nanosilver (Fewtrell, 2014). Furthermore, a study revealed that direct particle-specific antimicrobial effects of nanosilver are negligible. Instead, it served as a more effective carrier of Ag ions to deliver to the bacteria (Xiu et al., 2012). On the other hand, several studies in the literature showed that the antimicrobial action of nanosilver was not only due to ionic Ag release. In fact, Stabryla et al. (2018) reviewed 30 studies conducted for AgNP mechanisms. Among 30 studies reviewed, 39%, 16% and 45% of the studies were concluded as the ion-only mechanism, particle-only mechanism and combined ion-particle mechanism, respectively. In other review papers by Maillard and Hartemann (2013) and Rizzello and Pompa (2014), it was also mentioned that Ag ion release was not the major responsible mechanism for the antimicrobial activity of nanosilver.

Ribeiro et al. (2014) suggested that bactericidal effect of nanosilver might be a combination of both the toxicity of released Ag ion and particle-specific effect as a result of their studies on *Pseudokirchneriella subcapitata*, *Daphnia magna* and *Danio rerio* as model organisms. Parandhaman et al. (2015) researched the mechanism of action of nanosilver composite on gram-negative bacteria (*E. coli* and *P. aeruginosa*) under strictly anaerobic conditions to eliminate ionic Ag release by aerial conditions. They revealed that even if there was not any ionic Ag in the environment, nanosilver showed antibacterial activity under anaerobic conditions similar to that of aerobic conditions. This study confirms that the antibacterial action of nanosilver does not only depend on the ionic Ag release. Further studies by Parandhaman et al. (2015) showed that nanosilver resulted in membrane damage, which inhibits the respiratory chain, and alteration in proteins expressed in the absence of intracellular ROS production and dissolution of ionic Ag. Similar effects of nanosilver were discussed in several studies (Fewtrell, 2014; Jain and Pradeep, 2005; Le Ouay and Stellacci, 2015; Li et al., 2008; Quinteros et al., 2016; H. Zhang, 2013). Figure 2-4 shows the particle-specific antibacterial actions of nanosilver.
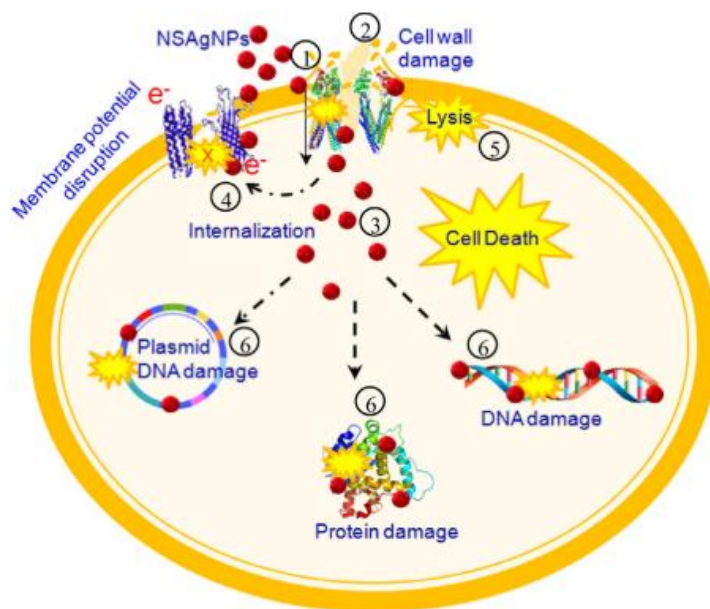
Figure 2-4. Particle-specific antibacterial actions of nanosilver composite (Parandhaman et al., 2015).

The mechanism and efficacy may also change depending on the target organisms since different organisms have different sensitivity in the function of the structures of the cell wall (Durán et al., 2016). A study (Jung et al., 2008) showed that the efficacy of the Ag ion on gram-negative *E. coli* would be better than that on the gram-positive *S. aureus*, possibly due to the thickness of the peptidoglycan layer, which may prevent the action of the Ag ions through the bacterial cell wall. On the other hand, Feng et al. (2000) proposed the same phenomenon occurred in the Ag^+ treated typical gram-negative and gram-positive cells although they observed slight morphological changes in gram-positive bacteria: Ag ions inhibited the DNA replication abilities due to both the denaturation effects of Ag ions and the interaction with thiol groups of Ag ions. Wong and Liu (2010) showed that a low concentration of AgNPs could inhibit the growth of yeast and *E. coli* resulted from free radicals and oxidative stress.

Some studies (Hong et al., 2016a; C. Liu et al., 2013; Nangmenyi et al., 2011; X. Yang et al., 2014; Zodrow et al., 2009) also specified that nanosilver was effective on virus inactivation but there were no detailed studies on the interaction between Ag and viruses. One theory states that viruses containing sulfhydryl termini may bind to Ag, resulting in the inhibition of their replication cycle (Silvestry-Rodriques et al., 2007). Another theory by Silvestry-Rodriques et al. (2007) states that continuous redox reactions occurred by metal binding to a biological molecule damage viruses. AgNPs (up to 10 nm) can bind virus' glycoproteins so that they prevent the viruses from binding to host cells (Q. Li et al., 2008) or it might block or destruct the host-cell receptors (Silvestry-Rodriques et al., 2007).

Toxicology research is focused generally on AgNPs. Even if the shape of the nanosilver may have different impacts on the antimicrobial efficacy (Rai et al., 2009), mechanism of action pathway for AgNWs are thought as mostly similar to that of AgNPs (Perk, 2016). Briefly, it is clear that the most common perspectives on the

mechanisms of action are cell membrane damage, DNA interactions and ROS generation. All may result in cell damage and death as discussed earlier.

2.3.2. Antimicrobial performance of nanosilver

The antimicrobial effect of nanosilver was mostly studied during early 2000s (Morones et al., 2005; Son et al., 2004; Sondi and Salopek-Sondi, 2004; Zaporojtchenko et al., 2006). There has been progress on the drinking water disinfection performance of nanosilver-based materials over the years. This thesis mostly focuses on the research studies targeting POU water disinfection. In this context, Table 2-2 summarizes the properties and results of the studies conducted with AgNPs or AgNWs in the field of drinking water disinfection (i.e. POU water disinfection).

Table 2-2. *Properties and results of the studies conducted with AgNPs or AgNWs for POU water disinfection.*

Nanosilver based material	Application	Voltage Application (V)	Flow Rate (ml/min)	Cell Type	Cell Concentration (CFU (or PFU)/ml)	Disinfection Efficiency	Silver Concentration	Silver Release (ppb)	Reference
Cellulose acetate/AgNPs membrane	F/P	0	600	E.coli	NG	99.95%	NG	NG	Beisl et al. (2019)
AgNWs-PAN/TPU membrane	F/G	0, 1.5, 3	10	E.coli, S. aureus	$10^3 - 10^5$	100%	0.5 – 2.0 mg	32.4 – 81.7	Tan et al. (2018)
PAN/PANI/AgNWs-CC	F/P	0, 3, 6	0.3	E.coli, S. aureus	$10^5 - 10^7$	100%	5.22 wt.%	<15	Wen et al. (2017)
AgNPs coated GAC	CC	0	<0.45	E.coli	10^4	100%	0.8 wt.%	29.8 ± 8.2	Biswas and Bandyopadhyaya (2016)
Silver modified zeolites-clinoptilolite	CC	0	2	E.coli	10^9	100%	43.4 mg Ag/g zeolite	50 – 230	Akhigbe et al. (2016)
Cu-Ag- TiO$_2$ membrane	F/P	0	5	E.coli / MS2	10^7 / 10^5	7.68±0.99 log / 4.06±0.27 log	2%	<100	Rao et al. (2016)
AgNP coated on cellulose paper	F/P	0	19800	E.coli	10^8	99-100%	0.141 – 0.676 mg/g	20-30	Praveena et al. (2016)
AgNW-Carbon fiber cloth nanocomposite membrane	F/G	0 – 10	2-10	E.coli / MS2	$10^2 - 10^{10}$	<5.95 log / <5.21 log	2 – 10 mg/ml	11.36 – 81.75	Hong et al. (2016a)
AgNP/AgNW and graphite coated porous cotton fibers	F/G	20	10	E.coli	$10^7 - 10^8$	6 log	NG	NG	Basheer and Abu-thabit (2014)

Table 2-2. (*Continued*)

Nanosilver based material	Application	Voltage Application (V)	Flow Rate (ml/min)	Cell Type	Cell Concentration (CFU(or PFU)/ml)	Disinfection Efficiency	Silver Concentration	Silver Release (ppb)	Reference
AgNPs containing silica beads	CC	0	30	E.coli	10^6	99.9%	0.38 wt.%	10 – 100	Quang et al. (2013)
AgNPs coated GAC	CC	0	800	E.coli	10^4	100%	20 mg AgNP/g GAC	NG	El-Aassar et al. (2013)
AgNPs attached to porous carbon foam	F/P	0	100	E.coli	10^3	99%	1.5 – 2.5 wt.%	NG	Karumuri et al. (2013)
Polyurethane sponge modified by CNTs/AgNWs	F/G	0-20	25	E.coli S. enterica E. faecalis B. subtilis / MS2	10^7	>6 log / 99.4 %	NG	70 – 94	C. Liu et al. (2013)
AgNPs coated cation resin beads	CC	0	2 – 10	E.coli	$10^2 – 10^4$	100%	NG	NG	Mthombeni et al. (2012)
AgNPs coated Polysulfone UF membrane	F/P	0	NG	E.coli	10^{17}	6 – 12 log	2 - 4 wt.%	0 – 200	Mollahosseini et al. (2012)
Ag-modified Fe₂O₃ nanoparticle impregnated fiberglass	F/G	0	1	E.coli / MS2	10^6 / 10^7	2 – 4 log / 0.5 – 1.6 log	0.1 – 1.4 wt.%	NG	Nangmenyi et al. (2011)
Blotting paper impregnated with AgNPs	F/G	0	10	E.coli / E. faecalis	10^9	4.5 – 7.5 log / 2.8 – 3.2 log	0.2 – 20.4 mg/g	47.5 ± 17.7	Dankovich and Gray (2011)
AgNWs/CNTs - cotton	F/G	-20 ; +20	16.7	E.coli	10^7	80 – 90 %	NG	NG	Schoen et al. (2010)

20

Table 2-2. (*Continued*)

Nanosilver based material	Application	Voltage Application (V)	Flow Rate (ml/min)	Cell Type	Cell Concentration (CFU (or PFU)/ml)	Disinfection Efficiency	Silver Concentration	Silver Release (ppb)	Reference
AgNP impregnated fiberglass mats	F/G	0	20	*E.coli*	10^6	100 %	5.0 wt.%	NG	Nangmenyi et al. (2009)
Polysulfone UF membranes impregnated with AgNPs	F/P	0	NG	MS2	$10^4 - 10^5$	100 %	0.9 wt.%	4 – 34	Zodrow et al. (2009)
AgNP coated polyurethane foam	F/G	0	500	*E.coli*	$10^3 - 10^5$	100 %	NG	NG	Jain and Pradeep (2005)

NG: Not Given
CC: Continuous Column Operation
F/P: Filtration by the pump
F/G: Filtration by gravity

21

Table 2-2 reveals that the desired antibacterial performance can be obtained with nanosilver-containing materials. Each individual study reported in Table 2-2 was conducted under different conditions in terms of material type, application type, cell type and concentration, and Ag concentration. As it is the case for the most studies using nanomaterials, the application method and material characteristics of each unique material change from one study to the other. It can be concluded that the antibacterial performance of nanosilver depends on several factors. The major factors discussed in the literature are coated materials, microbial culture, microbial concentration, Ag concentration, and water characterization (such as pH, temperature, turbidity, total organic carbon etc.). Each effect will be discussed in the following sections in detail.

2.3.2.1. Effect of different supporting materials on antimicrobial performance

It is mostly seen that Ag in the form of NPs or NWs can be coated onto different carriers in the literature. Fan et al. (2018), Song et al. (2016) and Parandhaman et al. (2015) tested antibacterial properties of AgNP-decorated chitosan cryogels, Ag containing graphene oxide (GO) and silica-silver nanocomposites, respectively, for water disinfection through directly applying these nanocomposites to bacterial suspensions. Cellulose acetate/AgNP (Beisl et al., 2019), AgNP/TiO$_2$ membrane (Rao et al., 2016), AgNP coated on cellulose paper (Praveena et al., 2016) and blotter paper (Dankovich and Gray, 2011), AgNP/GO sheet (Gu et al., 2016), AgNP coated on polyurethane foam (Jain and Pradeep, 2005; Phong et al., 2009), Ag modified iron oxide nanoparticle impregnated fiberglass (Nangmenyi et al., 2011), AgNP impregnated ball media (W. H. Yang et al., 2012), AgNP modified ceramic water filters (Kahler et al., 2016; Kallman et al., 2009; Mikelonis et al., 2016), Ag/lysozyme nanoparticles supported with montmorillonite clay (J. Jiang et al., 2016), AgNP attached porous carbon foam (Karumuri et al., 2013) and AgNP modified micro or ultrafiltration membranes (Diagne et al., 2012; Mollahosseini et al., 2012; Sawada et

22

al., 2012; Taurozzi et al., 2008; Zodrow et al., 2009) were also investigated for water disinfection. For POU water disinfection, AgNPs were coated on activated carbon granules in continuous packed column application (Biswas and Bandyopadhyaya, 2016; El-Aassar et al., 2013). In similar column applications, AgNPs were coated on modified silver zeolite (Akhigbe et al., 2016), silica beads (Quang et al., 2013), cation resin beads (Mthombeni et al., 2012) and alginate composite beads (Lin et al., 2013). Mpenyana-Monyatsi et al. (2012) compared the disinfection performance of Ag/anion resin, Ag/fiberglass resin, Ag/sand resin and Ag/cation resin, entirely. Among four different resin systems, Ag/cation resin was suggested for disinfection of drinking water, which achieved 100% removal of bacteria. Nangmenyi et al. (2009) also compared the activated carbon fibres and fiberglass impregnated with AgNPs in a filtration application. It was concluded that fiberglass mats impregnated with AgNPs showed superior performance over Ag-impregnated AC fibres.

AgNWs are less studied and are relatively new materials compared to AgNPs. In recent years, water disinfection studies conducted with AgNW-polyacrylonitrile/thermoplastic polyurethane (AgNW-PAN/TPU) (Tan et al., 2018), polyacrylonitrile/polyaniline/silver nanowires-carbon fiber cloth (PAN/PANI/AgNW-CC) composite nanofiber membrane (Wen et al., 2017), AgNW-Carbon fiber cloth nanocomposite (Hong, 2016a), composites made from AgNW, carbon nanotubes and cotton (Basheer and Abu-thabit, 2014; Schoen et al., 2010) and nanosponge filters made from polyurethane sponge modified by carbon nanotubes (CNTs) and AgNW (C. Liu et al., 2013) were also reported.

Some studies suggested a synergistic effect between nanosilver and coated medium. Ag modified iron oxide nanoparticles impregnated fiberglass showed superior disinfection performance over fiberglass impregnated with either Ag or iron oxide alone at higher concentrations (Nangmenyi et al., 2011). Rao et al. (2016) also

observed the synergistic effect of Ag and copper. Synergistic effects between AgNPs and decorated magnetic graphene oxide (MGO) (H. Z. Zhang et al., 2016), nanosilver and acid activated montmorillonite (Roy et al., 2017), silver and chlorine (Fewtrell, 2014; Tan et al., 2018) were also discussed in the literature.

In order to enhance the antimicrobial capability of nanosilver, low bias voltages were applied. This was due to the high conductivity of nanosilver (Basheer and Abu-thabit, 2014; Hong et al., 2016a; Schoen et al., 2010; Tan et al., 2018; Wen et al., 2017). Wen and his colleagues (2017) inactivated over 99.999% of sieved bacteria on PAN/PANI/AgNW-CC membrane at an applied potential of only 3V. Further study by the same group inactivated bacteria completely under an applied voltage of 1.5V to AgNW-PAN/TPU membrane (Tan et al., 2018). Hong et al. (2016a) indicated that the voltage application was the most effective way to enhance disinfection efficacy. Voltage application increased the removal of bacteria by at most 5 log more. Nanosilver coated materials also show biofouling mitigation of the filter or membrane. It was observed that polyacrylonitrile/polyaniline/silver nanowires-carbon fiber cloth (PAN/PANI/AgNW-CC) membrane showed approximately 1 log higher antifouling efficiency compared to membranes without AgNW (Wen et al., 2017). Taurozzi et al. (2008) suggested that Ag was effective in reducing intrapore biofouling in porous membranes of a wide range of porosities. Zodrow et al. (2009) studied with polysulfone ultrafiltration membrane, so did Taurozzi and his colleagues (2008). It has been concluded that the membrane containing nanosilver had anti-biofouling property against biofilm causing bacteria (*P.mendocina*). It was observed that *P.mendocina* were less likely to attach during filtration and they were inactivated when deposited onto the surface of the membrane. Hydrophilic polymer membranes containing AgNPs showed quite stable permeability whereas original membranes' permeability decreased sharply (Sawada et al., 2012). Another study confirmed that the modification of microfiltration membrane with AgNPs significantly mitigated organic and bacterial fouling (Diagne et al., 2012).

A few studies evaluated the nanosilver containing materials in field sites. Ceramic filters impregnated with AgNPs was investigated in the field in San Mateo Ixtatan, Rural Guatemala (Kallman et al., 2009). The average percent reduction in total coliforms and *E. coli* was 87% and 92%, respectively, by examining the filters in drinking waters of 62 households in this urban community. It has also been mentioned that public acceptance of the product was significant. Kahler et al. (2016) conducted a similar study in two field sites: Limpopo Province, South Africa and Dodoma Region, Tanzania with Ag impregnated ceramic cubes. The study focused on educational areas. The material reduced the total coliform by 3-4 logs. It was indicated that although students prejudged this novel treatment technology, they always preferred the treated water with silver-based materials, which showed sustained acceptance. A paper sheet containing AgNPs was also tested in contaminated streams in Limpopo, South Africa (Dankovich et al., 2016). The paper sheets completely inactivated total coliform bacteria in the samples taken from contaminated streams for those concentrations ranged between 250 – 15000 CFU/100 ml. When higher coliform bacteria (500000 – 1000000 CFU/100 ml) were present, AgNPs containing paper sheet resulted in 5.1 log removal in average.

2.3.2.2. Effect of different microbial culture on antimicrobial performance

Antimicrobial performance of nanosilver on various microbial cultures has been studied by several researchers. Although Ag has an antibacterial impact on a wide range spectrum of microorganism, the antimicrobial effectiveness of Ag would change depending on the microbial culture type. It was reported that the distinction between gram-positive (*B. Subtilis, S. aureus,* etc.) and gram-negative bacteria (*E. coli, Salmonella typhimurium,* etc.) was based on the cell wall structure. The gram-negative cell wall is chemically complex and consists of two layers, whereas gram-positive bacteria have a much thicker and single cell wall (Madigan et al., 2012). The thick cell wall of gram-positive bacteria helps them survive in the harsh conditions while the

more complex structure of gram-negative bacteria tends to interact with mineral surfaces and solutes (Pepper et al., 2015). However, the reticular structure of the peptidoglycan layer in Gram-negative bacteria is looser and exhibits a lower mechanical strength (Song et al., 2016).

Song et al. (2016) and Zhu et al. (2013) studied with GO-AgNPs material to investigate the antibacterial activity. The former conducted their studies by *E. coli* and *S. aureus* while the latter used *E. coli* and *B. subtilis* as gram-negative and gram-positive bacteria, respectively. Both concluded that nanosilver was more effective on gram-negative bacteria than gram-positive bacteria, resulted from their time kill and minimum inhibitory concentration (MIC) tests (Song et al., 2016; Zhu et al., 2013). Another study investigating the antibacterial effect of Chitosan/AgNPs cryogels on *E. coli* and *B. subtilis* revealed that *E. coli* was slightly more sensitive than *B. subtilis* (Fan et al., 2018). A blotter paper impregnated with AgNPs was tested against gram-negative *E. coli* and gram-positive *E. faecalis* (Dankovich and Gray, 2011). The study concluded that AgNPs paper is more lethal to *E. coli* than *E.faecalis* at all Ag doses in the range of 0.2 – 10.4 mg/g. C. Liu et al. (2013) conducted a more comprehensive study to examine the antibacterial effect of the conducting nanosponge made from low-cost polyurethane sponge coated with carbon nanotubes and AgNWs against gram-negative *E. coli,* and *S. Typhimurium* and gram-positive *E. faecalis* and *B. subtilis*. The disinfection performance was found to be higher for gram-negative ones compared to gram-positive counterparts. Tan et al. (2018) also evaluated the disinfection performance of AgNW-PAN/TPU membrane against *E. coli* and *S.aureus*. It has been found that there was not a significant difference in inhibition zones for two different bacteria, but the inactivation rate of *E. coli* was higher than that of *S. aureus* under the same conditions. The same conclusion was reached by Wen et al. (2017) via a PAN/PANI/ AgNW-CC composite nanofiber membrane. Unlike studies mentioned so far, Roy et al. (2017) showed that the zone of inhibition of nanosilver loaded acid activated montmorillonite for *E. coli* was less than that for *S.*

26

aureus. Another study resulted in higher MIC and minimum bactericidal concentration (MBC) values of AgNP obtained for *E. coli* than *B. subtilis* (Zain et al., 2014). Both implied that gram-negative *E. coli* is more resistant than gram-positive bacteria (*S. aureus* and *B. subtilis*). Park et al. (2017) studied with *L. pneumophila* as gram-negative unlike the other studies and *B. subtilis* as gram-positive. It has been concluded that *B. subtilis* was more sensitive to AgNPs-Magnetic Hybrid Colloids (MHC) than *L. pneumophila*. Doganay et al. (2019) investigated the AgNW decorated cotton fabrics for their antimicrobial activity against gram-positive coccus (*S. aureus*), a gram-negative bacillus (*E. coli*), a gram-positive and spore-forming bacillus (*B. cereus*), and a yeast-like fungus (*C. albicans*). The outcomes of this study implied that the maximum antibacterial effect is observed on *B. cereus* after a long period due to the spore-forming nature; moreover, the antibacterial activity of the material maintained its activity for a short period for *S. aureus* (Doganay et al., 2019).

Two studies comparatively investigated the antibacterial effect of Ag on different gram-negative bacteria strains (Mpenyana-Monyatsi et al., 2012; Nawaz et al., 2012). Nawaz et al. (2012) concluded their studies that *E. coli* was more sensitive than *P. aeruginosa*. Mpenyana-Monyatsi et al. (2012), on the other hand, found that *S. typhimurium* and *V.cholerae* are more susceptible ones whereas *E. coli* is the most resistant one among four different gram-negative bacteria (*E. coli, S. dysenteriae, V. cholera* and *S. typhimurium*).

Overall, the literature is confusing to understand the relative effectiveness of Ag against both gram-negative and gram-positive bacteria. Ruparelia et al. (2008) made a valuable contribution. They used three representative bacteria (*E. coli, B. subtilis* and *S. aureus*) with eight different strains, i.e., four *E. coli* strains, one *B. subtilis* strain and three *S. aureus* strains for the antimicrobial study of nanosilver by disk diffusion test, MIC and MBC tests. Finally, it has been concluded that the bactericidal efficiency

do not only depend on the structure of the bacterial membrane but also it changes based on strain specificity. Nanosilver showed higher antibacterial activity against *S. aureus* than some *E. coli* strains. Greater sensitivity of *B. subtilis* compared to *E. coli* and *S.aureus* is reported (Ruparelia et al., 2008).

The inhibitory effect of the silver-reduced GO composites against two bacteria in the marine environment, *V. natriegens* and *Bacillus sp.*, was also investigated (Gu et al., 2016). It has been concluded that *Bacillus sp.* is more resistant against the composite material than *V. natriegens*.

There are also studies to investigate the antibacterial effect of Ag on both *E. coli* and bacteriophage MS2, which is a virus infecting and replicating within bacteria and archaea, comparatively (Hong et al., 2016a; Rao et al., 2016; X. Yang et al., 2014; You et al., 2011). All concluded that Ag could inactivate bacteriophage MS2 except the one conducted by You et al. (2011) which failed to inactivate bacteriophage MS2 even at the highest silver concentration of AgNPs. In fact, Hong et al. (2016a) found out the higher antibacterial efficiency on bacteriophage MS2 (5.95 log) than *E. coli*, (5.21 log) although X. Yang et al. (2014) and Rao et al. (2016) revealed that nanosilver shows better inactivation against *E. coli* than bacteriophage MS2. It is seen that nanosilver might affect the bacteriophages and be effective for their removal. However, the effect of nanosilver on bacteriophages still needs further investigation.

2.3.2.3. Effect of different microbial concentration on antimicrobial performance

Microbial concentration can affect the antimicrobial performance of nanosilver. The general phenomenon is that higher bacterial concentration leads to lower removal efficiency.

As a result of the inhibition zone test conducted by El-Aassar et al. (2013) with AgNPs coated onto activated carbon granules, inhibition zone diameter decreased with an increase in bacterial concentration for the same Ag concentration. At 10^2 CFU/ml of *E. coli* concentration, inhibition zone diameter was 1.1 cm, whereas it was 0.9 cm when bacterial concentration increased to 10^6 CFU/ml. Hong and his colleagues (2016a) reported on effective removal of *E. coli* and bacteriophage MS2 using a composite AgNW-carbon fiber cloth. However, when the bacterial and viral concentration increased beyond 10^6 CFU (or PFU)/ml, the performance was found to decrease significantly especially for *E. coli*. The maximum reduction in the removal efficiencies of *E. coli* and MS2 was 73.84% and 13.7%, respectively, while concentration was increased from 10^2 CFU(PFU)/ml to 10^{10} CFU(or PFU)/ml in a flow test. Tan et al. (2018) showed that the disinfection efficiencies of the AgNW-PAN/TPU membranes were 48.7% and 45.0% for *E. coli* and *S. aureus* at 10^5 CFU/ml, respectively, when operated at 1.5 V for 1 min. Decreasing the bacteria concentration to 10^3 CFU/ml for both types increased the inactivation efficiencies to 58.7% and 51.3%, respectively. A similar behavior was obtained for 3 and 5-min long experiments. H.Z. Zhang et al. (2016) reported a prominent antibacterial effect with a removal rate of more than 99% even at high concentration of bacteria through the use of Ag nanoparticle-decorated MGO. In contrast, Mthombeni et al. (2012) reported on the improvement of inactivation of bacterial cells by increasing initial bacterial concentration during column experiment with AgNPs coated resin beans. However, the breakthrough point of the column experiment was reached faster. They explained this indicated result as the increase in cell concentration led to the increase in the probability of interaction between cells and AgNPs and resulted in an increase in inactivation rate. However, due to higher bacterial concentration, it has been observed that the breakthrough point of the column was decreased.

2.3.2.4. Effect of silver concentration on antimicrobial performance

There are two opposite ideas about the effect of Ag concentration on antimicrobial performance. One says there is no significant effect of changing the Ag dose on the performance and other claims improved performance by increasing the Ag dose. Doganay et al. (2019) reported that increasing AgNW loading on AgNW modified fabrics have no significant effect on the inhibition zone diameters; whereas Tan et al. (2018) found that inhibition zone diameters increase with increasing AgNW loading on PAN/TPU membrane. Like Tan et al.'s study, El-Aassar and his colleagues (2013) indicated an increase in inhibition zone diameter with increasing AgNP concentration. For 2.5 mg AgNP coated on gram activated carbon granules, inhibition zone diameter was seen as 1.1 cm, while 20 mg/g of AgNP concentration resulted in 1.4 cm zone diameter at same bacterial concentration. At least 1 cm more inhibition zone was observed when 10 mg/l AgNW was coated on carbon cloth compared to 2 mg/l AgNW for *E. coli* at a concentration of $10^2 - 10^6$ CFU/ml (Hong et al., 2016a). Gu et al. (2016) and Park et al. (2017) also supported this dose-dependent idea as a result of their studies. The idea that revealed the independency of antimicrobial performance of Ag dose by Doganay et al. (2019) was also investigated via MIC experiment by Roy et al. (2017). No significant difference in MIC values was found with at least 10 times lower Ag content. Similarly, increase in Ag concentration in the solution coated onto cellulose filter paper did not show a significant difference in log reduction values of *E. coli* after filtration. Log reduction values changed between 7-8 log for water sample containing 10^8 CFU/ml of *E. coli* at various Ag concentrations changing from 0.001 mole to 0.1 mole (Praveena et al., 2016). On the other hand, Song et al. (2016) and H.Z. Zhang et al. (2016) reported on a dose-dependent manner for both *E. coli* and *S. Aureus*. Song et al. (2016) used different concentrations of GO-Ag solution (40 mg/l, 120 mg/l, 200 mg/l and 280 mg/l). Bactericidal effect was found to increase with concentration. Similarly, H.Z. Zhang et al. (2016) suggested that the increase in nanosilver dose from 6.25 µg/ml to 50.00 µg/ml increased the inactivation from 91.16% to 99.999% for *E. coli*.

2.3.2.5. Effect of different water characterization on antimicrobial performance

Antimicrobial performance of nanosilver would depend on natural water characteristics such as pH, temperature, turbidity, hardness, total organic carbon (TOC) or natural organic matter (NOM).

Song et al. (2016) studied the influence of pH. With this aspect, solutions under acidic (pH=5.5), neutral (pH=7) and alkaline (pH=8.5) conditions at the same Ag dosage were prepared. It has been found that, for both *E. coli* and *S.aureus*, 200 mg/l GO-Ag nanocomposite show better antibacterial activity at lower pH compared to higher pH values. For *E. coli,* the bacterial reduction was 81.68%, 75.5% and 70.5% and for *S.aureus,* the percentages were 58.23%, 45.96% and 40.6% at the acidic, neutral and alkaline conditions, respectively. Lower pH values resulted in a more rapid release of Ag ions from AgNPs and higher antibacterial activity. In another study, Ag nanoparticle-decorated MGO was found to highly adapt to different pH values (H. Z. Zhang et al., 2016). Antibacterial activities of 50 µg/L MGO-Ag solution at different pH values (4, 5, 6, 7, 8 and 9) for *E. coli* and *S.aureus* were all close to 100% except for *S.aureus* at pH values of 4 and 5. There was a significant difference compared to other pH values when pH was changed from 4 to 5 (96% and ~100%, respectively). Compared to these two studies by Song et al. (2016) and H. Zhang et al. (2016), it is seen that there is a conflict with their arguments. Song et al. (2016) justified the pH effect on antibacterial performance, while H.Z. Zhang et al. (2016) concluded in the highly adaptable antibacterial effect of the nanosilver containing material to different pH values. The differences between these two studies might be different temperatures and contact time factors. Song et al. (2016) conducted their studies at room temperature (25 °C) for 25 min while H.Z. Zhang et al. (2016) worked at 37°C for 2h. Both factors can certainly affect the antibacterial performance.

Tartanson et al. (2014) found that the time needed for complete removal of the bacterial mixture by Ag containing material decreases as temperature increases from 22 to 37°C. A similar argument was disclosed by H. Z. Zhang et al. (2016). Antibacterial effect of silver-containing materials was found to improve as water temperature increases.

Another factor that influences the antibacterial efficacy of Ag is turbidity. Fan et al. (2018) mentioned that the turbidity of water play a major role on the bactericidal efficiency. Kahler et al. (2016) observed that the antibacterial efficiency of Ag impregnated ceramic cubes was 4.2 log reduction and 1.1 log reduction in less turbid water (5 NTU) and in more turbid water (11 NTU), respectively.

The effects of ionic strength, hardness and TOC were also studied by sodium nitrate, calcium, and, magnesium nitrate and humic acid, respectively (X. Yang et al., 2014). It has been shown that ionic strength and hardness only influence the viral inactivation performance at high concentrations only, while much lower TOC dramatically reduce the performance. In fact, 30 mg/l TOC as humic acid totally suppressed the antiviral performance. In the presence of dissolved NOM and divalent ions, such as humic acid and calcium carbonate, the antibacterial performance of nanosilver was found to decrease (H. Zhang et al., 2012). NOM could create a physical barrier between the nanoparticles and bacteria through being adsorbed on the AgNP surface resulting in a decreased bacterial toxicity. Therefore, it has been found that AgNPs show greater performance in groundwater compared to surface and brackish water due to their lower NOM content. Presence of anionic ligand (Cl$^-$) can drastically decrease the AgNPs activity since AgNPs tend to precipitate in AgCl form thus reducing their toxicity (X. Yang et al., 2014; H. Zhang et al., 2012). Antibacterial efficacy of AgNPs in seawater environment was the lowest compared to surface, brackish and groundwater due to the formation of large aggregates (H. Zhang et al., 2012). In

Tartanson et al.'s study (2014) presence of $CaCl_2$ inhibited the bactericidal effect of the material by 4 log due to the formation of AgCl aggregates. A study investigated the different ligands to reduce AgNP toxicity on nitrifying bacteria specified that ligands such as Cl^-, PO_4^{3-}, EDTA and S^{2-}, except the weak ligand SO_4^3, reduced AgNPs toxicity. Among those ligands, sulfide was found to be the most effective in controlling or reducing nanosilver toxicity by approximately 80% (Choi et al., 2009). Finally, Tan et al. (2018) investigated the effect of different salt solutions (NaCl, Na_2SO_4 or $NaNO_3$) on the electrochemical disinfection performance of AgNW-PAN/TPU membranes. Under an applied potential of 1.5V, an insignificant difference was found in inactivation rate between the salt solutions and sterile pure water. However, an increase in inactivation efficiencies for all three salt solutions was observed as the voltage was increased to 3.0V. The system with NaCl showed slightly higher inactivation efficiency than the others due to the presence of Cl^-. The concentration of Cl^- was found to decrease at 3.0V, while concentration of ClO_3^- increased. The high voltage promoted to form chlorine DBPs, which improved the electrochemical disinfection performance (Tan et al., 2018). Therefore, it can be said that voltage application increased the toxicity due to DBPs in the presence of Cl^- rather than a reduction observed due to the presence of ligands mentioned in other studies.

2.3.3. Silver release

Widespread research and the use of Ag raise a concern about the Ag release which may cause unwanted consequences for the environment and human health. In addition, it can reduce the lifetime of the antibacterial material. Ag is naturally found in groundwater, surface water or drinking water at a concentration above 5 ppb in the form of highly insoluble and immobile oxides, sulfides and some salts (WHO, 2011). WHO and USEPA specify the maximum Ag content in water and daily consumption as up to 0.1 mg/l (100 ppb) without risk to health (USEPA, 2018; WHO, 2011). The maximum daily intake of Ag for a 70 kg body was proposed as 2.85 µg/kg/day. Rosa

et al. (2016) evaluated the bioaccesibility of colloidal Ag and AgNPs. Colloidal Ag was reported to have higher bioaccesibility compared to AgNPs so that it would pose higher health risk after long-term exposure. It has been found that Ag release was higher in the gastric medium than in intestinal medium due to strongly acidic conditions. It has also been found that the larger Ag particle size lead to higher bioaccesibility. This study also revealed that the consequences of such bioaccumulation of Ag in the body appear only in long term. On the other hand, several studies investigating the toxicity of AgNPs discussed by Fewtrell (2014) did report no toxicity or relatively mild toxicity to human cells depending on the dose. LC_{50} value of AgNPs for mammalian cells in vitro was indicated as 11.3 mg/l (Bondarenko et al., 2013), which is much higher than the recommended limit value of 100 ppb.

Several studies conducted Ag release analysis to develop a novel material for POU disinfection. Table 2-2 provides silver release values obtained from these studies. It is seen that Ag values in the effluent change from one study to another due to different size of nanosilver, different chemicals used in nanosilver production, the stability of nanosilver changing with respect to the coating media type used, and different set-ups of the experiments as discussed in a review paper by Bondarenko et al. (2013). These studies mostly indicate the low Ag release compared to WHO's and USEPA's recommended limit. Thus, the Ag release is directly correlated with the life span of the materials containing nanosilver, which is investigated in a few studies. Based on the indicated Ag release amounts and rates, life-span of different materials varies from 50 liters (Tan et al., 2018) to a wide range of 30-130 liters (Dankovich et al., 2016) and even 148 liters (Hong et al., 2016a).

Ag release is found to increase with Ag content, as discussed in the literature (Hong et al., 2016a; Mpenyana-Monyatsi et al., 2012; Praveena et al., 2016; Tan et al., 2018).

Praveena et al. (2016) indicated that when Ag content on cellulose paper was above 0.451 mg/l, Ag concentration in the effluent was higher than the limit value. Size of the nanosilver also has an impact on Ag release (Dankovich and Gray, 2011; Mollahosseini et al., 2012). Mollahosseini et al. (2012) revealed that smaller AgNPs could be released from the polymeric matrix easier, as also discussed by Quang et al. (2013).

Voltage application is another factor affecting Ag release. Tan et al. (2018) showed that the silver release increases with the applied potential. For the AgNW-PAN/TPU membrane, the average Ag concentrations in effluent were 8.241 ± 5.041, 20.621 ± 6.320, and 29.391 ± 4.466 μg/l with applied voltages of 0, 1.5, and 3.0 V, respectively, in 10 cycles. A released Ag concentration of 70 ppb between applied potentials of 5-15V was reported, increasing to 94 ppb at 20V (Liu et al., 2013). Another study found that Ag concentrations were all below 15 ppb with applied voltages of 0-6 V (Wen et al., 2017).

Ag release also changes with time and volume. In a study conducted with AgNPs containing silica beads in column test (Quang et al., 2013), the Ag concentration in the effluent was not detectable after filtering 3 liters of clean water. Filtration of 12 liters of clean water increased Ag release to 0.04 mg/l, which became relatively constant in further filtration. Akhigbe et al. observed a decrease in Ag release as the flow rate increased since the residence time of the solution within the bed decreases (Akhigbe et al., 2016). However, *E. coli* removal breakthrough occurred earlier with an increase in the flow rate, decreasing the service life. It was indicated that the Ag release rate was higher in the first 10 minutes and then decreased with time (Mpenyana-Monyatsi et al., 2012). These results were in agreement with those of Tan et al. (2018) and Biswas and Bandyopadhyaya (2016).

Bacterial concentration might also affect the amount of Ag release. It was found by Quang et al. (2013) that Ag release is considerably higher when *E. coli* contaminated water is filtered compared to clean water. About 10^6 CFU/ml *E. coli* resulted in 0.01 mg/l and 0.17 mg/l after treating 0.5 liters and 2 liters water, respectively, which is much higher than results obtained by filtration of clean water as discussed earlier. This could be manipulated by Dankovich and Gray (2011) since Ag was taken up by the cells during filtration. Solution chemistry and other contaminants present in water also affect the Ag release due to Ag aggregation as discussed in the previous part (Section 2.3.2.5). Thus, Ag ion release in water conditions with high Cl^- and NOM content was found very small compared to deionized water (H. Zhang et al., 2012). On the other hand, presence of ammonium hydroxide (NH_4OH) was found to enhance Ag release due to the formation of a soluble silver-ammonia complex, whereas urea was found to reduce Ag ion release into the water (Quang et al., 2013). Acidic pH was also found to trigger the Ag release significantly as well as the PBS solution (Biswas and Bandyopadhyaya, 2016).

Surface modification is one of the approaches to control Ag release (J. Liu et al., 2010). According to a review paper by Tolaymat et al. (2010), sodium citrate is the most commonly used stabilizing agent followed by polyvinylpyrrolidone (PVP). Mikelonis et al. (2016) conducted a study with AgNPs on ceramic water filter with four different stabilizing agents, namely citrate, PVP, branched polyethyleneimine (BPEI) and casein. It has been found that citrate give the least Ag release results but also the least disinfection efficiency. Similarly, compared to membrane coated with PVP, the membrane without PVP showed a faster inhibitory effect and easier release of Ag ions (Beisl et al., 2019). H. Zhang (2012) conducted a comparative study with three different stabilizing agents including casein, dextrin and PVP in different water chemistries. In this study, it was proposed that PVP-stabilized AgNPs showed the highest colloidal stability followed by casein and dextrin, since nitrogen-containing PVP was more likely to bind on the surface of AgNPs than oxygen-containing dextrin.

Therefore, PVP-stabilized AgNPs was less likely to aggregate. H. Zhang (2012) also discussed that the three stabilizers did not show any toxicity and PVP considered as an environmentally friendly stabilizer. Nguyen et al. (2013) compared the toxicity of uncoated and coated AgNPs with PVP and citrate against two different mammalian cells. They revealed that although citrate coated AgNPs showed the least toxicity followed by PVP-coated and -uncoated AgNPs, it was observed that the uncoated AgNPs had significantly higher toxicity compared to coated AgNPs. However, AgNW-PAN/TPU material, without the top protective layer with electrospun nanofibers, increased the silver release by 5 times compared to the material with the top protective layer (Tan et al., 2018). Study with AgNW-carbon fiber cloth nanocomposites synthesized by UV curing adhesive indicated that UV curing adhesive could stabilize the AgNW on carbon cloth so that it significantly decrease the Ag release rate (Hong et al., 2016a).

CHAPTER 3

MATERIALS AND METHODS

This chapter covers the materials used in the experiments, methodology of the study, experimental set-ups (i.e. gravity filtration unit and filtration set-up with constant flow rate), all the methods, and experimental procedures and analyses in detail. Analytical methods are provided at the end of the chapter (Section 3.5).

3.1. Materials Used

The glass fiber filter (GF/A grade) used in the experiments was obtained from Whatmann^{TM}. The sheet diameter, thickness and mean pore size for the glass fiber (GF) filter are 150 mm, 0.26 mm and 1.6 μm, respectively. The calculated average grammage was 5.3 mg/cm^2.

Polyvnylpyrrolidone (PVP) (MW=55,000), ethylene glycol (EG), silver nitrate (AgNO$_3$) and sodium chloride (NaCl) used for AgNW synthesis were purchased from Sigma-Aldrich.

Nutrient Broth, Nutrient Agar, Luria-Bertani (LB) Agar and Mueller-Hinton (MH) Agar used for antibacterial tests were purchased from Merck. They were prepared as described in their product sheets. Ultra-pure water used throughout this study was obtained by MilliQ water purification system, Millipore.

3.2. Fabrication of AgNW-decorated Glass Fiber Filters

3.2.1. Synthesis of AgNW

AgNWs were synthesized via polyol method as described in Coskun et al.'s study (2011). This process is based on the reduction of an inorganic salt by a polyol at an elevated temperature. Here, ethylene glycol (EG) was used as both solvent and reducing agent, polyvinylpyrolidone (PVP) was used as a stabilizing agent and $AgNO_3$ was used as a Ag source. Following synthesis, the AgNWs were purified by washing several times with ethanol and centrifuging. Following purification, AgNWs were suspended in ethanol. A photo of AgNW suspension is provided in Figure 3-1.

Figure 3-1. A photograph of AgNW suspension.
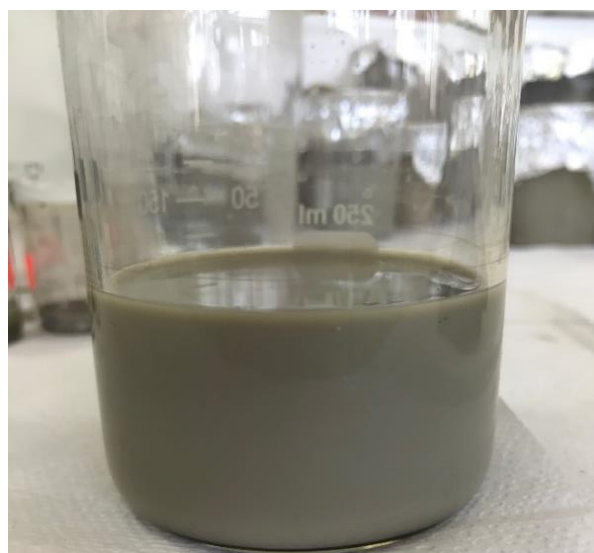
3.2.2. Fabrication of AgNW-decorated glass fiber filters

For the fabrication of AgNW-decorated glass fiber filters (AgNW-GF filters), a GF filter sheet was coated with AgNW via simple dip and dry method as shown schematically in Figure 3-2. First, a sheet of clean Whatmann^{TM} GF filter with 150 mm diameter was cleaned by immersing into absolute ethanol solution within an

ultrasonic cleaner for 5 minutes. Then, the GF filters were dried at 120 °C for 10 min. Synthesized AgNWs were dispersed in ethanol solution with a dilution ratio of 1/8. A cleaned sheet of GF filter was immersed into the diluted AgNW solution for 10 min; then, it was dried at 120 °C for 10 min. This procedure was repeated 4, 6 or 10 times in order to obtain different AgNW loadings. In order to produce control filters (bare GF filters with no AgNW loading); a sheet of GF filters was immersed in only ethanol solution (i.e. containing no synthesized AgNW) and dried under same conditions (120°C, 10 min). Prior to the experiments, each side of the AgNW-GF filters and control filters was kept under the UV-light for 30 min for both sterilization and removal of residual PVP.
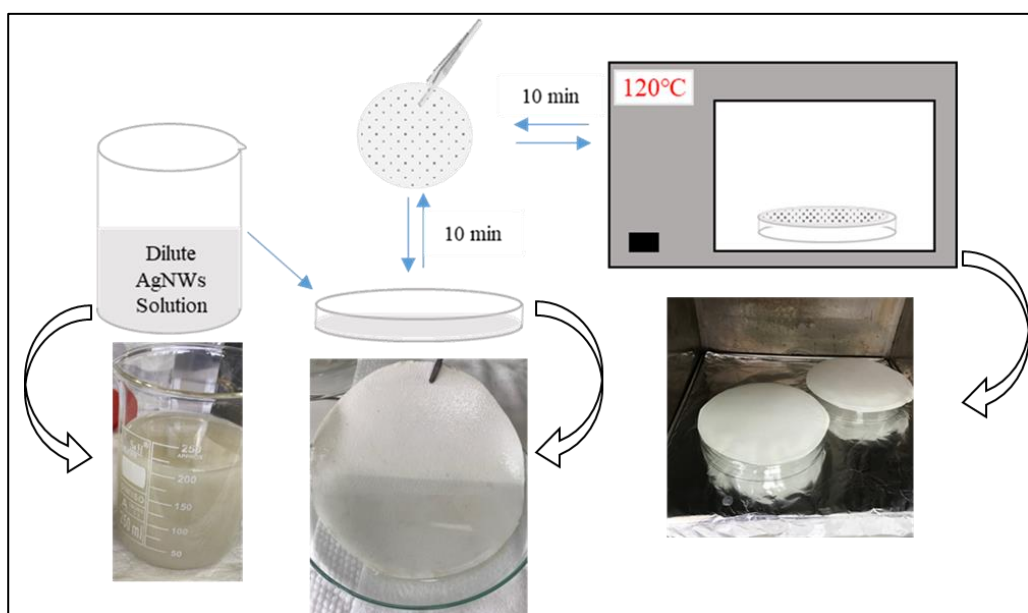

Figure 3-2. Coating of AgNWs on GF filters via simple dip-and-dry method

3.2.3. Methodology of AgNW-GF filters production

In order to develop an AgNW-GF filter for POU water disinfection, several sets of AgNW-GF filters were produced in sequence. The methodology of the production of AgNW-GF filters followed in this thesis is given in Figure 3-3. Based on that

methodology, each set of filter produced was initially investigated for its antibacterial performance by disk diffusion test and/or flow test (Figure 3-3). Mechanical durability of the produced filters for filtration process was another criterion for the improvement of the filters. Depending on the results of these tests, if required, the AgNW-GF filter production stage and the applied tests were improved. Accordingly, a new set of AgNW-GF filter was produced with the feedback from the previous set of production. This cyclic (or sequential) production lasted until the final set of AgNW-GF filters which are durable and have antibacterial effect. At the end, the final sets of AgNW-GF filters, namely, Group X and Group Y, were produced and used in further experiments/tests. Antibacterial tests and Ag release test results of Group X were also used to improve the production of Group Y AgNW-GF filters and experimental processes.
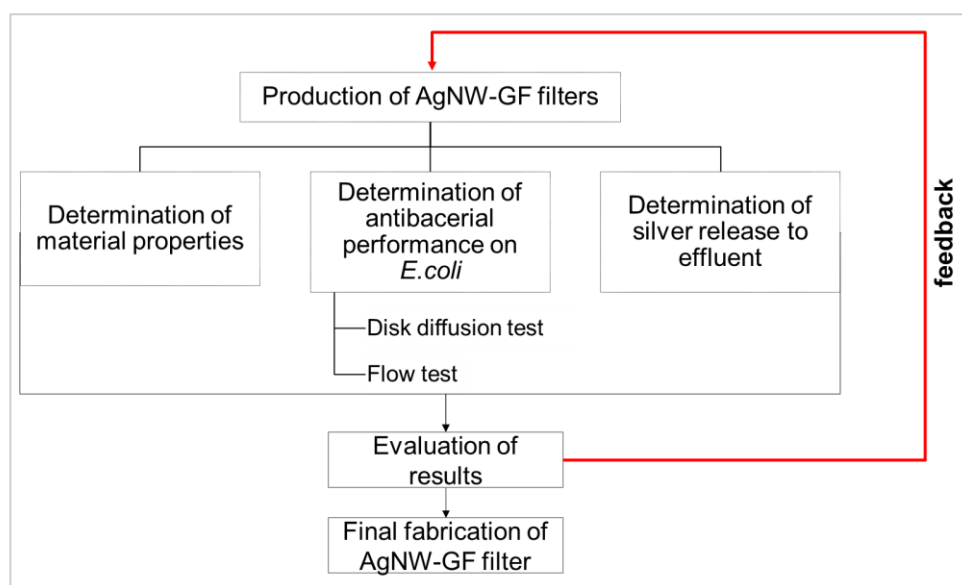

Figure 3-3. Methodology of AgNW-GF filter production

In the scope of the thesis, first, stand-alone AgNW foils were fabricated and used in the experiments. Stand-alone AgNW foils contained no supporting material as a scaffold but only Ag. The fabrication method of the stand-alone AgNW foils was

given in Appendix A. The mesh structure of AgNW webs was expected to provide the circulation of water within the foil and more contact with the bacteria. It was observed that the structure of stand-alone AgNW foils made the infiltration rate non-uniform due to nonhomogeneous pore sizes. Additionally, the developed stand-alone AgNW foils were very fragile and, thus, physically unstable to be used in POU water disinfection. Therefore, as a solution to physical instability, it was decided to produce another filter, this time with a scaffold, rather than stand-alone AgNW foils.

As an alternative to stand-alone AgNW foils, GF filter was chosen as a scaffold. GF filter was preferred since GF filters are more durable and flexible as it has high strength to weight ratio and resist to wide range of moisture, pH, temperature or chemical corrosives (Bauer and Manville, 2004). The mesh structure of GFs can provide the circulation and more contact due to its more defined and large pore structure. Therefore, the AgNW-GF filters to be produced might allow rapid gravity flow and provide low fouling affinity. The AgNW-GF filters to be produced would be also more economical compared to stand-alone AgNW foils due to the fact that the former has low scaffold material cost and lower amount of Ag is needed for coating. Therefore, AgNW-GF filters are likely to be more suitable for POU water disinfection.

Four sets of stand-alone AgNW foils and three sets of AgNW-GF filters were fabricated and tested until the fabrication of final AgNW-GF filters (Group X and Group Y). The results of these tests are discussed in the Results and Discussion Chapter (Section 4.1.1 and Section 4.1.2).

Group X and Group Y AgNW-GF filters were produced as final filters and tested for POU water disinfection according to the all methods given in the Experimental Procedures Section (Section 3.4).

In Group X, five sheets of AgNW-GF filters (X1-X5) were produced in order to investigate the effect of AgNW loading. Three of the five sheets, namely, X1, X2 and X3, were produced by 10 dip-and-dry cycles. The other two, X4 and X5, were produced by 6 and 4 dip-and-dry cycles, respectively.

In Group Y AgNW-GF filter production, four sheets of AgNW-GF filters were fabricated (Y1-Y4) in order to investigate the effect of AgNW loading. Two of the four sheets, namely, Y2 and Y3, were produced by 6 dip-and-dry cycles. The other two, Y1 and Y4, were produced by 4 and 10 dip-and-dry cycles, respectively.

The results obtained from the studies conducted with Group X and Group Y AgNW-GF filters are given and discussed in Section 4.2 and Section 4.3, respectively.

3.3. Experimental Set-Up

One of the experiments performed to determine *E. coli* removal efficiency of AgNW-GF filters was flow test. It is required for flow tests to be performed under gravity in order to simulate energy-efficient POU water disinfection unit. Gravity flow also provides higher contact time than typical vacuum filtration. At the very beginning of the experiments, it was realized that typical vacuum filters were not suitable for gravity flow and resulted in leakage, which would have misled the results. Therefore, two different filtration set-ups were designed for flow test using gravity filtration. These experimental set-ups are discussed in the following sections.

3.3.1. Gravity filtration unit

Gravity filtration unit (Figure 3-4) was designed for the flow test experiments. Flow tests for Group X AgNW-GF filters were conducted with gravity filtration unit.

The unit consists of two separate glass funnels connected with Teflon plates and screws. In order to prevent leakage during gravity filtration, an O-ring was placed between two Teflon plates. In the unit, there was a 3 cm-diameter por-2 glass filter. While using the unit, the fabricated AgNW-GF filters were placed on the por-2 glass filter between the Teflon plates and the plates were closed by the screws. All materials used in the unit were initially sterilized. During the flow tests, it was observed that water can flow through the filters with gravity and no leakage occurs during the process. However, it was also observed that the flow rate cannot be controlled in this gravity filtration unit.
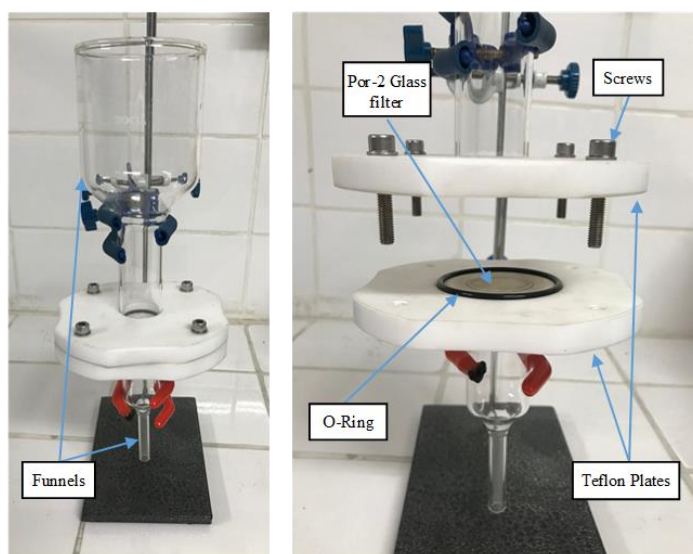
Figure 3-4. Photos of the gravity filtration unit used in the experiments.

3.3.2. Filtration set-up with constant inflow rate

Flow tests for Group Y AgNW-GF filters were conducted at constant flow rate with the set-up shown in Figure 3-5. In order to adjust constant flow rate during the flow tests, a peristaltic pump (Masterflex L/S) was used. The pump transmits the water through the AgNW-GF filters at an adjusted flow rate. AgNW-GF filters were placed into Millipore bacteriological field monitor filter cassette with 37 mm-diameter

(Figure 3-5 a, b). The filtered water was collected in the effluent erlen. All materials used in this system were initially sterilized.
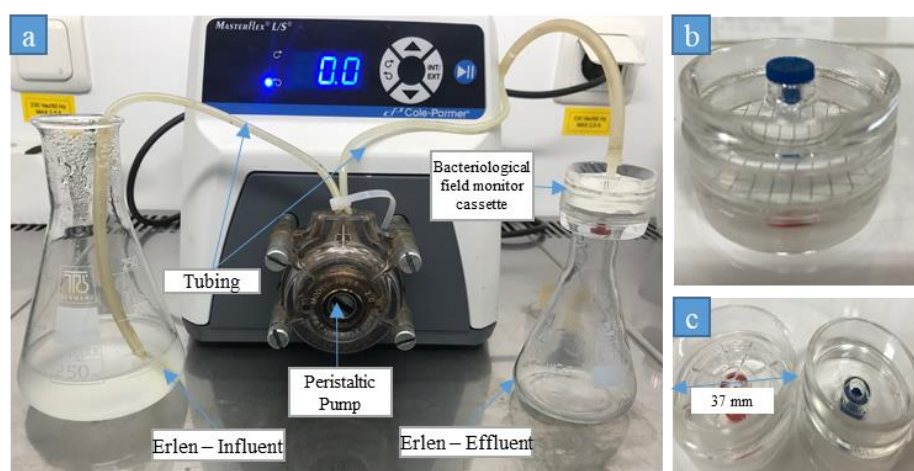
Figure 3-5. Photos of the filtration set-up with peristaltic pump (a) and Millipore bacteriological field monitor filter cassette (b, c)

3.4. Experimental Procedures

Experiments given in this section were conducted for the final AgNW-GF filters, namely, Group X and Group Y AgNW-GF filters. In order to understand the performance of AgNW-GF filters, experiments were performed in three main experimental steps, which are 1) characterization of the fabricated AgNW-GF filters, 2) antibacterial testing and 3) Ag release analyses. In this section, procedures of these main experiments are given.

3.4.1. Characterization of AgNW-GF filters

In order to understand the structure of the Group X and Group Y AgNW-GF filters, SEM analyses using FEI NOVA NANO SEM 430 microscope (FEI, Hillsboro, OR)

were performed in METU, Department of Metallurgical and Materials Engineering. A thin gold layer (5–10 nm) was deposited onto the fabrics prior to SEM analysis.

Electrical resistance (ohm/sq) of each Group X and Group Y AgNW-GF filter was also measured and recorded. Resistance was measured at 10 different points for both sides of the AgNWs-GF filters using resistivity probe (Signatone) connected to a Keithley 2400 SourceMeter. The average values with standard deviations are reported in corresponding figures and tables.

In order to understand the exact Ag amount (i.e. Ag loading) coated on AgNW-GF filter, Group X and Group Y AgNW-GF filters were analyzed via inductively coupled plasma mass spectrometry (ICP-MS) by METU Central Laboratory.

Characterization of synthesized AgNW, which were used for coating of Group Y AgNW-GF filters, was also performed in terms of length distribution, absorption spectra and concentration analysis. Length distribution of synthesized AgNW was evaluated via ImageJ software using SEM images. The optical properties (absorption spectra) of AgNW solutions, which were used for coating of GF filters, were analyzed by UV-Visible absorption spectrophotometer (HACH Lange DR39000) over the wavelength range of 320-800 nm. Concentration of AgNW in ethanol solutions was recorded via Exstar SII TG/DTA 7300.

3.4.2. Antibacterial testing

The antibacterial property of AgNW-GF filters and control GF filters were tested against gram-negative *E. coli*. The reason of selecting *E. coli* in this thesis is that *E. coli* is one of the most important indicator organisms and well represents the fecal

contamination in water (Okafor, 2011; Pepper et al., 2015; Percival et al., 2013). In order to investigate antibacterial effect, disk diffusion tests and flow tests were conducted as given below. Mentioned antibacterial tests were conducted in a laminar flow cabinet (NÜVE MN090) in order to obtain sterile environment unless otherwise specified.

3.4.2.1. Disk diffusion test

In order to evaluate the effect of both bacterial concentration and AgNW loading on antibacterial property of the fabricated AgNW-GF filters, disk diffusion tests were conducted, initially. If AgNW-GF filters have antibacterial property, it is expected to see a circular zone at which no growth is visible around the filter (i.e. free of bacterial growth). This clear zone is defined as inhibition zone.

Disk diffusion tests performed for the initially produced filters (the ones produced before Group X and Group Y AgNW-GF filters) were conducted with nutrient agar, LB agar and MH agar. For disk diffusion tests in Group X and Group Y AgNW-GF filters, MH agar was used as a culture medium. In these tests, initially, the selected agar medium was poured on plastic sterilized Petri dishes and then solidified. Disk diffusion test was performed by uniformly spreading 100 microliters of *E. coli* solution ($\sim 10^5$, 10^7 and 10^9) over the agar medium in petri dishes. One cm diameter of circular bare GF filter piece (as control) and AgNW-GF filter pieces with different AgNW loadings were placed over the agar gel. Petri dishes were incubated at 37 °C for 24 h. After the incubation period, the diameter of the inhibition zone developed around the pieces was measured with a ruler. The correlation of antibacterial performance of AgNW-GF filters with both AgNW loading and *E. coli* concentration were simply calculated by Pearson correlation coefficient factor (r). Although correlation analysis does not determine cause and effect because of other variables influencing the results, the factor establishes possible connections between variables (djs research, 2019). The

correlation factors were calculated via Microsoft Excel 2016 (Microsoft Corporation, Washington, USA).

3.4.2.2. Flow test

In order to investigate *E. coli* removal efficiency of the AgNW-GF filters from water, flow tests were conducted. To this purpose, four cm diameter of circular AgNW-GF filter pieces were placed into the gravity filtration unit (Figure 3-4) and the bacteriological field monitor filter cassette (Figure 3-5) for Group X and Group Y AgNW-GF filters, respectively. Overnight growth *E. coli* solution was initially centrifuged at 2500xg for 10 min. Then, the centrifuge were re-suspended with PBS and diluted with ultra-pure water (Milli-Q water) to represent the model-contaminated water (*E. coli*-contaminated water). A-100-ml of this model-contaminated water was passed through an AgNW-GF filter via gravity filtration unit or filtration set-up with constant inflow rate. The viable *E. coli* amount in the influent water and effluent water (filtrate) was counted by spread plate method (Section 3.5.3). The removal efficiency was calculated as given in Equation 1.

$$\text{Removal efficiency (\%)} = \frac{\text{Influent } E.coli \text{ (CFU/ml)} - \text{Effluent } E.coli \text{ (CFU/ml)}}{\text{Influent } E.coli \text{ (CFU/ml)}} * 100 \qquad (1)$$

The effects of flow rate, AgNW loading and *E. coli* concentration on removal efficiency were investigated via flow tests for Group Y AgNW-GF filters. Initially, the effect of flow rate was investigated. The flow rate, resulting in the highest removal efficiency was used in the following flow tests. Then, the optimal AgNW loading resulting in the highest removal efficiency was determined and used in the following flow tests. Finally, the influent *E. coli* concentration at which the AgNW-GF filters perform with the highest efficiency was investigated. All these tests were performed

in duplicate and the average values of the results (as % removal and log removal) are reported. In order to assess the correlation of antibacterial performance of AgNW-GF filters with flow rate, AgNW loading and *E. coli* concentration, Pearson correlation coefficient factors (r) were calculated (via Microsoft Excel 2016).

For the effect of flow rate on removal efficiency, flow tests were performed with the flow rates of 1, 2.5 and 5 ml/min. The *E. coli* concentration and AgNW loading were set as 10^8 CFU/ml and 4.49 mg/g, respectively, for all flow rates studied. These values used were selected according to literature given in Table 2-2.

For the effect of AgNW loading on removal efficiency, flow tests were performed with the AgNW loadings of 0.95, 4.8 and 9.9 mg/g (Table 2-2). The *E. coli* concentration and flow rate were set as 10^8 CFU/ml and 1 ml/min, respectively, for all AgNW loadings studied.

For the effect of *E. coli* concentration on removal efficiency, flow tests were performed with *E. coli* concentration of 10^3, 10^5, and 10^8 CFU/ml (Table 2-2). The AgNW loading and flow rate were 9.9 mg/g and 1 ml/min, respectively, for all *E. coli* concentrations studied.

Finally, it was aimed to investigate how the two-stage serial filtration application of AgNW-GF filters will improve the *E. coli* removal from water. To this purpose, the flow test was conducted with two similar Y4 AgNW-GF filters. The model *E. coli* solution was first filtered through an AgNW-GF filter; then the collected filtrate was passed through a second AgNW-GF filter. In this study, as flow rate, AgNW loading and *E. coli* concentration, the predetermined optimum values resulting in the highest removal efficiency were used. In other words, the flow rate, AgNW loading and the

50

influent *E. coli* concentration were set as 1 ml/min, 9.9 mg/g and 10^3 CFU/ml, respectively.

3.4.3. Determination of silver release from AgNW-GF filters

In order to investigate the trends in Ag release from the AgNW-GF filters, Ag release analyses were conducted for the effluents of each flow test performed with different flow rates, AgNW loadings and *E. coli* concentrations. The tests were performed in duplicate and the average values of the results are reported. The released Ag concentrations were analyzed via ICP-MS in METU Central Laboratory.

Ag release analysis was also conducted in order to investigate the effect of volume of filtrate on Ag release in long-term operation. One-liter of ultra-pure water was passed through the AgNW-GF filter with AgNW loading of 9.9 mg/g. The flow rate was adjusted to 1 ml/min. Filtrate samples were collected at each 100 ml filtered for the analysis of amount of Ag released .

3.5. Analytical Methods

3.5.1. Preparation of standard *E. coli* solution

Gram-negative *E. coli*, which was isolated from chicken manure, was obtained from Assoc. Prof. Dr. Yesim Soyer's Lab in METU, Food Engineering Department and used in the tests performed with Group X and Group Y AgNW-GF filters. For the initially produced filters (the ones produced before Group X and Group Y), the *E. coli* that was isolated from the wastewater of METU WWTP was used in the tests.

To cultivate the fresh bacteria (*E. coli*), streak plate method on EMB agar (Figure 3-6 in Section 3.5.4) was conducted once a week. EMB agar is a selective culture medium, which inhibits the growth of Gram-positive bacteria, yet let the Gram-negative bacteria grow on the agar. EMB agar allows differentiating *E. coli* from the others visually. *E. coli* cultures are observed as metallic green sheen on EMB agar.

To prepare standard *E. coli* culture, a colony of *E. coli* from EMB agar was added into 100 ml of nutrient broth solution autoclaved at 121°C for 15 min. The suspension was incubated overnight (18 h) in a shaker incubator at 37 °C (18 h) and 160 rpm.

3.5.2. OD calibration curve

OD calibration curve was obtained to estimate initial *E. coli* concentration. The exact number of *E. coli* of prepared standard solution was initially counted by spread plate method (Section 3.5.3). Afterwards, the standard solution was diluted by factors of 1/2, 1/4, 1/8, 1/16, 1/5, 2/5, 3/5, 4/5, 1/10, 3/10, 9/10, 1/100. Absorbance of the diluted solutions was measured at 600 nm by UV-vis spectrophotometry. Counted viable cells were multiplied with these factors. Finally, absorbance vs. number of colony count graph was obtained. The formula on the linear part of graph was used to estimate the initial *E. coli* concentration of the solution. OD calibration curve and related data are given in Appendix B.

3.5.3. Spread plate method

Spread plate method can be used in many antimicrobial tests for quantitative analysis of viable cells (Collins, Lyne, Grange, & Falkinham, 2004). This method was performed as described in Standard Method 9215C (APHA, 1999). In this method, the samples collected for spread plate method analysis are first subjected to serial dilutions. Then, 0.1 ml of appropriately diluted culture is homogeneously spread on

the surface of nutrient agar plate using a sterile glass L-spreader. After the plates are incubated at 37°C for 24 hr, the number of visible colonies is counted (Madigan et al., 2012). The total number of viable cells is calculated by the formula given in Equation 2. In this thesis, whenever the plating was done, it was performed duplicate. The experiments were conducted in a sterile environment in a laminar flow cabinet.

$$\text{Total number of } E.\,coli(\text{CFU/ml}) = \frac{\sum_{i=1}^{n} \frac{\text{mean bacteria count(i)}}{\text{Dilution factor}}}{0.1*n} \tag{2}$$

3.5.4. Streak plate method

Streak plate method, which is also known as looping-out method, is easy and quick method to obtain pure culture. A loopful of *E. coli* was initially spread on the part A of nutrient agar or EMB agar (Figure 3-6). Then, the loop was flamed and spread again from part A to part B with the parallel streaks and so on. The method was conducted in aseptically sterile conditions.
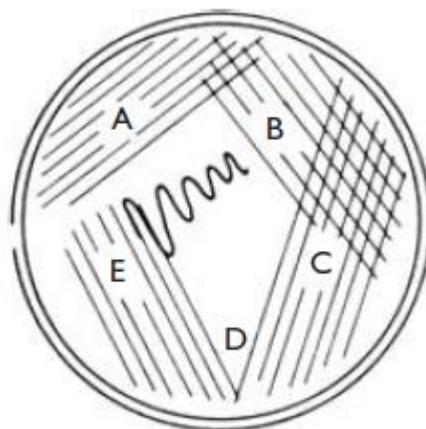

Figure 3-6. Streak-plate method (Collins et al., 2004)

3.5.5. Fixation method for SEM analysis

SEM analyses were performed usually to investigate the bacterial attachment on the AgNW-GF filters after flow tests. In order to analyze the AgNW-GF filters via SEM, a fixation method mentioned by Doganay et al. (2019) was used. This method is known to prevent deformation of the *E. coli* containing filters due to vacuum and voltage applications. In this method, each AgNW-GF filter used is initially immersed into a 2.5% glutaraldehyde solution in PBS for 30 min, which is followed by the immersion into graded ethanol series (60, 70, 80, 90 and 100% ethanol/PBS solutions) for 10 min each. After fixation, SEM analyses were performed as previously described in Section 3.4.1.

3.5.6. Silver analyses

Ag analyses were performed in order to determine the Ag concentration both on AgNW-GF filters and in the filtrate. In order to examine the Ag loading of AgNW-GF filters, pieces punched from produced sheet of AgNW-GF filters were first analyzed. Four circular AgNW-GF pieces with 1 cm diameter were punched from different locations of the AgNW-GF filter sheet. Then, 2 pieces were digested together in 30% HNO_3 solution. The remaining 2 pieces were also digested together in another dilute HNO_3 solution. At the end, there were two samples to analyze AgNW loading of a sheet of AgNW-GF filters. The liquid samples were analyzed as soon as possible. The average values are reported in corresponding figures and tables.

In order to determine Ag release from AgNW-GF filters into the filtrate, the filtrates of the flow tests were collected. The filtrate samples were stored in falcon tubes at pH<2 in order to prevent Ag aggregation. pH values of the samples were reduced below 2 by several drops of HNO_3. The samples were analyzed as soon as possible.

As previously mentioned (Section 3.4.3), all analyses were conducted in METU Central Laboratory via ICP-MS.

CHAPTER 4

RESULTS AND DISCUSSION

In order to develop an AgNW-GF filter for POU water disinfection, four sets of stand-alone AgNW foils and three sets of AgNW-GF filters are produced and tested initially until the final sets of AgNW-GF filter production (Group X and Group Y). The results of these preliminary production studies, which form the basis of Group X and Group Y AgNW-GF filters, are briefly discussed in Section 4.1.1 and Section 4.1.2. Later on, results of the studies conducted with Group X and Group Y AgNW-GF filters are given and discussed in Section 4.2 and Section 4.3, respectively.

4.1. Preliminary Fabricated Stand-alone AgNW foils and AgNW-GF Filters

4.1.1. Stand-alone AgNW foils

In the scope of the thesis, first, stand-alone AgNW foils (Figure 4-1, a) were produced as POU filter. The first observations were that stand-alone AgNW foils were very fragile. Additionally, autoclaving for sterilization at 121°C for 20 min led to the dispersion/deformation of the foils. Therefore, for the following productions, it was decided that the foils should be sterilized via UV.

Figure 4-1 (b) shows the SEM image and the structure of the stand-alone AgNW foil. It was observed that AgNW foil has nonhomogeneous web-like porous structure. The web-like porous structure of AgNWs might have provided better circulation of water within the foil and, thus, more contact of bacterial solution with AgNW.
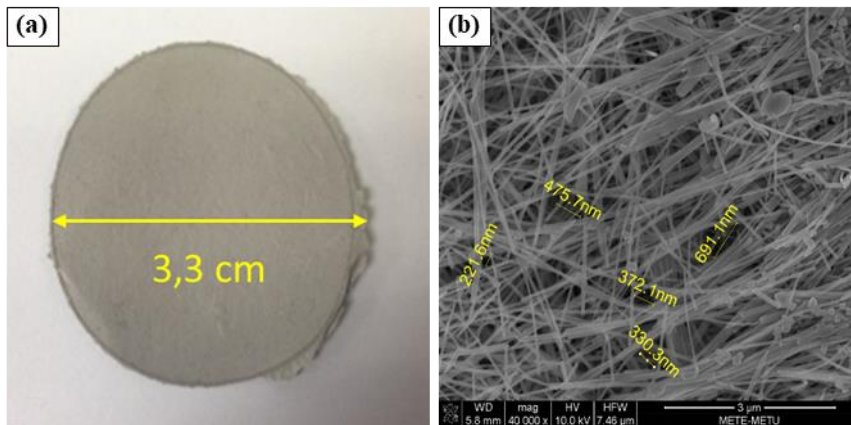
Figure 4-1. Stand-alone AgNW foils photo (a) and SEM image (b)

Stand-alone AgNW foil, which was used in the flow test and thus in contact with the *E. coli* solution, was incubated on nutrient agar for 24 hours at 37 ° C and it was observed that there was bacterial growth on the foil. This was an unexpected result for nanosilver since it has well-known antibacterial effect and, thus, stand-alone AgNW foil would also have. This was attributed to the presence of residual PVP on foils (Coskun et al., 2011). AgNW foils have PVP and that residual PVP might have reduced the contact surface between Ag and bacteria (Bayraktar et al., 2019). According to Jones et al. (2018), PVP is not required to synthesize AgNWs, but it is beneficial for prevention of aggregation (i.e. uniformity) of the synthesized AgNWs. Thus, it was decided to decrease residual PVP for the further productions.

4.1.2. AgNW-GF filters

AgNW-GF filters have more defined and larger pore structure than stand-alone AgNW foils. The web-like structure of AgNW-GF filters, as it is the case in the stand-alone AgNW foils, could provide more circulation and contact due to the structure of both GFs and AgNW. In addition, AgNW-GF filters were found to be more durable than stand-alone AgNW foils for POU water disinfection. Besides, for having a scaffold,

they are more economical compared to AgNW foils. Thus, they are more suitable to be used in POU water disinfection studies.

Figure 4-2 shows the pictures and SEM images of both bare GF filters and AgNW-GF filters. AgNW decorated onto GFs can be seen in Figure 4-2 (d).
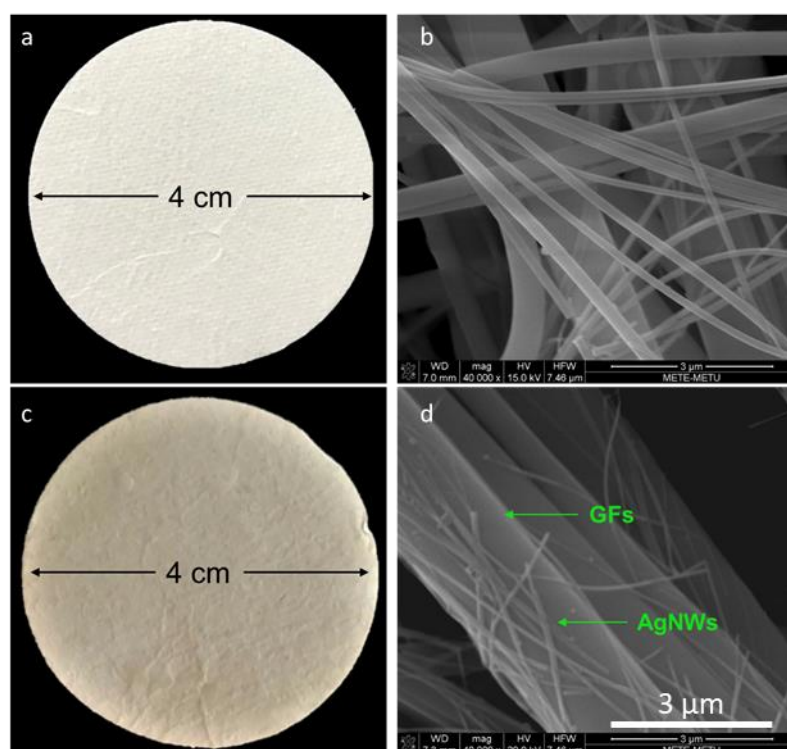

Figure 4-2. A photo of bare GF filter (a), SEM image of bare GF filter (b), a photo of AgNW-GF filter (c), and SEM image of AgNW-GF filter (d)

Three sets of AgNW-GF filters were produced in the scope of the preliminary production studies. Results and speculations obtained from each set were used to improve the subsequent AgNW-GF filter production and experimental procedures. When a stand-alone AgNW foil and a AgNW-GF filter were compared by disk diffusion test, it was observed that the antibacterial effect of AgNW-GF filters on *E. coli* was same as or even better than that of the foil (Appendix C, Figure C1). However,

disk diffusion tests performed for the subsequently produced AgNW-GF filter sets had inconsistent results. Besides, they were not repeatable. An inhibition zone or fuzzy zone was observed on some of the disk diffusion tests whereas it was not observed on other disk diffusion tests conducted with AgNW-GF filters (Appendix C, Figure C2).

Figure 4-3 represents a typical fuzzy zone on agar. According to Tendencia (2004), fuzzy zones might be observed with mixed bacterial cultures that are used in disk diffusion tests. Therefore, fuzzy zones observed with AgNW-GF filters might have been due to the presence of mixed bacterial culture, i.e. contamination, during the disk diffusion tests. EUCAST (2019) suggests to check for purity in case of fuzzy zones. For this purpose, a loop of culture taken from inner and outer parts of the fuzzy zones was incubated on EMB agar. All cultures grown on EMB agar were observed as metallic green sheen, which is a characteristic for *E. coli* as mentioned in Section 3.4.4.1. It was concluded that bacteria utilized in these experiments was pure *E. coli* culture (data not shown), unlike Tendecia (2004) suggested.
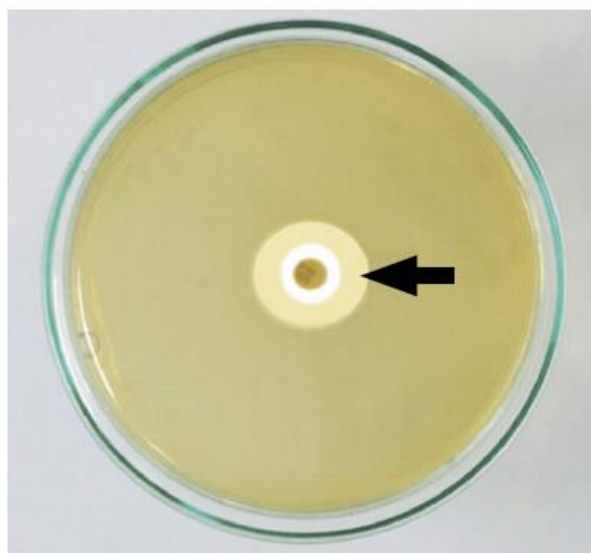

Figure 4-3. Fuzzy zone on agar (Tendencia, 2004).

Another reason of fuzzy zones and inconsistent results obtained from disk diffusion tests could be non-homogeneity of the AgNW-GF filters. It was thought that the AgNW might not have been impregnated homogeneously on the GF filter. Therefore, the pieces taken from the different regions of the AgNW-GF filter sheets were used for the disk diffusion test. However, results did not change, and still fuzzy zones or no inhibition zones were observed (data not shown). Thus, it was speculated that the reason of fuzzy zones and inconsistent results was not caused by non-homogeneity of impregnated AgNW on the filters.

The other possibility of observing unrepeatable results, fuzzy and even no inhibition zones during disk diffusion tests was related to the bacterial resistance against Ag. *E. coli*, which was used for the tests until that time, was isolated from wastewater taken from WWTP in METU. Wastewater from the university may contain Ag compounds since wastewater from laboratories, where studies with Ag are conducted, is also discharged to this WWTP. In addition, with the increase in use/application of nanosilver-containing products, it is known that nanosilver is being released into the wastewater treatment systems (Guo et al., 2019). Therefore, microbial community in the wastewater (e.g. *E. coli*) can evolve a resistance against Ag (Graves et al., 2015; Guo et al., 2019; Panáček et al., 2018; Randall, Gupta, Jackson, Busse, & O'Neill, 2014) occurring by genomic changes. In order to investigate if there is any *E. coli* resistance to Ag, a new isolation source was tried; *E. coli* was obtained from chicken manure. However, the unclear results still did not change with the new isolation source. Therefore, it could not be concluded that the previous *E. coli* source was resistant to Ag. Nevertheless, due to the possibility of the Ag resistivity, it was decided to use the *E. coli* culture isolated from chicken manure for the further studies.

The other possibility of not observing consistent inhibition zones might be attributed to the ineffective dissolution of AgNW on nutrient agar (Schoen et al., 2010). Physico-

61

chemical composition of the agar gel could influence the Ag ion release as well as the ion diffusion (Zaporojtchenko et al., 2006). Therefore, disk diffusion test was performed this time with different agar mediums, namely, Luria-Bertani (LB) agar and Mueller-hinton (MH) agar, in addition to the nutrient agar, which was used in previous tests. The composition of the agar mediums is given in Table 4-1. Nutrient agar contains peptone and meat extract while LB agar is composed of Tryptone, yeast extract and NaCl. MH agar contains meat infusion, casein hydrolysate and starch.

Table 4-1. *Agar medium compositions*

Agar medium	Composition (g/L)
Nutrient agar	Peptone (5.0), Meat extract (3.0), Agar-agar (12.0)
Luria-Bertani agar (LB agar)	Tryptone (10.0), Yeast extract (5.0), NaCl (5.0), Agar-agar (15.0)
Mueller-hinton agar (MH agar)	Meat infusion (2.0), Casein hydrolysate (17.5), starch (1.5), Agar-agar (13.0)

The results of disk diffusion tests performed with three different agar mediums are shown in Figure 4-4. As seen in Figure 4-4a and 4-4b, clear inhibition zones were not observed in the tests conducted with the nutrient agar and LB agar, respectively. Schoen et al. (2010) attributed the reason of not observing inhibition zones to very little Ag dissolution on the agar from the AgNW film. However, they did not specify the type and/or content of the agar medium that they used in their experiments and its potential effect on Ag dissolution. MH agar, on the other hand, resulted in perfectly clear inhibition zones (Figure 4-4c). Similarly, Zaporojtchenko et al. (2006) observed higher inhibition zone of Ag-Au coatings on polytetrafluorethylene (PTFE) in MH agar than that in LB agar. It was speculated in this thesis that the composition of the agar medium might have affected the antibacterial performance of nanosilver. For example, one of the components of agar medium may result in higher dissolution of

Ag in MH agar. Johnston et al. (2018) compared the Ag ion release from AgNPs in MH broth and LB broth. They observed that the total percentage of Ag ion release in LB broth was lower than that in MH broth. They also found that soluble starch and yeast extract are the two major components contributing to Ag release among others in MH and LB broth, respectively (Johnston et al., 2018). In addition, starch in the MH agar also acts as a colloid that absorb toxins produced by bacteria, so that they cannot interfere with the antibacterial agents (Hardy Diagnostics, 2019) and probably become more prone to the Ag compound. Literature shows that there are still unknowns regarding this topic in the field to be researched. Nevertheless, the agar content is likely to be the main factor resulting in higher and more clear inhibition effect of Ag. The disk diffusion test results revealed that the inconsistent inhibition zones and/or fuzzy zones observed so far were due to the agar medium type used. Among three different agar types used (nutrient, LB and MH agar), MH agar was the most appropriate for disk diffusion test and, thus, a better indicator for inhibition effect of AgNW-GF filters.
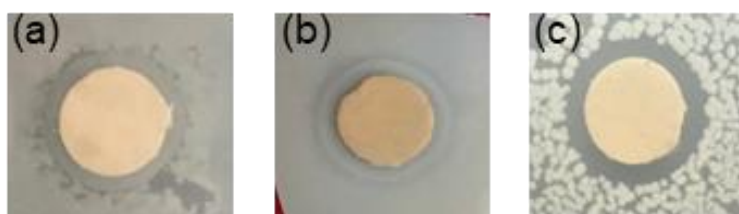

Figure 4-4. Inhibition zones on nutrient agar (a), LB agar (b) and MH agar (c)

After disk diffusion tests, a flow test was also performed for AgNW-GF filter. *E. coli* solution with a concentration of 10^6 CFU/mL was infiltrated through an AgNW-GF filter via gravity filtration unit. The average flow rate was 8.8 mL/min. Bacteria concentration in the inlet water and filtrate was analyzed by viable cell count method. Removal efficiency was found to be 15%. This value is very low compared to the

literature, where efficiencies of more than 90% were achieved (Table 2-2). This might be due to the effect of flow rate, influent *E. coli* concentration, AgNW loading and/or amount of Ag release. These parameters, therefore, were investigated in the following AgNW-GF filter productions

4.2. AgNW-GF Filters – Group X

4.2.1. Characterization of Group X AgNW-GF filters

In Group X, five sheets of AgNW-GF filters (X1-X5) were produced. Each has different AgNW loading and electrical resistance as shown in Table 4-2. The highest AgNW loading belonged to X1 (21.74 mg/g). Although X2 and X3 were produced by 10 dip-and-dry cycles as X1, their AgNW loadings were lower as 17.13 mg/g and 16.77 mg/g, respectively. Nevertheless, 10 dip-and-dry cycles resulted in higher AgNW loadings compared to X3 and X4. AgNW loading of X4 was 11.32 mg/g. Even in the non-conductive X5 AgNW-GF filter sheet, AgNW loading was found as 5.81 mg/g. Expectedly, as dip-and-dry cycle decreased, AgNW loading on the GF filter also decreased and electrical resistance increased.

Table 4-2. *Characterization of AgNW-GF filters – Group X.*

AgNW-GF filter sheet	Dip-and-dry cycle	AgNW loading (mg/g)	AgNW loading (wt.%)	Electrical resistance (ohm/sq)
X1	10	21.74	2.17	15.74 ± 4.34
X2	10	17.13	1.71	21.74 ± 5.75
X3	10	16.77	1.68	36.21 ± 9.54
X4	6	11.32	1.13	1245.84 ± 615.85
X5	4	5.81	0.5	Non-conductive

The SEM images of Group X AgNW-GF filters are shown in Figure 4-5. Web-like structure of both AgNW and GFs are clearly seen in the figure. Due to this web-like

structure, pores are non-uniform. As AgNW loading of the AgNW-GF filters increases, the AgNW around the GFs becomes more dense as seen in Figure 4-5.
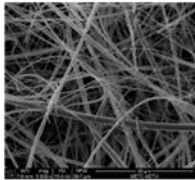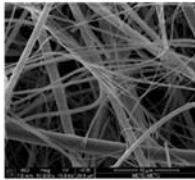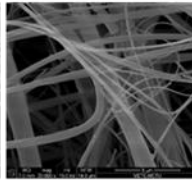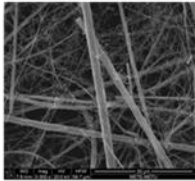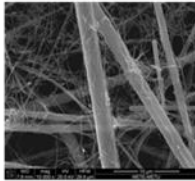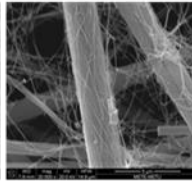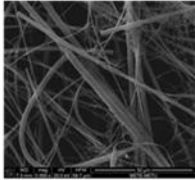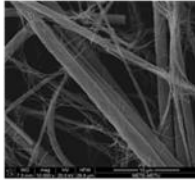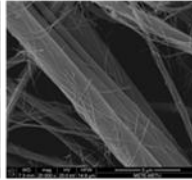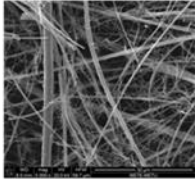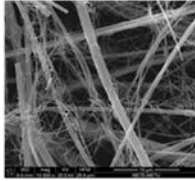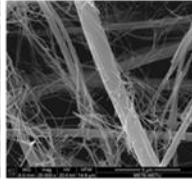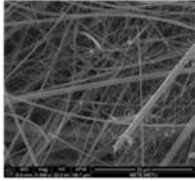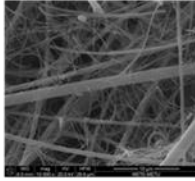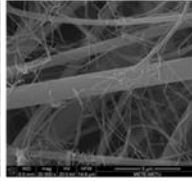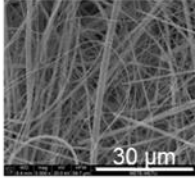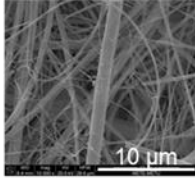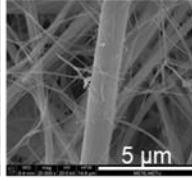
	AgNW Loading (mg/g)	SEM Magnification		
		x5000	x10000	x20000
Control	0			
X1	21.74			
X2	17.13			
X3	16.77			
X4	11.32			
X5	5.81			

Figure 4-5. SEM images of AgNW-GF filters – Group X

4.2.2. Antibacterial testing of Group X AgNW-GF filters

4.2.2.1. Disk diffusion test results of Group X AgNW-GF filters

Figure 4-6 shows the results obtained from disk diffusion test conducted with Group X AgNW-GF filters. The test was conducted for three different *E. coli* concentration and five AgNW-GF filters having different AgNW loadings (X1-X5). The results are given in Figure 4-6 and in Appendix D (Table D1). Overall, the diameters of inhibition zones of AgNW-GF filters were found to change between 1.1 – 1.4 cm. Control (bare) GF filters did not show any inhibition zone diameter. This indicated that control GF filters have no antibacterial effects while Group X AgNW-GF filters have.
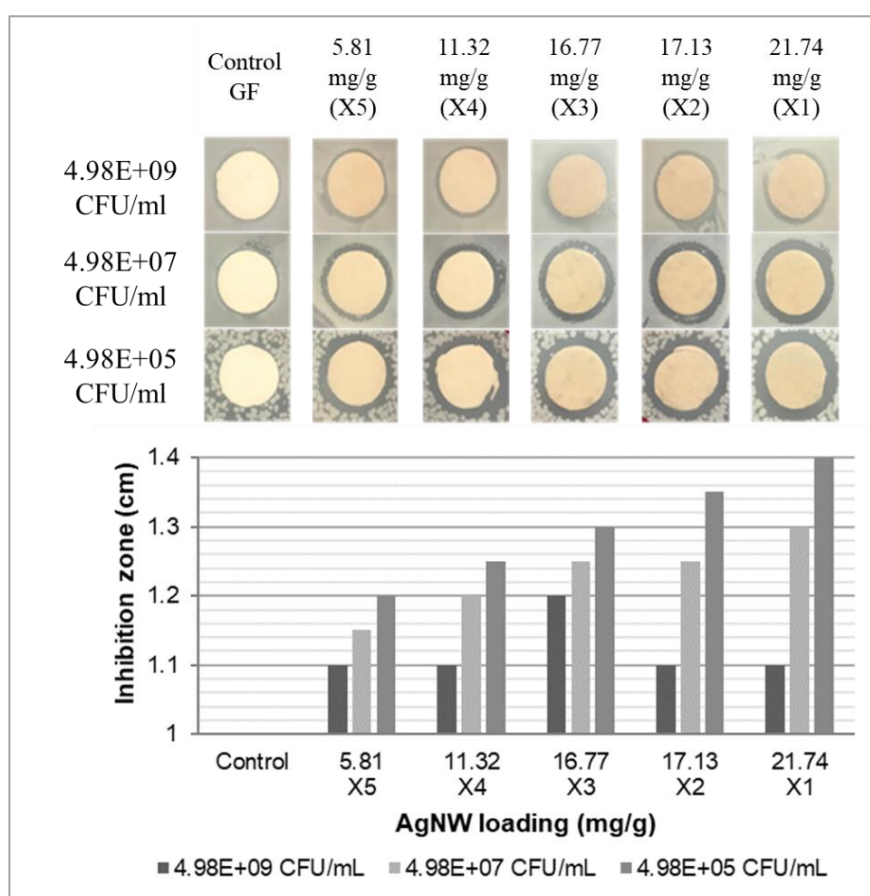
Figure 4-6. Disk diffusion test results of Group X AgNW-GF filters

AgNW-GF filter (X1) having a Ag concentration of 21.74 mg/g shows 1.1 cm, 1.2 cm, and 1.4 cm inhibition zone diameters for 4.98E+09 CFU/mL, 4.98E+07 CFU/mL and 4.98E+05 CFU/mL, respectively. For AgNW-GF filter (X2) having a Ag concentration of 17.13 mg/g, the inhibition zone diameters were measured as 1.1 cm, 1.25 cm, and 1.35 cm for 4.98E+09 CFU/mL, 4.98E+07 CFU/mL and 4.98E+05 CFU/mL, respectively. For AgNW-GF filter (X3) having a Ag concentration of 16.77 mg/g, the inhibition zone diameters were observed as 1.2 cm, 1.25 cm, and 1.3 cm for 4.98E+09 CFU/mL, 4.98E+07 CFU/mL and 4.98E+05 CFU/mL, respectively. AgNW-GF filter (X4) having a Ag concentration of 11.32 mg/g was the one with fabricated through six dip-and-dry cycles. The inhibition zones for X4 were measured as 1.1, 1.2 cm, and 1.25 cm for 4.98E+09 CFU/mL, 4.98E+07 CFU/mL and 4.98E+05 CFU/mL, respectively. Finally, the lowest Ag concentration was 5.81 mg/g due to four dip-and-dry cycles. The results for this filter (X5) having the lowest Ag concentration were 1.1, 1.15 cm, and 1.2 cm for 4.98E+09 CFU/mL, 4.98E+07 CFU/mL and 4.98E+05 CFU/mL, respectively.

In order to eliminate the combined effect of *E. coli* concentration on antibacterial performance, correlation between AgNW loading and inhibition zone was individually investigated for each *E. coli* concentration. According to that approach, AgNW loading and inhibition zone diameters were found to be positively correlated for 4.98E+07 CFU/ml (r=0.99) and 4.98E+05 CFU/ml (r=0.97) of *E. coli* concentrations. As AgNW loading of the filters increased, inhibition zone diameters also increased. On the other hand, for the highest *E. coli* concentration studied (4.98E+09 CFU/ml), all AgNW-GF filters resulted in almost same inhibition zone diameters (r=0.20). This can be explained by MIC value. MIC value depends on bacteria concentration (Dankovich & Gray, 2011; J. Li et al., 2017). As bacteria concentration increases, resistance to antibacterial material also increases (J. Li et al., 2017). Udekwu et al. (2009) clarify the reason behind this relation as the reduction in ratio of available antimicrobial molecules per target organisms due to the reduced

effective antimicrobial concentration. Thus, the Ag release from AgNW-GF filters for the highest *E. coli* concentration might not be enough to differ in AgNW loadings.

The correlation between antibacterial performance (inhibition zone diameter) and *E. coli* concentration was individually observed for each AgNW loading, with the attempt to eliminate the combined effect of AgNW loading. It was found that *E. coli* concentration was inversely proportional to the inhibition zone diameter for all AgNW loadings. As *E. coli* concentration increased, the antibacterial effect of AgNW-GF filters decreased (r=-0.87 and -0.95). This was also expected as explained by Udekwu et al. (2009). Decreasing the concentration of target organism might lead to an increase in ratio of available antimicrobial molecules per target organisms; i.e. effective antimicrobial concentration.

4.2.2.2. Flow test results of Group X AgNW-GF filters

Flow tests were conducted for control (bare) GF filter, X1, X2, and X3 AgNW-GF filters via gravity filtration unit. Table 4-3 gives the flow test results of Group X AgNW-GF filters. The control filter provided 49.05% *E. coli* removal from 100 mL of model-contaminated water having approximately 10^8 CFU/mL *E. coli*. In X1, X2 and X3 AgNW-GF filters, *E. coli* removal efficiencies were 93.44%, 90.25% and 79.56%, respectively, for approximately 10^8 CFU/mL *E. coli*. It can be said that as AgNW loading decreased, *E. coli* removal efficiency also decreased gradually. On the other hand, a strong correlation was not observed (r=0.72). Although average AgNW loadings of X2 and X3 were close, *E. coli* removal efficiencies were different compared to removal efficiencies of X1 and X2. This could be attributed to the differences in flow rates of the tests.

Table 4-3. *Flow test results of Group X AgNW-GF filters.*

Type	Average AgNW loading (mg/g)	Flow rate (ml/min)	*E. coli* removal efficiency (%)
Control	0	12.5	49.05
X1	21.74	1.6	93.44
X2	17.13	4.4	90.25
X3	16.77	6.9	79.56

As mentioned previously, flow rate could not be controlled by the gravity filtration unit. Once 100 ml of contaminated water was put into the unit, the water head was starting to decrease. Reduction of head in time resulted in decreasing flow rate. Heterogeneous (web-like) structures of the filters might also lead to the changes in flow rates. These uncontrollable changes in flow rate could affect the removal efficiency as well. Hong et al. (2016a) investigated the effect of flow rate on bacterial removal efficiency of AgNW-CC nanocomposites. They observed that as flow rate increased removal efficiency decreased. Mthombeni et al. (2012) also analyzed the flow rate effect on the breakthrough point of AgNPs coated resin beads in fixed bed columns. They concluded that the breakthrough point was reached faster as flow rate increased.

Figure 4-7 shows the correlation between flow rate and E. coli removal efficiency on a graph obtained from the flow test results of Group X AgNW-GF filters. This graph gives an opinion about the effect of flow rate on removal efficiency. As flow rate increased, the *E. coli* removal efficiency decreased (r=-0.97). Therefore, the removal efficiency performance of the AgNW-GF filters should not be explained only by AgNW loadings of the filters; the flow rate might also affect the *E. coli* removal efficiency of the AgNW-GF filters.
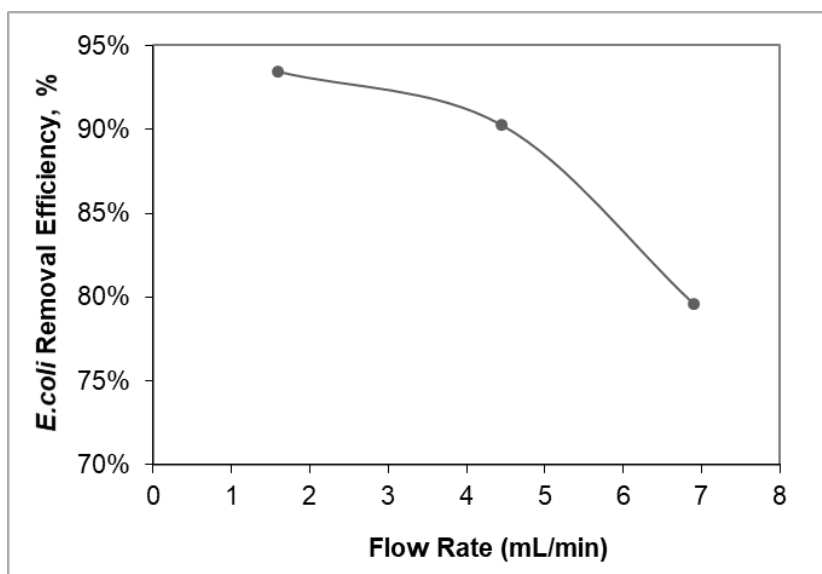
Figure 4-7. E. coli removal efficiencies at different flow rates (Group X).

Since the flow rate could be a factor that affects the removal efficiency, flow rate should be controlled during flow test. Therefore, the constant flow rate filtration set-up was provided for Group Y AgNW-GF filters in order to eliminate the consequences of variable flow rates and to investigate the effect of flow rate and effect of AgNW loadings on removal efficiency separately.

4.2.3. Silver release of Group X AgNW-GF filters

Ag release potential of the AgNW-GF filters was investigated by analyzing the filtrate produced after 100 mL of *E. coli* contaminated water was passed through the X1, X2 and X3 AgNW-GF filters during flow tests. Table 4-4 gives AgNW loadings of the filters, flow rate during flow tests, removal efficiency of *E. coli*, amount of Ag released from the AgNW-GF filters. Ag release values of X1, X2 and X3 were measured as 220, 120 and 180 ppb, respectively, which were all higher than the recommended Ag value in drinking water (100 ppb) (USEPA, 2018; WHO, 2011).

Table 4-4. *Ag release results of Group X AgNW-GF filters*

Type	Average AgNW loading (mg/g)	Flow rate (mL/min)	*E. coli* removal efficiency (%)	Ag Release (ppb)
X1	21.74	1.6	93.4	220
X2	17.13	4.4	90.2	120
X3	16.77	6.9	79.6	180

Figure 4-8 shows AgNW loadings of AgNW-GF filters and corresponding Ag release from the filters. The maximum Ag release was observed from X1 having the highest AgNW loading. Hong et al. (2016a) and Tan et al. (2018) investigated that Ag release was directly correlated with Ag content. However, it was not exactly the case for this study conducted with Group X AgNW-GF filters. It was observed that although X2 and X3 have close AgNW loadings (the latter with slightly lower amount), X3 released almost 50% more Ag than X2. Therefore, significant correlation was not also observed (r=0.76). Yet, it should be noted that flow rate cannot be controlled with the gravity filtration unit as mentioned before and, thus, it was not the same for these three flow tests performed.
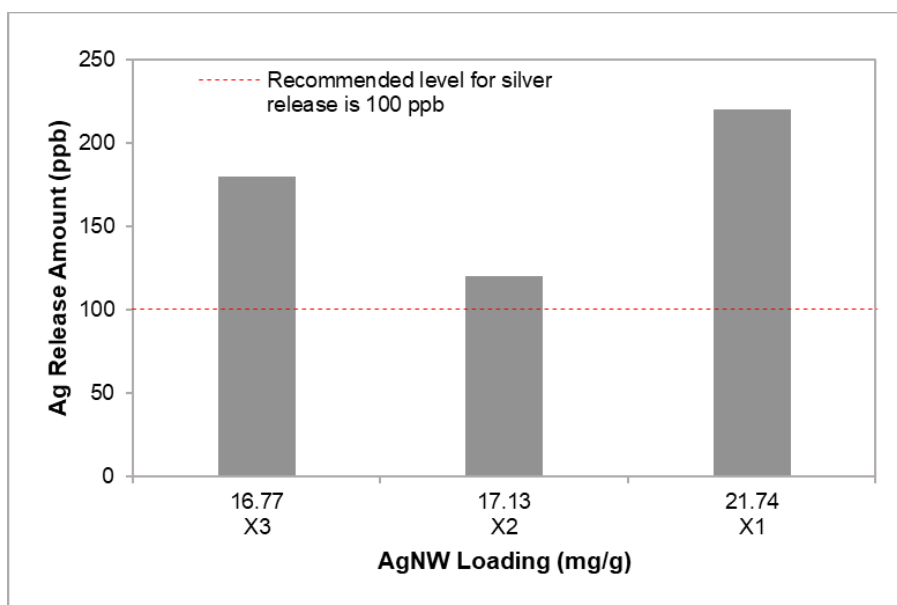
Figure 4-8. Average AgNW loading and Ag release correlation

71

Flow rate might also change the Ag release amount. Akhigbe et al. (2016) suggested that as the flow rate increased, the amount of Ag released decreased. On the contrary, Hong et al. (2016a), the longer the infiltration time was (the lower the flow rate), the higher the Ag released. In this study (Table 4-4), a significant correlation between flow rate and Ag release was not observed (r= -0.43) for Group X AgNW-GF filters.

Considering both the removal efficiencies of *E. coli* and Ag release of X1, X2 and X3 AgNW-GF filters with respect to the AgNW loadings, the removal efficiency of *E. coli* might be correlated with Ag release (r=0.88). X1, which released the highest amount of Ag, was the most efficient AgNW-GF filter against *E. coli*. However, X2 released the lowest amount of Ag but it was not the least efficient AgNW-GF filter against *E. coli*. Accordingly, X3, releasing 180 ppb Ag into the filtrate, removed minimum amount of *E. coli* from water. These contradictory results might be due to the flow rate effect (Table 4-4).

The experiments in Group X AgNW-GF filters were conducted via gravity filtration unit with variable (uncontrollable) flow rates. Since flow rate might be an important factor affecting the removal performance of AgNW-GF filters, the separate effects of the studied factors (*E. coli* concentration, Ag loadings, and flow rate) could not be determined. Therefore, experiments in Group Y AgNW-GF filters were conducted with constant flow rates.

4.3. AgNW-GF filters – Group Y

4.3.1. Characterization of synthesized AgNW for Group Y AgNW-GF filters

The physical and optical properties of synthesized AgNW that were used for coating of GF filters (Group Y) were analyzed by SEM (Figure 4-9 and Figure 4-10) and UV-

Visible absorption spectrophotometer (Figure 4-11). It was seen that the synthesized solution contain only nanowires but not nanoparticles.
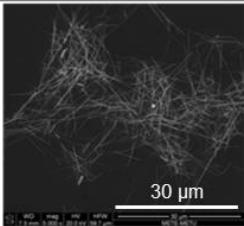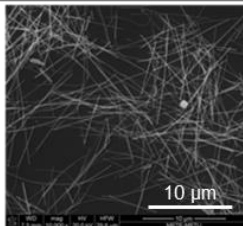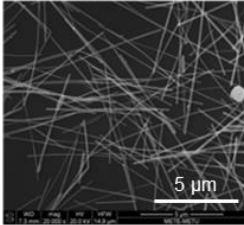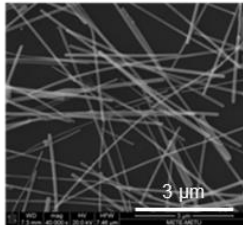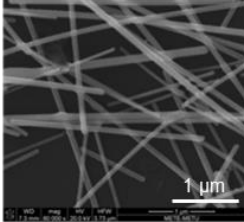
SEM Magnification	SEM Images	SEM Magnification	SEM Images
x5000		x10000	
x20000		x40000	
x80000			

Figure 4-9. SEM images of synthesized AgNW.

Based on the SEM images, the average diameter of AgNW was found as 0.1 μm. Length distribution analysis of AgNW was also done based on SEM images using ImageJ software. Figure 4-10 shows the length distribution histogram of the synthesized AgNW. The average length of AgNW was 8.1 ± 4.7 μm.
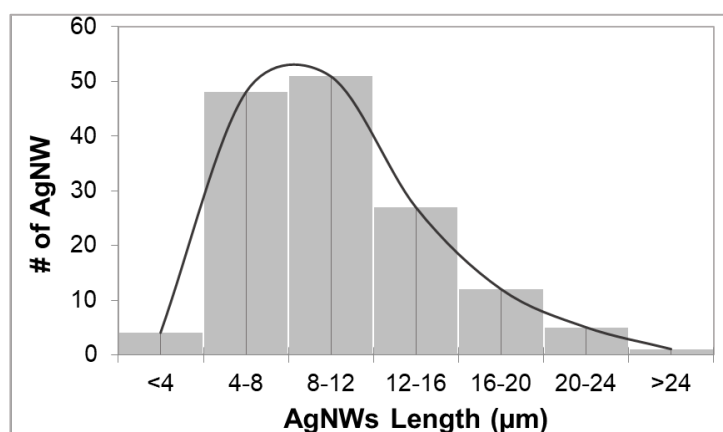
Figure 4-10. Length distribution of synthesized AgNW.

Figure 4-11 shows the absorption spectra of synthesized AgNW in ethanol solution. The spectrum has two characteristic absorption peaks at 350 and 385 nm. These absorption peaks are associated with typical surface plasmon resonance (SPR) of AgNW (E. J. Lee, Chang, Kim, & Kim, 2013; Y. Li et al., 2019; B. Liu et al., 2017; Nair, Jayaseelan, & Biji, 2015). The former and latter peaks generally corresponds to longitudinal plasmon resonance and transverse plasmon resonance, respectively (Ramasamy, Seo, Kim, & Kim, 2012). Presence of two peaks in the absorption spectrum is due to the low symmetry of the pentagonal cross section of AgNW (Luu et al., 2011).
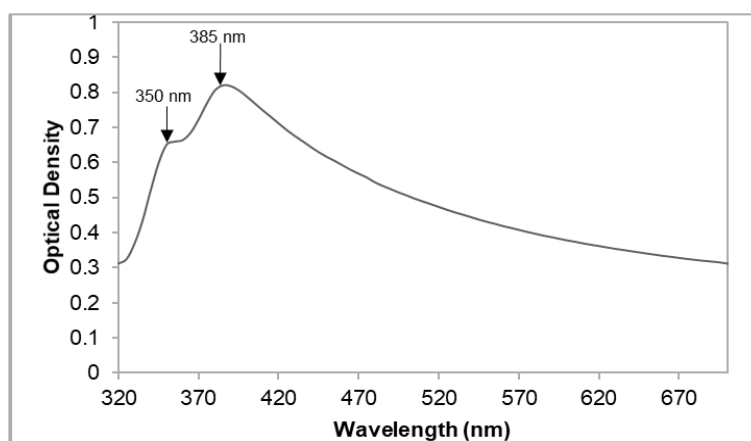
Figure 4-11. Absorption spectrum of synthesized AgNW solution.

4.3.2. Characterization of Group Y AgNW-GF filters

In Group Y AgNW-GF filter production, four sheets of AgNW-GF filters were fabricated (Y1-Y4). The concentration of AgNW in ethanol solution used in fabrication of Group Y AgNW-GF filters was recorded as 0.5 mg/ml.

Table 4-5 gives the electrical resistance and AgNW loading (as mg/g and as wt.%) values of Group Y AgNW-GF filters. Y1, Y2, Y3 and Y4 were fabricated with 4, 6, 6 and 10 dip-and-dry cycle, respectively. Therefore, as expected, Y4 has the highest AgNW loading, which is 9.9 mg/g. AgNW loading of Y1, Y2, and Y3 were calculated as 0.95, 4.5 and 4.8, respectively. As AgNW loading increases, electrical resistance decreases. Y1 was non-conductive.

Table 4-5. *Characterization of AgNW-GF filters – Group Y.*

AgNW-GF filter sheet	Dip-and-dry cycle	Average AgNW loading (mg/g)	Average AgNW loading (wt.%)	Electrical resistance (ohm/sq)
Y1	4	0.95	0.09	Non-conductive
Y2	6	4.5	0.45	60.91 ± 22.42
Y3	6	4.8	0.48	40.02 ± 20.55
Y4	10	9.9	0.99	8.49 ± 3.4

Group Y AgNW-GF filters achieved the same electrical resistance by lower AgNW loading compared to Group X AgNW-GF filters (Table 4-2). For example, electrical resistance of X4 with a AgNW loading of 11.32 mg/g was measured as 1245.84 ohm/sq. On the other hand, electrical resistance of Y4 having lower AgNW loading (9.9 mg/g) was three order of magnitude lower than that of X4 (8.49 ohm/sq). Electrical resistance of AgNW-based materials can be affected by length, diameter, quality of dispersion, surface roughness, and morphology of AgNW. Among the

factors, length and diameter are the major factors improving the electrical conductivity under theory of percolation (Kalakonda, 2016). Longer and thinner nanowires could achieve better electrical performance (Kalakonda, 2016). Besides, Bellew et al. (2015) found that nanowire-nanowire junctions and/or network skeleton would affect electrical resistance. PVP coating of nanowires in polyol method may result in low conductivity (Bellew et al., 2015). Wang et al. (2014) suggests that PVP layer on AgNW provides electrically insulating barrier at wire-wire junctions. They found out that adjusting PVP layer in order to improve contact between the wires significantly enhanced the electrical properties of AgNW (Wang et al., 2015). The difference between electrical resistance of Group X and Group Y might be due to the difference between their physical properties. The dimension of AgNW used for Group X and Group Y could be different. Thickness of PVP on AgNW could be different as well. Unfortunately, SEM images of synthesized AgNW used for production of Group X AgNW-GF filters could not be provided. Thus, the speculation behind the difference in electrical resistances of Group X and Group Y AgNW-GF filters cannot be verified and remains to be researched.

Figure 4-12 shows the SEM images of both control (bare) GF filter and Group Y AgNW-GF filters. As it was also mentioned in Section 4.2.1 for Group X AgNW-GF filters, the AgNW around the glass fibers seem to become denser as AgNW loading of the AgNW-GF filters increases.
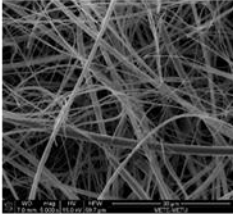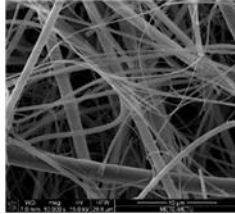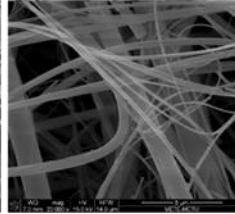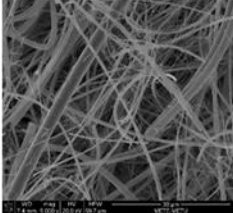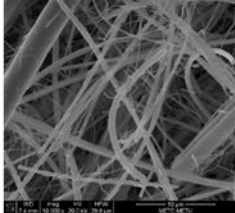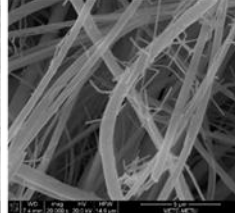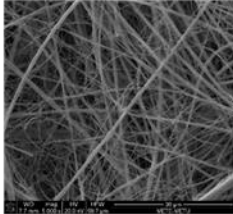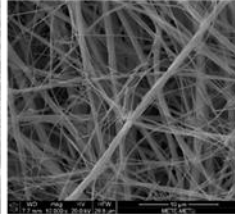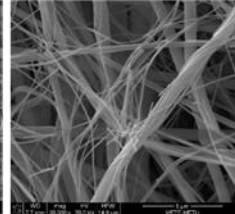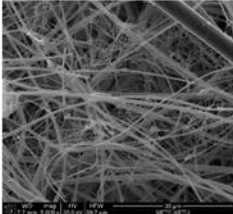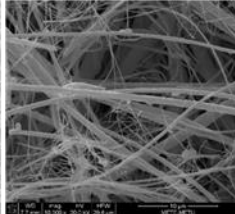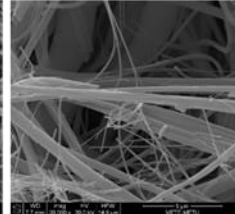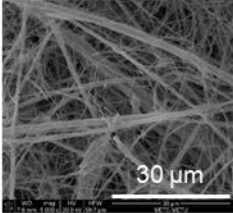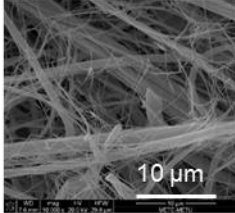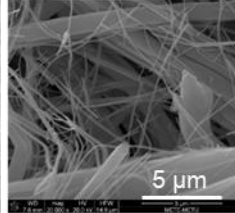
	AgNW Loading (mg/g)	SEM Magnification		
		x5000	x10000	x20000
Control	0			
Y1	0.95			
Y2	4.49			
Y3	4.79			
Y4	9.93	30 µm	10 µm	5 µm

Figure 4-12. SEM images of Group Y AgNW-GF Filters

77

4.3.3. Antibacterial testing of Group Y AgNW-GF filter

4.3.3.1. Disk diffusion test results of Group Y AgNW-GF filters

Figure 4-13 shows the disk diffusion test results conducted for Group Y AgNW-GF filters. Four different AgNW-GF filters in Group Y (Y1 – Y4) and control GF filter were used in this test. Like in the test performed for Group X AgNW-GF filters, the test was conducted with three different *E. coli* concentrations. Overall, the disk diffusion test results for Group Y AgNW-GF filter indicated that the diameter of inhibition zones were in the range of 1.15 – 1.35 cm (Figure 4-13 and Appendix D, Table D2).
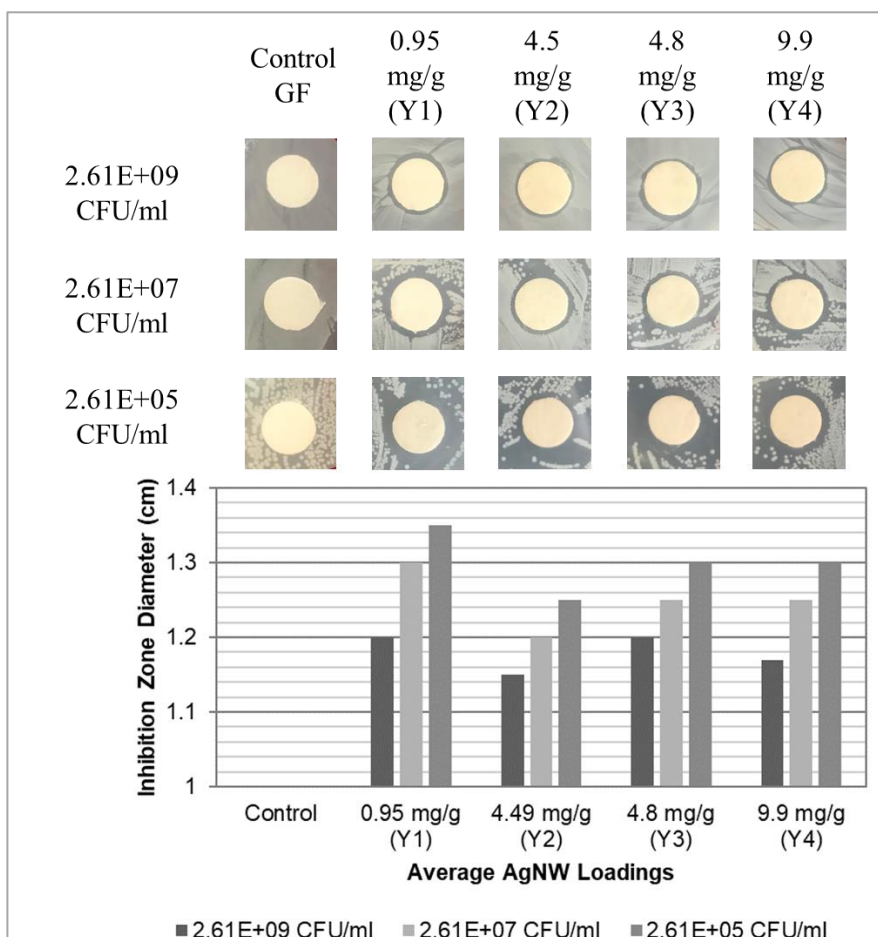
Figure 4-13. Disk diffusion test results of Group Y AgNW-GF filters

Inhibition zones caused by Y1 filter, with a AgNW loading of 0.95 mg/g, were observed as 1.2 cm, 1.3 cm and 1.35 cm for 2.61E+09 CFU/ml, 2.61E+07 CFU/ml, and 2.61E+05 CFU/ml *E. coli* concentrations, respectively. For Y2 AgNW-GF filter with a AgNW loading of 4.5 mg/g, inhibition zone diameters were measured as 1.15 cm, 1.2 cm and 1.25 cm for 2.61E+09 CFU/ml, 2.61E+07 CFU/ml, and 2.61E+05CFU/ml *E. coli* concentrations, respectively. For AgNW-GF filter with a AgNW loading of 4.8 mg/g (Y3), for 2.61E+09 CFU/ml, 2.61E+07 CFU/ml, and 2.61E+05 CFU/ml *E. coli* concentrations, inhibition zone diameters were measured as 1.2 cm, 1.25 cm and 1.3 cm, respectively. For AgNW-GF filter with a AgNW loading of 9.9 mg/g (Y4), inhibition zone diameters were measured as 1.17 cm, 1.25 cm and 1.3 cm for 2.61E+09 CFU/ml, 2.61E+07 CFU/ml, and 2.61E+05 CFU/ml *E. coli* concentrations, respectively. Control GF filters did not show any inhibition zone for any *E. coli* concentration, as expected.

It was observed that the decrease in *E. coli* concentration resulted in an increase in inhibition zone diameter of all Group Y AgNW-GF filters (r= -0.87 – -0.95), which is compatible with the disk diffusion test results of Group X AgNW-GF filter (Figure 4-6). This inverse correlation with bacteria concentration and inhibition zone diameter was also mentioned in literature (El-Aassar et al., 2013; Hong et al., 2016a) and no studies claims against this argument have been found.

AgNW loading, on the other hand, might not be affecting the inhibition zone diameters as much as *E. coli* concentration. Interestingly, among Group Y AgNW-GF filters, Y1, which has the lowest AgNW loading, showed the highest inhibition zone diameter at equal *E. coli* concentrations. Correlation between AgNW loading and inhibition zone diameters was not remarkable for all *E. coli* concentrations (r=-0.39 – -0.44). For Group X AgNW-GF filters, correlation was not significant at the highest *E. coli* concentration but this was not the case for the lower *E. coli* concentrations (Figure

4-6). AgNW loadings of Group X AgNW-GF filters were much higher than that of Group Y AgNW-GF filters. This difference might cause the correlation of AgNW loading with inhibition zone diameter. Yet, Hong et al. (2016a) suggests that the higher AgNW concentration results in the larger inhibition zone diameter. On the other hand, Doganay et al. (2019) and Shameli et al. (2011) did not find any dependency of inhibition zone diameter on AgNW loading, as well.

4.3.3.2. Flow test results of Group Y AgNW-GF filters

Flow tests for Group Y AgNW-GF filters were conducted in four groups in order to investigate the effect of (i) flow rate, (ii) AgNW loading, (iii) *E. coli* concentration, and (iv) two-stage serial filtration application on removal efficiency of the filters. The tests were performed via filtration set-up with constant flow rate. In the two-stage serial filtration application, it was made sure that the system was optimized according to the results obtained from the first three groups in terms of flow rate, AgNW loading and influent *E. coli* concentration.

In order to investigate the effect of flow rate on *E. coli* removal efficiency, flow tests for both control GF filter and AgNW-GF filter, were conducted at three different flow rates: 1 ml/min, 2.5 ml/min and 5 ml/min, at *E. coli* concentration of 10^8 CFU/ml. AgNW-GF filter (Y2) used in this test had a AgNW loading of 4.5 mg/g. The average *E. coli* removal efficiencies of control GF filter at 1 ml/min, 2.5 ml/min and 5 ml/min were found as 22.0% (0.11 log), 26.7% (0.13 log) and 20.0% (0.10 log), respectively (Appendix E, Table E1). For Y2-AgNW-GF filters, the removal efficiencies increased to 79.6% (0.69 log), 56.3% (0.36 log) and 51.9% (0.32 log) at 1 ml/min, 2.5 ml/min and 5 ml/min, respectively. This difference between the removal efficiencies of control GF filter and AgNW-GF filter was attributed to the antibacterial activity of AgNW and the potential increase in the filtration capacity of AgNW-GF filter due to the presence of nanowires in addition to the GF.

Figure 4-14 shows the results in order to understand the changes in *E. coli* removal efficiencies at different flow rates. For control GF filter, there was not seen any significant relation between flow rate and removal efficiency (r=-0.42). When log-removal efficiencies were considered, the maximum difference between log-removal values of control GF filters at different flow rates was 0.03. On the other hand, it was seen that there was a negative relation between flow rate and removal efficiency for AgNW-GF filter (r=-0.86). The similar results were also observed by Hong et al. (2016a) and Wen et al. (2017). In both studies, when flow rate was increased from 2 ml/min to 4 ml/min, the removal efficiencies decreased almost 0.5 – 1 log (68 – 90%) at 6 V. In this study, as flow rate increased from 1 to 2.5 ml/min, *E. coli* removal efficiency decreased significantly by 23%. The further increase in flow rate from 2.5 to 5 mL/min resulted in a slight decrease in removal efficiency by 4%. In other words, removal efficiency at 1 ml/min was 0.37 log higher (almost doubled) than removal efficiency at 2.5 ml/min. However, there was only 0.04 log difference between removal efficiencies at flow rates of 2.5 ml/min and 5 ml/min. The possible reason of this observation might be due to the Ag release from the filters, which is further discussed in Section 4.3.4. Nevertheless, the results revealed that maximum removal efficiency was obtained at the lowest flow rate studied, which is 1 ml/min.
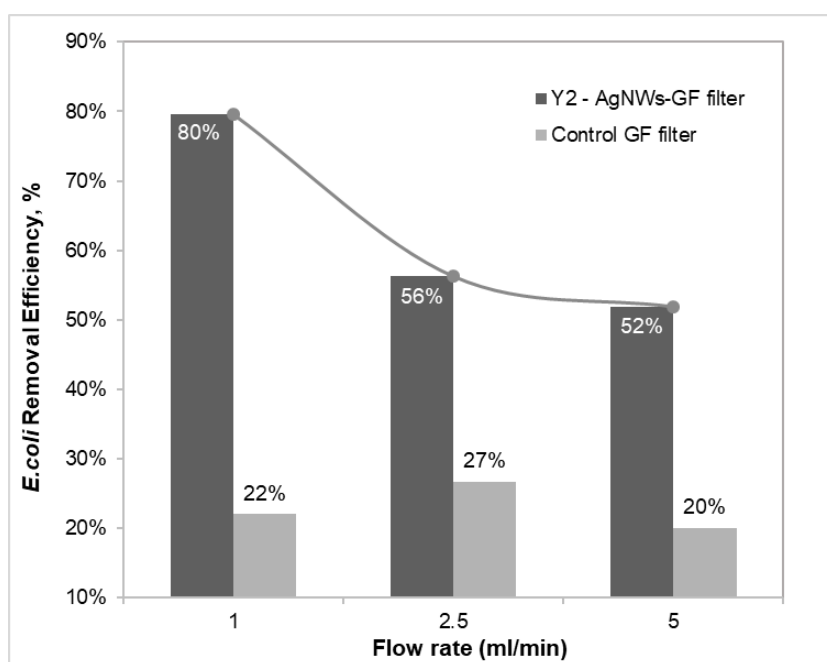
Figure 4-14. E. coli removal efficiency results at different flow rates

After optimizing flow rate, another group of flow test was performed in order to investigate the effect of AgNW loading on *E. coli* removal efficiency of AgNW-GF filters. Flow tests were conducted at zero-AgNW loading and three different AgNW loadings of 0 mg/g (control), 0.95 mg/g (Y1), 4.8 mg/g (Y3), and 9.9 mg/g (Y4). Flow rate was 1 ml/min based on previous group of flow test. *E. coli* concentration of model-contaminated water was 10^8 CFU/ml as an order of magnitude. The average *E. coli* removal efficiencies of control GF filter, Y1, Y3 and Y4 were found as 27.4% (0.14 log), 34.3% (0.18 log), 76.6% (0.63 log), and 89.0% (0.96 log), respectively. Detailed results are given in Appendix E, Table E2.

Figure 4-15 shows the results in order to understand the changes in *E. coli* removal efficiencies at different AgNW loadings. It should be recalled that the results of disk diffusion tests performed for Group Y AgNW-GF filters showed weak correlation between AgNW loading and antibacterial effect (Figure 4-13, Section 4.3.3.1). On the

other hand, for Group X AgNW-GF filters, AgNW loading and inhibition zone diameters were found to be correlated, except for the highest *E. coli* concentration. Similarly, the results obtained herein from flow tests conducted at different AgNW loadings showed that *E. coli* removal efficiency might depend on AgNW loading of the filters (r=0.95).

According to the results obtained (Figure 4-15), as AgNW loading increased, *E. coli* removal efficiency also increased. There are studies explaining the relation between nanosilver concentration and *E. coli* inactivation as a nanosilver concentration-dependent manner (Hong et al., 2016a; Song et al., 2016; H. Z. Zhang et al., 2016). Compared to the removal efficiency of control GF filter, Y1 AgNW-GF filter, having minimum AgNW loading, did not make a significant improvement on removal efficiency. The difference between removal efficiencies of control GF filter and Y1 filter was only 6.9% (or 0.04 log). This could be explained by MIC value as aforementioned (Section 4.2.2.1). In order to achieve effective removal efficiencies, AgNW should be above the MIC value (Dankovich & Gray, 2011). Y3 and Y4 AgNW-GF filters, on the other hand, achieved much better *E. coli* removal efficiency from influent model-contaminated water. When AgNW loading increased to 4.8 mg/g (Y3) from 0.95 mg/g (Y2), removal efficiency increased by 42%. On the other hand, removal efficiency gradually increased by 12% as AgNW loading changed from 4.8 mg/g (Y3) to 9.9 mg/g (Y4). *E. coli* concentration in the model-contaminated water was 10^8 CFU/ml. This high *E. coli* concentration might reduce the antibacterial efficacy like discussed in disk diffusion test results (Section 4.2.2.1). For example, at lower *E. coli* concentration, the difference between the removal efficiencies of Y3 and Y4 could be bigger. Among the three AgNW-GF filters and loads tried, Y4 achieved the highest removal efficiency of 89.0%.
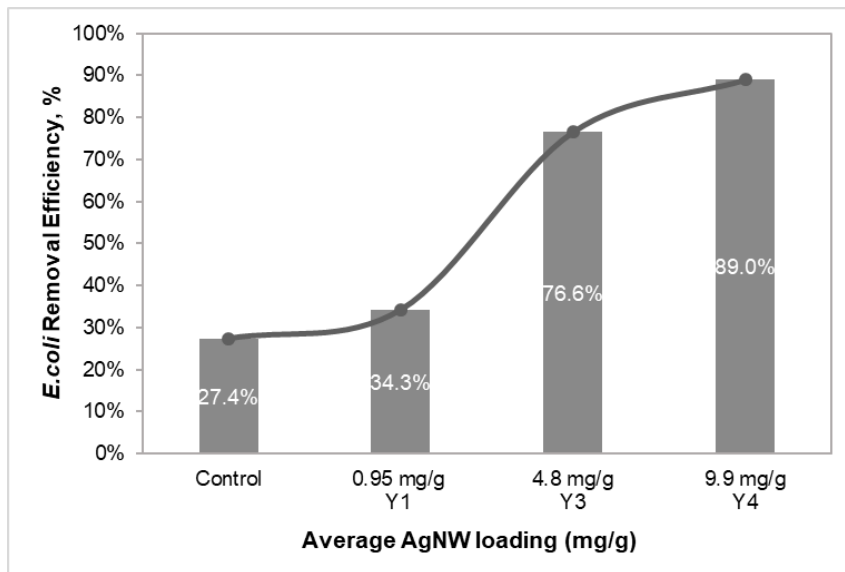
Figure 4-15. E. coli removal efficiency r*esults at different AgNW loadings*

After both flow rate and AgNW loading of AgNW-GF filters were optimized, flow tests were performed once again in order to investigate the effect of influent *E. coli* concentration on *E. coli* removal efficiency. Flow tests were conducted at three different influent *E. coli* concentration (as an order of magnitude) of 10^3 CFU/ml, 10^5 CFU/ml and 10^8 CFU/ml. Y4 AgNW-GF filter used for these tests had 9.9 mg/g AgNW loading and flow rate was 1 ml/min. *E. coli* removal efficiencies of control GF filter were calculated as 27.4% (0.14 log), 55.3% (0.35 log) and 61.5% (0.41 log) for 10^8 CFU/ml, 10^5 CFU/ml, and 10^3 CFU/ml, respectively. Removal efficiencies of Y4 AgNW-GF filter was found as 89.0% (0.96 log), 94.3% (1.24 log) and 99.0% (2 log) for 10^8 CFU/ml, 10^5 CFU/ml, and 10^3 CFU/ml, respectively. Detailed results are given in Appendix E, Table E3.

Figure 4-16 shows the results on a graph in order to understand the changes in *E. coli* removal efficiencies with different influent *E. coli* concentrations. Percent removals of Y4 AgNW-GF filter on the graph (Figure 4-16 – a) was not enough to compare the results properly since the percent removals were close. Therefore, in order to examine

the changes in removal efficiencies according to influent *E. coli* concentration, it was preferred to express the removal efficiency values based on log-removal on the graph (Figure 4-16 – b). As observed in the disk diffusion tests (Figure 4-13, Section 4.3.3.1), removal efficiency increased as the influent *E. coli* concentration decreased (r=-0.88). The removal efficiency decreased by 4.7% (0.28 log) when influent *E. coli* concentration increased from 10^3 CFU/ml to 10^5 CFU/ml. On the other hand, when influent *E. coli* concentration increased from 10^5 CFU/ml to 10^8 CFU/ml, more reduction (5.3% or 0.76 log) was observed. Hong and his colleagues (2016b) reported that the antibacterial performance of AgNW-carbon fiber cloth significantly decreased at *E. coli* concentrations greater than 10^6 CFU/ml. Tan and colleagues (2018) also discussed the concentration dependent results. They found 10% increase in removal efficiency of *E. coli* when the influent *E. coli* concentration decreased to 10^3 CFU/ml from 10^5 CFU/ml. Among all influent *E. coli* concentrations studied in the tests with AgNW-GF filters, the highest removal efficiency (99.0%) was achieved at 10^3 CFU/ml.

Similar to the AgNW-GF filters, *E. coli* removal efficiency increased as the influent *E. coli* concentration decreased (r=-0.98) for control GF filters as well. The highest removal efficiency (66%, 0.41 log removal) was also obtained at 10^3 CFU/ml. However, it should be noted that this value is almost 40% lower (1.6 log removal difference) than that of its AgNW-GF filter counterpart.
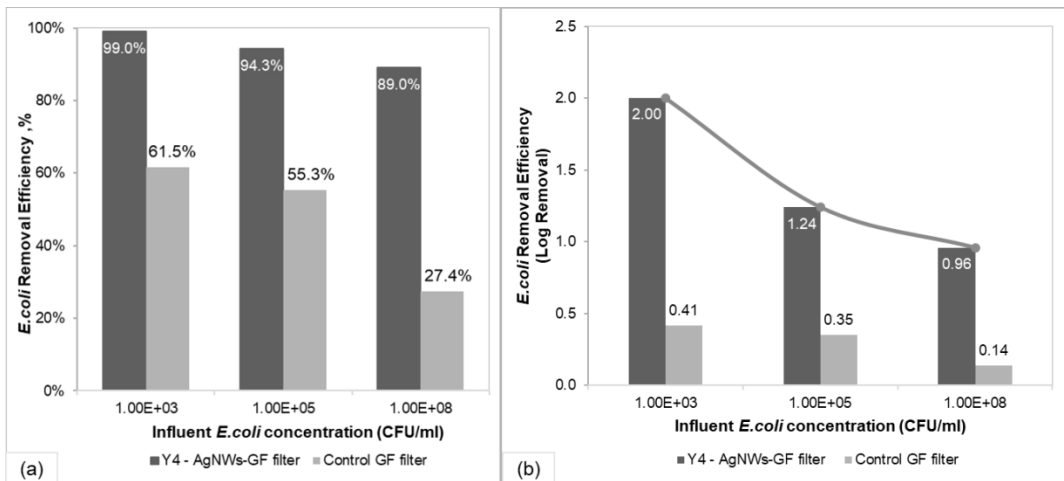
Figure 4-16. E. coli removal efficiency results as (a) percent removal and (b) log-removal at different E. coli concentration in influent water

Up to this point, the factors, namely, the flow rate, AgNW loading and *E. coli* concentration, were optimized and the values leading to the highest *E. coli* removal efficiency via AgNW-GF filters were determined as 1 ml/min, 9.9 mg/g (Y4) and 10^3 CFU/ml. Finally, two-stage serial filtration application was performed in order to investigate the further improvement on *E. coli* removal efficiency of AgNW-GF filters developed.

The results, in terms of both percent removal and log-removal, are given below in Figure 4-17. The detailed results are also given in Appendix E, Table E4. For control GF filter, *E. coli* removal efficiency increased to 86.8% (0.47 log) from 61.5% (0.88 log) after 2nd stage filtration. For Y4 AgNW-GF filter, *E. coli* removal efficiency increased from 91.6% (1.08 log) to 99.2% (2.12 log) after 2nd stage filtration. It was observed that log-removals were approximately doubled for both control GF and AgNW-GF filters (Figure 4-17).
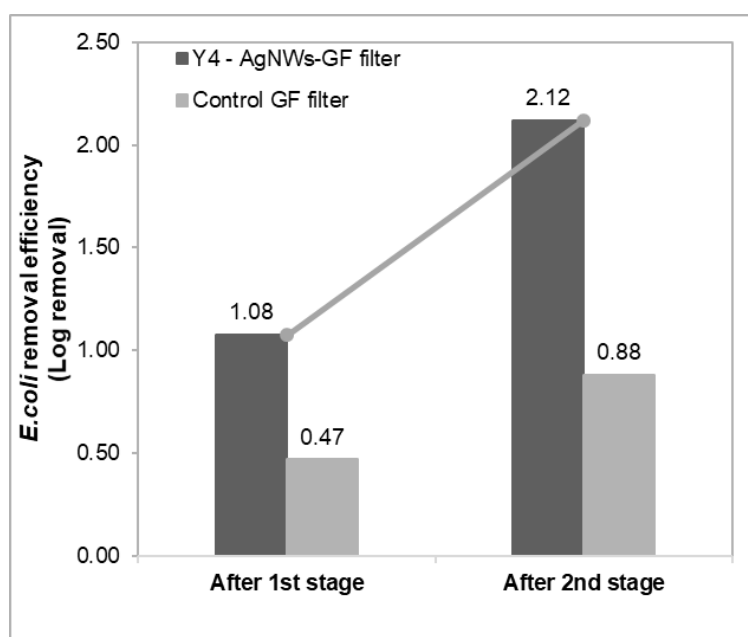
Figure 4-17. E. coli removal efficiency r*esults in two-stage serial filtration application*

4.3.4. Silver release analysis results of Group Y AgNW-GF filters

Filtrate samples collected from each flow test discussed in the previous Section (Section 4.3.3.2) were analyzed in order to investigate the effect of (i) flow rate, (ii) AgNW loading, (iii) *E. coli* concentration, and (iv) two-stage serial filtration application on Ag release from AgNW-GF filter. The amount of Ag released to the filtrate changes the quality of the drinking water. Thus, WHO (2011) and USEPA (2018) set that the maximum Ag content in drinking water should not be more than 100 ppb to prevent human health.

In order to investigate the effect of flow rate on Ag release, the filtrates of the flow tests performed with Y2 AgNW-GF filter at three different flow rates, namely, 1 ml/min, 2.5 ml/min and 5 ml/min (Section 4.3.3.2) were analyzed. AgNW-GF filter (Y2) used in these tests had a AgNW loading of 4.5 mg/g. Influent *E. coli* concentration was 10^8 CFU/ml as an order of magnitude. The analyzed average Ag

release values in the filtrates were found as 47.0 ppb, 42.5 ppb, and 43.0 ppb at 1 ml/min, 2.5 ml/min and 5 ml/min, respectively (Table 4-6). At all flow rates, Ag amount released to the filtrates were below the limit value (100 ppb). Detailed results are given in Table E1, Appendix E.

Table 4-6. *Average Ag release values at different flow rates.*

Flow Rate, ml/min	Average Ag release (ppb)
1	47.0
2.5	42.5
5	43.0

As seen in Table 4-6, first, Ag release value decreased by 4.5 ppb when flow rate was increased from 1 ml/min to 2.5 ml/min. Then, it was mildly increased by 0.5 ppb when the flow rate was further increased to 5 ml/min. Ag release in Group X AgNW-GF filters was observed as similar to this trend (Table 4-4). In AgNWs synthesis, PVP was used as a stabilizing agent. H. Zhang (2012) mentioned less Ag release from PVP-stabilized AgNPs. However, PVP can dissolve in water (Wang et al., 2015). The slower flow rate increased contact time of water with AgNW-GF filter, which would result in more Ag release at lower flow rates due to PVP dissolution. The higher Ag release at lower flow rates was also indicated by Gemici et al. (2018) and Akhigbe et al. (2016). On the other hand, Ag release at 5 ml/min was not expected to be higher than that of at 2.5 ml/min according to Hong et al. (2016a). AgNW on GF filter might be washed out at higher flow rate (5 ml/min) due to the higher velocity of water while passing through the AgNW-GF filters. This hypothesis should be investigated kinetically in more detail.

E. coli removal efficiency at different flow rates was discussed previously (Figure 4-14, Section 4.3.3.2). A significant difference (only 4%) was not found between removal efficiencies at flow rates of 2.5 ml/min and 5 ml/min (56.3 and 51.9%,

respectively). This might be associated with Ag release. As mentioned in Section 1.3.1., both Ag^+ release and particle-specific effect could be reasons of antibacterial effects of nanosilver. Since the difference between Ag release at 2.5 ml/min and 5 ml/min was almost the same (the difference was 0.5 ppb), Ag release at 5 ml/min might prevent much more reduction in *E. coli* removal efficiency. Therefore, the removal efficiency might not decrease as much as expected as flow rate increased.

In order to investigate the effect of AgNW loading on Ag release, the filtrates of the flow tests performed with four different AgNW loadings, namely, 0.95 mg/g (Y1), 4.8 mg/g (Y3) and 9.9 mg/g (Y4) (Section 4.3.3.2) were analyzed. The flow rate in these tests was 1 ml/min and influent *E. coli* concentration was in the order of 10^8 CFU/ml. The average Ag release values were found as 26.5 ppb, 34.5 ppb, and 62.5 ppb from Y1 (0.95 mg/g), Y3 (4.8 mg/g) and Y4 (9.9 mg/g) AgNW-GF filters, respectively (Figure 4-18). For all AgNW loadings, Ag amount released to the filtrates were below the recommended limit value of 100 ppb. Detailed results are given in Table E2, Appendix E.
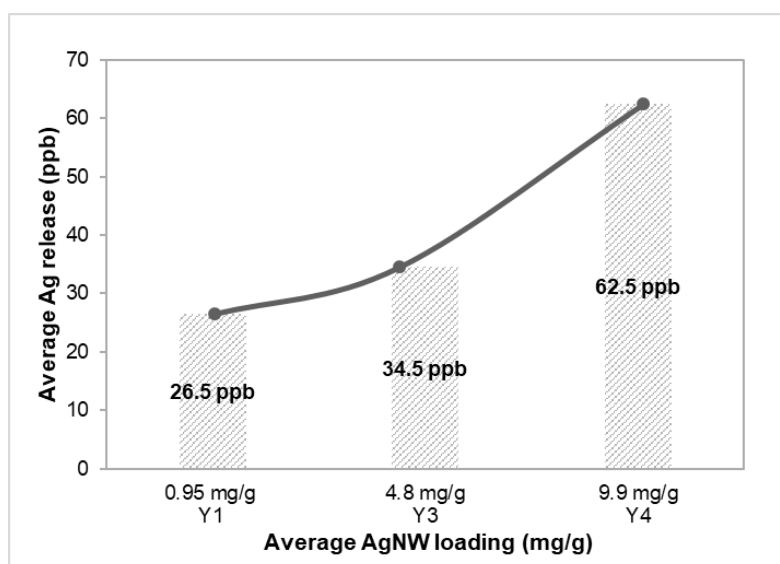
Figure 4-18. Ag release from AgNW-GF filters with different AgNW loading.

As seen in Figure 4-18, as AgNW loading increased Ag release also increased (r=0.93) as also observed for *E. coli* removal efficiency (Figure 4-15, Section 4.3.3.2). In literature, research studies confirmed this observation (Hong et al., 2016a; Mpenyana-Monyatsi et al., 2012; Praveena et al., 2016; Tan et al., 2018). Considering Ag release analyses of Group X AgNW-GF filters (Figure 4-8, Section 4.2.3), all Ag release values were higher than the limit value. It was confirmed that this would occur mostly due to higher AgNW loadings of Group X AgNW-GF filters (16.77 mg/g – 21.74 mg/g) than that of Group Y AgNW-GF filters (0.95 mg/g – 9.9 mg/g).

In order to investigate the effect of influent *E. coli* concentration on Ag release, the filtrates of the flow tests performed with three different influent *E. coli* concentrations of 10^3 CFU/ml, 10^5 CFU/ml and 10^8 CFU/ml (Section 4.3.3.2) were used. Y4 AgNW-GF filter used for these tests had a AgNW loading of 9.9 mg/g. Flow rate was 1 ml/min. The average Ag release amounts were found as 17.5 ppb, 16.5 ppb, and 62.5 ppb for 10^3 CFU/ml, 10^5 CFU/ml, and 10^8 CFU/ml, respectively (Figure 4-19). It was seen that Ag releases to filtrate were all below the limit value of 100 ppb. Detailed results are given in Table E3, Appendix E.

As seen in Figure 4-19, the difference between Ag release at 10^3 and 10^5 CFU/ml is negligible. On the other hand, Ag release significantly increased by 46 ppb when influent *E. coli* concentration was increased from 10^5 to 10^8 CFU/ml. Release of Ag from AgNW-GF filters would not only occur during the passage of water through the filters; Ag might be also entrapped by bacterial cells during percolation of model-contaminated water through the filters as suggested by Dankovich and Gray (2011). Dankovich and Gray (2011) found out that half of the Ag released to the filtrate was caused by Ag absorption into the cells. Thus, a higher number of bacteria-containing water would lead to higher amount of Ag released into the filtrate. S. Jiang and Teng (2017) proposed another explanation for the increase in Ag release with the increase

in *E. coli* concentration. They suggested that hydrophobic part of PVP molecule on AgNW provided interaction of AgNW with bacterial cells. Thus, cells would attach to the surface. The higher the number of cells attached to the AgNW, the more the Ag ion would be released from AgNW (S. Jiang and Teng, 2017). Meanwhile, during percolation of water, the Ag released due to cell attachment would flow into the filtrate. SEM images of both control GF filter and AgNW-GF filter after a flow test (Figure 4-20) partially confirmed the attachment of larger number of cells on AgNW-GF filter than that of control GF filter during percolation of model-contaminated water. Red circles in the figure shows some of the *E. coli* cells as example.
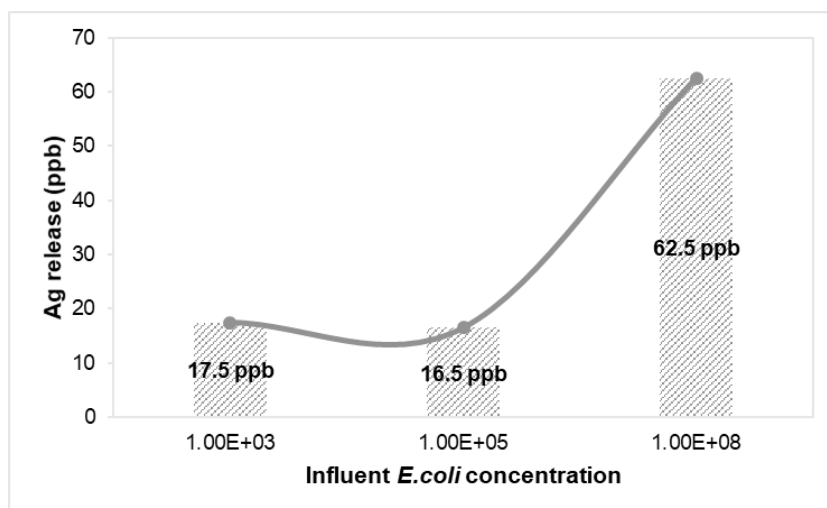
Figure 4-19. Ag release with different influent *E. coli* concentration
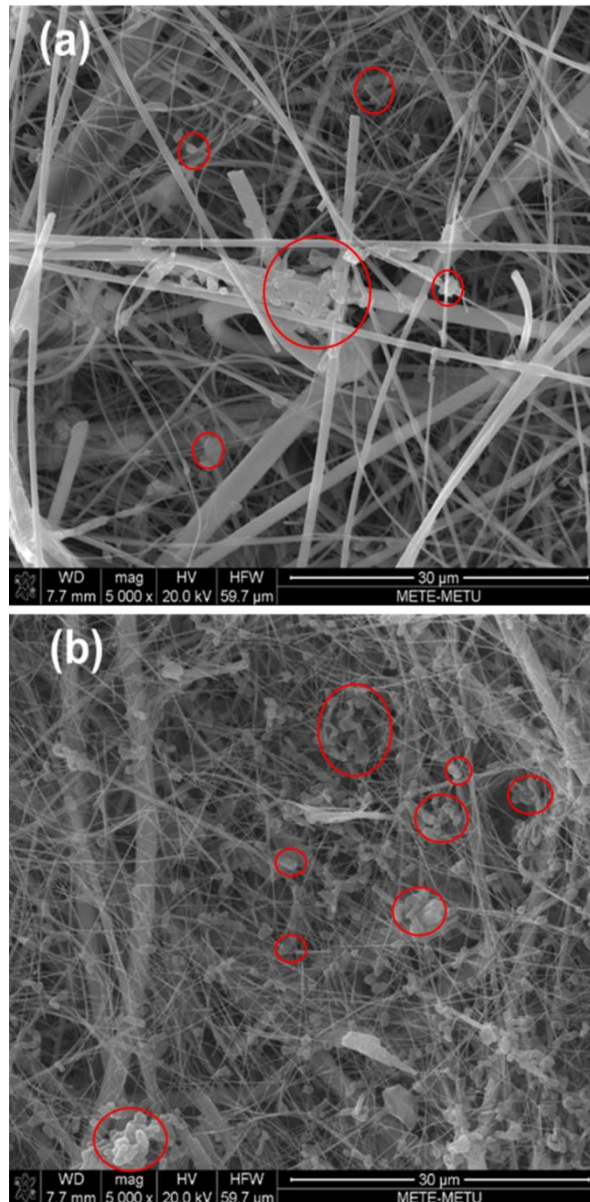
Figure 4-20. SEM images of control GF filter (a) and AgNW-GF filter (b) after flow test (Red circles indicates *E. coli* cells as example).

The amount of Ag released in the filtrates of the flow test conducted with two-stage serial filtration application was also analyzed for both the 1st and 2nd stage. The results are presented in Figure 4-21. The Ag release amount after 1st stage was found as 13 ppb. The filtrate was subsequently passed through the 2nd stage. After 2nd stage, total

Ag release was analyzed as 22 ppb which is still below the limit of 100 ppb. Detailed results are provided in Table E4, Appendix E.

AgNW-GF filters used in both stages had similar characteristics. Yet, the increase in the amount of Ag release via the application of 2nd stage was only 9 ppb, which was less than the amount released after 1st stage (13 ppb). This might be due to the removal of *E. coli* concentration after the 1st stage. The decrease in influent *E. coli* concentration might decrease the Ag release as aforementioned. After 1st stage filtration, 1.08 log removal was achieved (Figure 4-17, Section 4.3.3.2), thus, a decrease in Ag release was expected after 2nd stage filtration. The other reason of the observed decrease in Ag released amount might be due to the 2nd stage AgNW-GF filter only; the AgNW-GF filter at the 2nd stage might act as a barrier to the transfer of released Ag from the 1st stage to the filtrate of 2nd stage.
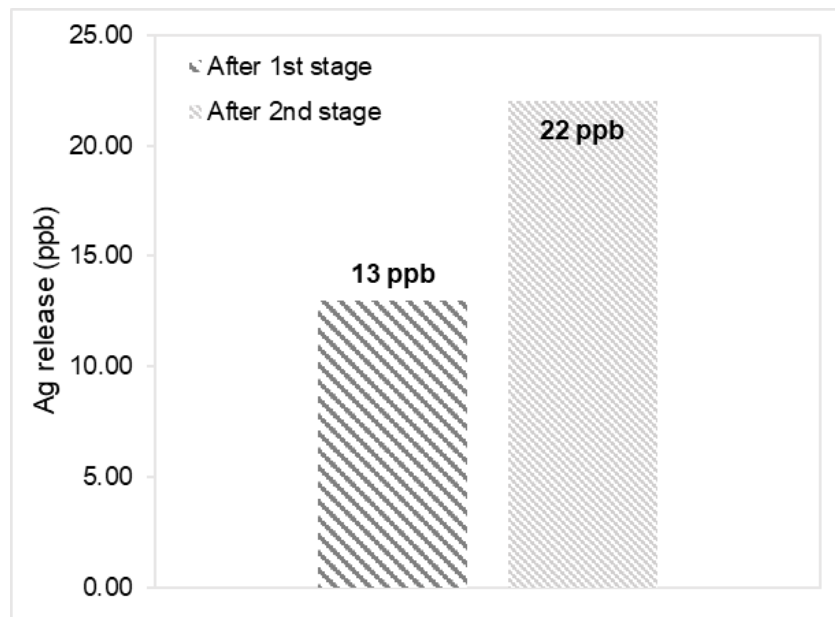
Figure 4-21. Ag release in two-stage serial filtration application

In two-stage filtration application, SEM analysis was made on a sample collected from the filtrate of 2nd stage (Figure 4-22). *E. coli* can be seen on the image. On the other hand, AgNW were not observed in the SEM image, although Ag release amount was analyzed in the filtrate (22 ppb). It should be noted that the device used for Ag analyses (ICP-MS) cannot distinguish Ag form (Ag ion or nanosilver). Therefore, the Ag released from the filter and detected by ICP-MS might possibly be in the form of Ag ions instead of AgNW. Although Ag was released from AgNW-GF filters, the antibacterial efficacy probably might not drastically reduce since it is not in nanosilver form, which is an effective carrier of Ag ions (Xiu et al., 2012) as mentioned in Section 1.3.1. In other words, for not releasing AgNWs, the developed AgNW-GF filters might be still stable and effective antibacterial agents. On the other hand, this outcome was based on only one filtrate sample. In order to make better judgements about the stability of AgNW-GF filters and form of released Ag, further analyses should certainly be done. Yet, investigation of the form of Ag released from the filters was not in the scope of the thesis and further analyses were not performed.
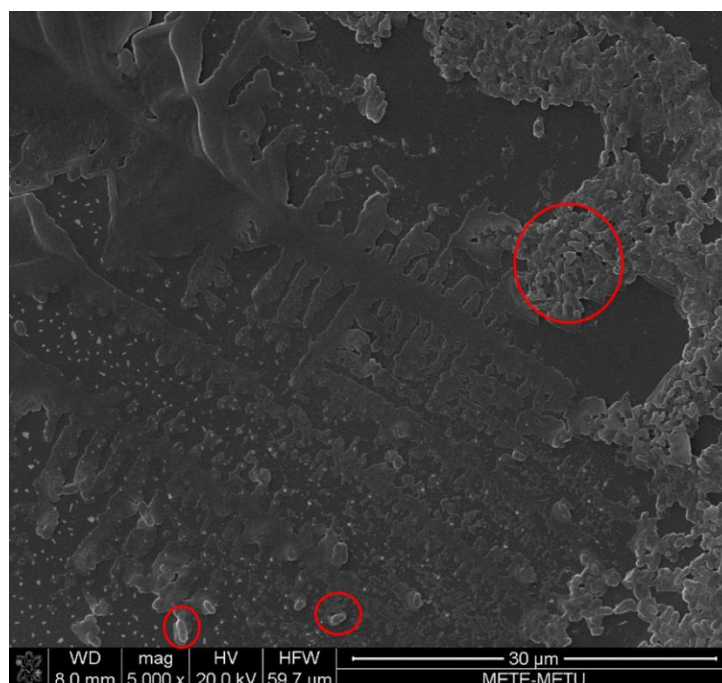
Figure 4-22. SEM image of filtrate (Red circles indicates *E. coli* cells as example).

Finally, a flow test was conducted in order to investigate the Ag release in long-term operation. One-liter ultra-pure water was filtered through the Y4 AgNW-GF filter having a AgNW loading of 9.9 mg/g. The flow rate was adjusted at 1 ml/min. Figure 4-23 shows Ag release at each 100 ml and the cumulative Ag release. As seen in figure 4-23, the release rate gradually decreased as volume of filtrate increased until 300 ml of filtrate volume. After passing 300 ml of water, Ag release rate became relatively constant until the end of operation. This result was compatible with the studies by Quang et al. (2013) and Biswas and Bandyopadhyaya (2016). Quang et al. (2013) described the higher release rate at the early stages of filtration. They suggest that nanosilver which has weak attraction with the substrate materials was likely to release first. In this study, the cumulative Ag release after 1-liter of ultra-pure water filtration was 46.7 ppb, which was less than half of the limit value (100 ppb).
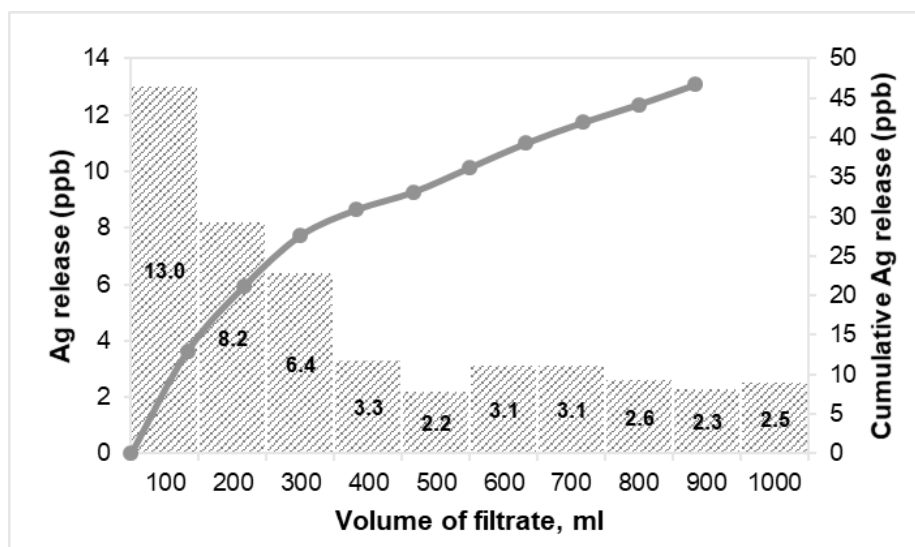
Figure 4-23. Ag release in long-term operation

Ag release is not only important for possible human health issues but also affects lifespan of the Ag containing materials. The calculation of the AgNW-GF filters' lifespan was done according to the equation 3. To this purpose, the Ag analyses results

95

of the flow tests conducted at 1 ml/min with a AgNW loading of 9.9 mg/g (0.053 mg/cm^2) and 10^3 CFU/ml influent *E. coli* concentration were used. Accordingly, the released Ag amount from AgNW-GF filter was 16 ± 4.3 ppb (Figure 4-19 and Figure 4-21), which was only 0.2% Ag after percolation of 100 ml contaminated-water. On this basis, it was roughly estimated that AgNW-GF filters might be used for 42 liters of contaminated water before all Ag on the filters is washed out. Studies estimated lifespan of the nanosilver-containing materials as between 50-148 liters (Dankovich et al., 2016; Hong et al., 2016a; Tan et al., 2018). In this study, however, lifespan was estimated a bit lower than the literature. It should be noted that the calculated lifespan is the minimum period possible to observe at the given highest Ag release rate. As seen in Figure 4-23, in long-term operation, the release rate decreases after 300 ml of water filtration. Therefore, considering the reduction in Ag release rate with the increase in volume of water filtrated, the lifespan of the developed AgNW-GF filter might increase in long-term operations. As seen in Figure 4-23, after 300 ml of water filtration through the AgNW-GF filter, the Ag amount released after each 100 ml of water filtered decreased to less than 3.3 ppb. Thus, as the Ag release rate decreases, the lifespan of the AgNW-GF filter might increase to about 245 liters, which is even more than the lifespan of the materials estimated in literature (50 – 148 liters).

$$\% \text{ Release of Ag} = \frac{\text{Ag release in 100 ml (µg)}}{\text{Average AgNW loading (µg/(cm}^2\text{)}*\text{Filtration area (cm}^2\text{)}} * 100 \qquad (3)$$

Presence of microbial cells could increase the amount of Ag release. Quang et al. (2013) obtained much more Ag release in filtration of bacterial water (10^5 CFU/ml) than that in ultra-pure water. However, this was not the case in this study. Average Ag release after the flow tests conducted with model-contaminated water under optimum conditions (at 1 ml/min, with a AgNW loading of 9.9 mg/g and 10^3 CFU/ml influent *E. coli* concentration) was 16 ± 4.3 ppb (Figure 4-19 and Figure 4-21). After filtering 100 ml ultra-pure water, Ag release was 13 ppb. A remarkable difference was not

observed between Ag release (only 3 ppb) by filtering *E. coli* contaminated water and ultra-pure water. On the other hand, as mentioned before (Figure 4-19), Ag release suddenly increased when influent *E. coli* concentration reached to 10^8 CFU/ml.

4.4. Evaluation of the Use of Developed AgNW-GF Filters for POU Water Disinfection

The final AgNW-GF filters (Group Y) developed in this thesis at optimum conditions achieved 2.12 log removal for 10^3 CFU/ml *E. coli* contaminated water via two-stage serial filtration application. Control GF filter, on the other hand, achieved only 0.88 log removal for the same conditions. Not only for the optimal conditions but also in all disk diffusion tests and flow tests, there were appreciable differences between antibacterial results of AgNW-GF filter and control GF filters. This difference was most probably due to the improvement of antibacterial effect of GF filters by AgNW. The maximum removal efficiency of AgNW-GF filter obtained at higher influent *E. coli* concentration (10^8 CFU/ml), which is almost equal to that of typical wastewater's *E. coli* content (Table 2-1, Section 2.1), was 89% (0.96 log) (Figure 4-15). At the same conditions, control GF filter achieved only 27.4% (0.14 log) removal.

The *E. coli* removal mechanisms of AgNW-GF filters from water might be the filtration process, the antibacterial activity of AgNW or combination of both. Although it is not in the scope of the thesis, it was tried, as an attempt, to differentiate these mechanisms, and the removal mechanism of AgNW-GF filters was tried to be investigated numerically. To do this, it was first planned to measure OD difference between influent and filtrate in flow tests (data not shown). Since *E. coli* causes turbidity in ultra-pure water, OD reduction in the water passing through the AgNW-GF filters might give the amount of *E. coli* (as percentage) attached on the filters. Accordingly, the difference between percent removal obtained by viable cell count (spread plate method) and percent OD reduction might reveal the removal mechanism.

If percent viable cell reduction is equal to OD reduction, the removal mechanism might be only filtration. If percent viable cell reduction is greater than OD reduction, the removal mechanism would not be only filtration but also the antibacterial activity of AgNW. This approach could performed only for 10^8 CFU/ml *E. coli* concentration because the OD reductions were not applicable to lower concentrations. Yet, even for the highest concentration (10^8 CFU/ml *E. coli)*, OD reduction ratio was calculated as higher than the calculated viable cell reduction in more than one flow test. This was not something expected and also not possible according to the aforementioned approach. Thus, the removal mechanisms of the AgNW-GF filters could not be estimated by this approach. Therefore, in order to understand the removal mechanism of AgNW-GF filters, SEM analyses for both control GF and AgNW-GF filters were performed before (not shown) and after the flow tests (Figure 4-20). Yet, a quantitative analysis could not be done based on the SEM images. However, it is clear from SEM analyses that there is an attachment of *E. coli* on the filters. As already discussed in Section 4.3.4, the attachment of the cells to the filter surface might be due to the interaction of hydrophobic part of PVP and bacterial cells. Therefore, the difference between removal efficiencies of AgNW-GF filters and control GF filters might be due to filtration mechanism. Yet, it cannot be said that the difference was only due to filtration. The antibacterial results of disk diffusion tests revealed that AgNW-GF filters have antibacterial effect and thus the AgNW in the filters would also contribute to the removal mechanism. Thus, both filtration and antibacterial activity of AgNW might be effective on removal performance of AgNW-GF filters. In order to understand which mechanisms dominate the removal, further studies should be conducted.

Table 2-2 (Section 1.3.2) gives the removal efficiency results obtained from literature. It is seen that the removal efficiencies of the materials studied in literature are comparable to the results obtained in this study. AgNPs attached to porous carbon foam developed by Karumuri et al. (2013) also achieved 2 log removal for 10^3 CFU/ml

E. coli concentration. On the other hand, AgNW-PAN/TPU membrane (Tan et al., 2018) and PAN/PANI/AgNW-CC (Wen et al., 2017) achieved 100% removal efficiencies for 10^3-10^5 CFU/ml *E. coli* concentration. Yet, Tan et al. (2018) and Wen et al. (2017) explained these high performances due to holding of *E. coli* on the membrane/filters (by filtration). Hong et al. (2016a) reported that AgNW-CC nanocomposite membrane reached at most 1 log removal for 10^6 CFU/ml *E. coli* without voltage application. Schoen et al. (2010) found 20% removal with AgNW/CNT coated cotton filter for 10^7 CFU/ml *E. coli* contaminated water. Similarly, polyurethane sponge modified by CNTs/AgNW achieved less than 1 log removal of 10^7 CFU/ml *E. coli* without voltage application. In contrast, blotting paper impregnated with AgNPs (Dankovich and Gray, 2011) achieved 4.5 – 7.5 log removal of 10^9 CFU/ml *E. coli* contaminated water depending on Ag content of the papers under no voltage application.

Voltage application certainly enhanced the removal efficiency. 10 V voltage application on AgNW-CC nanocomposite membrane (Hong et al., 2016a) increased the removal efficiency up to 5 log removal for 10^6 CFU/ml whereas only 1 log removal was achieved under no voltage. On the other hand, the highest removal efficiency was obtained as only 80% for 10^8 CFU/ml *E. coli* concentration under 6 V voltage application (Hong et al., 2016a). Similarly, composite filter fabricated by a mixture of AgNPs/AgNW and graphite (Basheer and Abu-thabit, 2014) achieved 6 log removal for 10^7-10^8 CFU/ml under 20 V voltage application. AgNW/CNT coating on cotton filter (Schoen et al., 2010) achieved 20%, 89% and 77% under 0 V, +20V and -20V for 10^7 CFU/ml *E. coli* contaminated water. C. Liu et al. (2013) studied with polyurethane sponge modified by CNTs/AgNW. The antibacterial performance was increased by more than 6 log with 10 V compared to no voltage application for 10^7 CFU/ml *E. coli* contaminated water.

Compared to these research studies, AgNW-GF filters fabricated in this study, achieved a good performance although no voltage was applied. Although Hong et al. (2016a) applied 6V voltage and achieved 80% removal, AgNW-GF filters, in this study, reached better removal efficiency (89%) for 10^8 CFU/ml. Similarly, compared to Schoen et al. (2010), AgNW-GF filters have superior performance over AgNW/CNT coating cotton filter for even the higher *E. coli* concentration. In contrast, AgNW-GF filters were found less efficient against *E. coli* than blotting paper impregnated with AgNPs. Blotting paper impregnated with AgNPs (Dankovich and Gray, 2011) achieved 4.5 – 7.5 log removal for 10^9 CFU/ml *E. coli* contaminated-water changing with respect to Ag content of the papers under no voltage. There are several reasons of that much of difference. First, the thickness of GF filter used in this study was 0.26 mm, which is smaller than that of blotter paper (0.5 mm). Pore size was unknown in Dankovich and Gray's study (2011); however, this is an important parameter for filtration. On the other hand, AgNW used in this study could be less toxic than AgNPs as it was discussed in Section 1.2. Lastly, synthesis method of AgNPs (Dankovich and Gray, 2011) and AgNWs (this study) were different. Dankovich and Gray (2011) did not use PVP, which might possibly lower the antibacterial performance.

It was found out that the removal efficiency increases with the decrease in influent *E. coli* concentration. AgNW-GF filters were found to be efficient for contaminated-water containing less than 10^3 CFU/ml *E. coli*. On the other hand, the maximum removal efficiency (2.12 log removal) obtained in this study might be improved by further studies through further investigating for optimal conditions (AgNW loading or flow rate). It is believed that if voltage is applied, the antibacterial performance would be improved more and the filter might be even appropriate to use for higher *E. coli* concentrations. It should be noted that non-homogeneity (in terms of both size and distribution) of nanofibers does not ensured the uniform porosity and uniform filtration performance. Flow tests conducted with AgNW-GF filters resulted in

variable *E. coli* removal efficiencies under the same conditions (Appendix E). This might occur possibly due to non-homogeneity and high average pore size (1.6 μm) of GF filters. Thus, better removal efficiency results can be achieved using a more uniform scaffold material.

Finally, in this thesis, the Ag amount released to the filtrate was found as 22 ppb, which is far below the recommended limit (100 ppb). In literature, a wide range of Ag release amount is reported as 10 – 200 ppb (Table 2-2). Thus, Ag release from AgNW-GF filters to the effluent water was evaluated as safe for drinking water.

For POU water treatment, cost is an important consideration for possible uses of the materials on site (Backer, 2019). Cost analysis was not within the scope of thesis. Even so, it was estimated that the developed AgNW-GF filters was low-cost since it did not require any power source for filtration but only gravity. Thus, this might be lowering the treatment cost of POU application compared to the conventional methods. However, the fabrication cost and corresponding lifetime of AgNW-GF filters should be investigated and optimized if required.

Considering all these discussions, it can be concluded that AgNW-GF filters were found to be very promising to be furtherly developed for low-cost, safe (in terms of Ag release) and highly-efficient POU water disinfection to be used in contaminated natural water, in particular for waters having less than 10^3 CFU/ml.

CHAPTER 5

CONCLUSIONS

In this thesis, AgNW-GF filters were developed for POU water disinfection. Within the scope of the study, initially, novel stand-alone AgNW foils were produced and investigated. Because of their low durability and flexibility characteristics, it was difficult to conduct antibacterial studies. Therefore, as an alternative to stand-alone AgNW foils, a commercially available glass fiber filter, which is more durable and flexible, has more defined porous structure and large pores and would be economical for production compared to bare AgNW foils, was used as scaffold in the further studies.

The effect of flow rate, AgNW loading and *E. coli* concentration on both *E. coli* removal efficiency and Ag release were investigated. The optimum values of these parameters (i.e. flow rate, AgNW loading and *E. coli* concentration) leading to the highest removal efficiencies were utilized in two-stage serial application. The significant observations and main conclusions are listed as follows:

- Agar medium composition significantly affects the disk diffusion test results. Among three different agar (nutrient, LB and MH agar), MH agar is the most proper one for disk diffusion test and, thus, a better indicator for detection of antibacterial effect of AgNW-GF filters.

103

- It was concluded (via both disk diffusion test and flow test) that AgNW-GF filters have higher antibacterial effect on *E. coli* compared to control (bare) GF filters.

  o While control GF filters did not show any inhibition zone in disk diffusion tests, inhibition zone diameters were measured in the range of 1.15 – 1.35 cm for AgNW-GF filters, changing with respect to the *E. coli* concentration and AgNW loadings.

  o Control GF filters achieved 20% - 61.5% (0.1 log – 0.41 log) *E. coli* removal in flow tests while the *E. coli* removal efficiency of AgNW-GC filters were calculated as 34.3 – 99% (0.18 log – 2.00 log) changing with respect to the flow rate, AgNW loading and *E. coli* concentration.

- Flow rate was found to be one of the major factors affecting *E. coli* removal efficiency of AgNW-GF filters. As flow rate increased, *E. coli* removal efficiency decreased. Thus, flow rate should be kept constant during passage of water through the filters.

  o *E. coli* removal efficiencies in flow tests were obtained as 79.6%, 56.3% and 51.9% at 1 ml/min, 2.5 ml/min and 5 ml/min, respectively, with AgNW-GF filter having a AgNW loading of 4.5 mg/g and 10^8 CFU/ml influent *E. coli* concentration.

- Although disk diffusion test results did not show a significant relation between AgNW loading and antibacterial efficiency (r=-0.39 – -0.44), it was observed that as AgNW loading increased, *E. coli* removal efficiency increased according to flow test results (r=0.95).

o *E. coli* removal efficiencies in flow tests were obtained as 34.3%, 76.6% and 89.0% with AgNW-GF filters having a AgNW loading of 0.95mg/g, 4.8 mg/g and 9.9 mg/g, respectively, for 10^8 CFU/ml influent *E. coli* concentration at 1 ml/min flow rate.

- Both disk diffusion test and flow test results revealed the *E. coli* concentration-dependent antibacterial effect of AgNW-GF filters. As *E. coli* concentration decreased, antibacterial effect of AgNW-GF filters enhanced.

   o *E. coli* removal efficiencies in flow tests were obtained as 89.0%, 94.3% and 99.0% for influent *E. coli* concentration of 10^8 CFU/ml, 10^5 CFU/ml and 10^3 CFU/ml, respectively, with AgNW-GF filters having a AgNW loading of 9.9 mg/g AgNW loading at 1 ml/min flow rate.

- According to flow test results, optimal flow rate, AgNW loading and influent E. coli concentration were determined as 1 ml/min, 9.9 mg/g and 10^3 CFU/ml, respectively.

- Two-stage serial filtration application doubled the log-removals for both control filter and AgNW-GF filter under the optimal conditions. The removal efficiency which was 1.08 log after the 1st stage increased to 2.12 log removal after 2nd stage.

- Ag amount released from AgNW-GF filters (flow tests results) ranged between 13 – 62.5 ppb, changing with respect to the flow rate, AgNW loading and *E. coli* concentration. Ag release amounts were all below the recommended limit

value for drinking water, 100 ppb. Thus, AgNW-GF filters were safe in terms of Ag release amounts.

- o At lower flow rates (less than and equal to 1 ml/min), there was more time to solubilize PVP in water due to higher contact time. At higher flow rates, AgNW might be detached from AgNW-GF filters easily due to higher velocity of water during filtration.

- o A direct relation was found between AgNW loading and Ag release. Ag release increases with AgNW loading.

- o Influent *E. coli* concentration could affect Ag release beyond a certain value. When influent *E. coli* concentration increased from 10^5 to 10^8 CFU/ml, Ag release was almost increased by four times.

- o The increase in Ag released amount via the application of 2nd stage was only 9 ppb which was less than that of the 1st stage (13 ppb). This might be due to the decrease in influent *E. coli* concentration after 1st stage and/or AgNW-GF filter at the 2nd stage acting as a barrier to the transfer of Ag released in the filtrate of 1st stage.

- o After a long-term operation (1-liter), cumulative Ag release was still less than the recommended limit value (100 ppb). The release rate was gradually decreased with the increasing filtrate volume due to tendency to release at the early stages of AgNW having weak attraction with the filters.

- o It was roughly estimated that AgNW-GF filters could be used for 41.7 liters of contaminated water before all Ag was washed out. Considering the decrease in the Ag release rate with the increase in the volume of water filtrated, the lifespan can increase to 245 liters.

- o Difference between Ag releases after percolation of 100 ml of ultra-pure water and 100 ml of *E. coli* contaminated water with 10^3 CFU/ml

106

was not significant. However, 10^8 CFU/ml *E. coli* contaminated water raised Ag release suddenly.

- AgNWs were not observed in the SEM image of a filtrate sample. Thus, it was assumed that AgNW-GF filters have good stability. Possibly, released Ag might be in the form of Ag ions.

In conclusion, this thesis revealed important results that might fill the gap in literature on investigation of AgNW based filters for POU water disinfection and the effect of flow rate, Ag loading and influent *E. coli* concentration on removal efficiency. Ag release into water is less studied in literature. This study also investigated the Ag release from AgNW-GF filters comprehensively. A novel AgNW-GF filter was fabricated and found to be promising for POU water disinfection under optimal conditions. In order to achieve better removal efficiencies and obtain more promising POU water disinfection for highly contaminated water or even wastewater, further studies should be conducted.

CHAPTER 6

FUTURE RECOMMENDATIONS

Recommendations for future work based on the findings in this study are as follows:

- Literature indicates that the applied voltage remarkably enhances the removal efficiency. Therefore, a voltage application can be integrated to the AgNW-GF POU water disinfection system in order to improve removal efficiency.

- It is known that antibacterial activity of nanosilver varies based on microbial cultures. *E. coli*, used in this study, was gram-negative bacteria. In literature, there are studies conducted with different microbial cultures. However, investigation of removal efficiency based on other microbial groups in flow tests is limited and remains to be investigated.

- A comparative study with different form of nanosilver (e.g. AgNPs, AgNWs or AgNCs) can be performed in terms of both Ag release (i.e. stability) and POU water disinfection.

- Natural water characteristics (e.g. pH, temperature, turbidity, TOCs or NOMs) affect the antibacterial efficacy of nanosilver. A matrix study can be performed in order to investigate the effect of different water characteristics.

- Based on the findings obtained from this study, Ag release kinetics can be studied in detail.

- The determined optimum flow rate (1 ml/min) is low for POU application. Studies should be performed to increase the flow rate without decreasing the removal efficiency.

- The effect of agar medium composition and the concentrations on disk diffusion test can be studied in detail.

- In order to understand removal mechanism of AgNW-GF filters, a method can be developed and mechanism can be investigated in detail.

- GF filters with smaller pore sizes can be investigated in order to enhance the removal efficiency.

- AgNW-GF filters resulted in less repeatable results due to non-homogeneous porous structure of GF filters. Pore size distribution changes within the filters could influence the removal efficiencies. Provided that filters that are more homogeneous are utilized better results can be obtained. Therefore, in addition to the recommendations given above, more homogenous porous filter media should be preferred as a scaffold for decorating with AgNWs. The scaffold material can be selected by taking into consideration of better stability with AgNW and material reusability.

REFERENCES

Ahamed, M., AlSalhi, M. S., & Siddiqui, M. K. J. (2010). Silver nanoparticle applications and human health. *Clinica Chimica Acta*, *411*(23–24), 1841–1848. https://doi.org/10.1016/j.cca.2010.08.016

Akhigbe, L., Ouki, S., & Saroj, D. (2016). Disinfection and removal performance for Escherichia coli and heavy metals by silver-modified zeolite in a fixed bed column. *Chemical Engineering Journal*, *295*, 92–98. https://doi.org/10.1016/j.cej.2016.03.020

APHA. (1999). *Standard Methods for the Examination of Wastewater* (20th Ed.; L. S. Clesceri, A. E. Greenberg, & A. D. Eaton, eds.). Washington, DC, USA: America Public Health Association.

Atay, H. Y., Yaşa, İ., & Çelik, E. (2014). Antibacterial Polymeric Coatings with Synthesized Silver Nanoparticles. *Synthesis and Reactivity in Inorganic, Metal-Organic, and Nano-Metal Chemistry*, *45*(6), 784–798. https://doi.org/10.1080/15533174.2013.843561

Backer, H. (2019). Chapter 5 - Water Disinfection for International Travelers. In *Travel Medicine* (Fourth Ed.). https://doi.org/10.1016/B978-0-323-54696-6.00005-7

Basheer, R., & Abu-thabit, N. (2014). *Nanostructured Conductive Composite Filter Electrodes Sterilization by Application of Low Electrical Current for Water*. 1–6.

Bauer, J. F., & Manville, J. (2004). Properties of Glass Fiber for Filtration: Influence of Forming Process. *International Nonwovens Journal*, *os-13*(4), 1558925004os – 13. https://doi.org/10.1177/1558925004os-1300401

Bayraktar, I., Doganay, D., Coskun, S., Kaynak, C., Akca, G., & Unalan, H. E. (2019). 3D printed antibacterial silver nanowire/polylactide nanocomposites. *Composites Part B: Engineering*, *172*(January), 671–678. https://doi.org/10.1016/j.compositesb.2019.05.059

Beisl, S., Monteiro, S., Santos, R., So, A., Lemos, F., Minhalma, M., … Pinho, D. (2019). Synthesis and bactericide activity of nano fi ltration composite membranes e Cellulose acetate / silver nanoparticles and cellulose acetate / silver ion exchanged zeolites. *Water Research*, *149*, 225–231. https://doi.org/10.1016/j.watres.2018.10.096

Bellew, A. T., Manning, H. G., Gomes da Rocha, C., Ferreira, M. S., & Boland, J. J. (2015). Resistance of Single Ag Nanowire Junctions and Their Role in the Conductivity of Nanowire Networks. *ACS Nano*, *9*(11), 11422–11429. https://doi.org/10.1021/acsnano.5b05469

Biswas, P., & Bandyopadhyaya, R. (2016). Water disinfection using silver nanoparticle impregnated activated carbon: Escherichia coli cell-killing in batch and continuous packed column operation over a long duration. *Water Research*, *100*, 105–115. https://doi.org/10.1016/j.watres.2016.04.048

Bondarenko, O., Juganson, K., Ivask, A., Kasemets, K., Mortimer, M., & Kahru, A. (2013). Toxicity of Ag , CuO and ZnO nanoparticles to selected environmentally relevant test organisms and mammalian cells in vitro : a critical review. *Archives of Toxicology*, *87*, 1181–1200. https://doi.org/10.1007/s00204-013-1079-4

Choi, O., Clevenger, T. E., Deng, B., Surampalli, R. Y., Ross, L., & Hu, Z. (2009). Role of sulfide and ligand strength in controlling nanosilver toxicity. *Water Research*, *43*(7), 1879–1886. https://doi.org/10.1016/j.watres.2009.01.029

Choi, O., Deng, K. K., Kim, N. J., Ross, L., Surampalli, R. Y., & Hu, Z. (2008). The inhibitory effects of silver nanoparticles, silver ions, and silver chloride colloids on microbial growth. *Water Research*, *42*(12), 3066–3074. https://doi.org/10.1016/j.watres.2008.02.021

Cicek, S., Gungor, A. A. J., Adiguzel, A., & Nadaroglu, H. (2015). *Biochemical Evaluation and Green Synthesis of Nano Silver Using Peroxidase from Euphorbia (Euphorbia amygdaloides) and Its Antibacterial Activity. 2015*.

Clasen, T. F., & Bastable, A. (2003). Fecal contamination of drinking water during collection and household storage : The need to extend protection to the point of use Faecal contamination of drinking water during collection and household storage : the need to extend protection to the point o. *Journal of Water and Health*, (June), 109–115. https://doi.org/10.2166/wh.2003.0013

Collins, C. H., Lyne, P. M., Grange, J. M., & Falkinham, J. O. (2004). *Collins and Lyne's Microbiological Methods* (Eighth Ed.). Retrieved from http://mmstcchemistry.weebly.com/uploads/2/4/1/2/24121933/microbiological_methods.pdf

Coskun, S., Aksoy, B., & Unalan, H. E. (2011). Polyol synthesis of silver nanowires: An extensive parametric study. *Crystal Growth and Design*, *11*(11), 4963–4969. https://doi.org/10.1021/cg200874g

Dankovich, T. A., & Gray, D. G. (2011). Bactericidal paper impregnated with silver nanoparticles for point-of-use water treatment. *Environmental Science and*

Technology, *45*(5), 1992–1998. https://doi.org/10.1021/es103302t

Dankovich, T. A., Levine, J. S., Potgieter, N., Dillingham, R., & Smith, J. A. (2016). Inactivation of bacteria from contaminated streams in Limpopo, South Africa by silver- or copper-nanoparticle paper filters. *Environ. Sci.: Water Res. Technol.*, *2*(1), 85–96. https://doi.org/10.1039/C5EW00188A

Dankovich, T. a. (2012). *Bactericidal Paper Containing Silver Nanoparticles for Water Treatment by*. McGill University.

Diagne, F., Malaisamy, R., Boddie, V., Holbrook, R. D., Eribo, B., & Jones, K. L. (2012). Polyelectrolyte and silver nanoparticle modification of microfiltration membranes to mitigate organic and bacterial fouling. *Environmental Science and Technology*, *46*(7), 4025–4033. https://doi.org/10.1021/es203945v

djs research. (2019). No Title. Retrieved from Correlation Analysis - Market Research website: https://www.djsresearch.co.uk/glossary/item/correlation-analysis-market-research

Doganay, D., Kanicioglu, A., Coskun, S., Akca, G., & Unalan, H. E. (2019). Silver-nanowire-modified fabrics for wide-spectrum antimicrobial applications. *Journal of Materials Research*, *34*(04), 500–509. https://doi.org/10.1557/jmr.2018.467

Dogru, E., Demirbas, A., Altinsoy, B., Duman, F., & Ocsoy, I. (2017). Formation of Matricaria chamomilla extract-incorporated Ag nanoparticles and size-dependent enhanced antimicrobial property. *Journal of Photochemistry & Photobiology, B: Biology*, *174*(May), 78–83. https://doi.org/10.1016/j.jphotobiol.2017.07.024

Durán, N., Durán, M., de Jesus, M. B., Seabra, A. B., Fávaro, W. J., & Nakazato, G. (2016). Silver nanoparticles: A new view on mechanistic aspects on antimicrobial activity. *Nanomedicine: Nanotechnology, Biology, and Medicine*, *12*(3), 789–799. https://doi.org/10.1016/j.nano.2015.11.016

Duran, N., Marcato, P., Conti, R., Alves, O., Costa, F., & Brocchi, M. (2010). Potential Use of Silver Nanoparticles on Pathogenic Bacteria, their Toxicity and Possible Mechanism of Action. *Journal of Brazilian Chemical Society*, *21*(6), 949–959.

El-Aassar, A. H. M., Said, M. M., Abdel-Gawad, A. M., & Shawky, H. A. (2013). Using Silver Nanoparticles Coated on Activated Carbon Granules in Columns for Microbiological Pollutants Water Disinfection in Abu Rawash area, Great Cairo, Egypt. *Australian Journal of Basic and Applied Sciences*, *7*(1), 422–432. Retrieved from http://search.ebscohost.com/login.aspx?direct=true&profile=ehost&scope=site

&authtype=crawler&jrnl=19918178&AN=88911596&h=IZgRtHVSejk3hLuW
w+59p1N425CqKY9ztdCFSkFj5UQxpxWt1OpFbX336js9IX/Hu1bfX6S2k6s6
YUxjUdM9/Q==&crl=c%5Cnhttp://www.ajbasweb.com/ajbas/2013/J

Eltugral, N., & Simsir, H. (2016). Preparation of nano-silver-supported activated carbon using different ligands. *Research on Chemical Intermediates*, *42*(3), 1663–1676. https://doi.org/10.1007/s11164-015-2110-6

Erdem, R., & Akal, M. (2015). *Characterization and evaluation of antimicrobial properties of electrospun chitosan / polyethylene oxide based nanofibrous scaffolds (with / without nanosilver).* https://doi.org/10.1177/1528083713503000

European Committee on Antimicrobial Susceptinility Testing (EUCAST). (2019). *EUCAST disk diffusion method for antimicrobial susceptibility testing - Reading guide*. Retrieved from http://www.eucast.org/fileadmin/src/media/PDFs/EUCAST_files/Disk_test_doc uments/2019_manuals/Reading_guide_v_6.0_EUCAST_Disk_Test_2019.pdf

Fan, M., Gong, L., Huang, Y., Wang, D., & Gong, Z. (2018). Facile preparation of silver nanoparticle decorated chitosan cryogels for point-of-use water disinfection. *Science of The Total Environment*, *613–614*, 1317–1323. https://doi.org/10.1016/j.scitotenv.2017.09.256

Feng, A., Cao, J., Wei, J., Chang, F., & Yang, Y. (2018). Facile Synthesis of Silver Nanoparticles with High Antibacterial Activity. *Materials*, *11*(2948). https://doi.org/10.3390/ma11122498

Feng, Q. L., Wu, J., Chen, G. Q., Cui, F. Z., Kim, T. N., & Kim, J. O. (2000). A mechanistic study of the antibacterial effect of silver ions on Escherichia coli and Staphylococcus aureus. *Journal of Biomedical Materials Research*, *52*(4), 662–668. https://doi.org/10.1002/1097-4636(20001215)52:4<662::AID-JBM10>3.0.CO;2-3

Fewtrell, L. (2014). Silver: water disinfection and toxicity. In *Centre for Research into Environment and Health*.

Gao, M., Sun, L., Wang, Z., & Zhao, Y. (2013). Controlled synthesis of Ag nanoparticles with different morphologies and their antibacterial properties. *Materials Science and Engineering C*, *33*(1), 397–404. https://doi.org/10.1016/j.msec.2012.09.005

Gemici, B. T., Karel, F. B., Karaer, F., & Koparal, A. S. (2018). Water Disinfection With Advanced Methods : Successive and Hybrid Application of Antibacterial Column With Silver , Ultrasound and Uv Radiation. *Applied Ecology and*

Environmental Research, *16*(4), 4667–4680.

Gorka, D. E., Osterberg, J. S., Gwin, C. A., Colman, B. P., Meyer, J. N., Bernhardt, E. S., … Liu, J. (2015). Reducing Environmental Toxicity of Silver Nanoparticles through Shape Control. *Environmental Science and Technology*, *49*(16), 10093–10098. https://doi.org/10.1021/acs.est.5b01711

Graves, J. L., Tajkarimi, M., Cunningham, Q., Campbell, A., Nonga, H., Harrison, S. H., & Barrick, J. E. (2015). Rapid evolution of silver nanoparticle resistance in Escherichia coli. *Frontiers in Genetics*, *5*(FEB), 1–13. https://doi.org/10.3389/fgene.2015.00042

Gu, D., Chang, X., Zhai, X., Sun, S., Li, Z., Liu, T., … Yin, Y. (2016). Efficient synthesis of silver-reduced graphene oxide composites with prolonged antibacterial effects. *Ceramics International*, *42*(8), 9769–9778. https://doi.org/10.1016/j.ceramint.2016.03.069

Guo, Y., Cichocki, N., Schattenberg, F., Geffers, R., Harms, H., & Müller, S. (2019). AgNPs change microbial community structures of wastewater. *Frontiers in Microbiology*, *10*(JAN), 1–12. https://doi.org/10.3389/fmicb.2018.03211

Hardy Diagnostics. (n.d.). Mueller Hinton Media. Retrieved from https://catalog.hardydiagnostics.com/cp_prod/Content/hugo/MuellerHintonMed.htm

Hong, X., Wen, J., Xiong, X., & Hu, Y. (2016a). Silver nanowire-carbon fiber cloth nanocomposites synthesized by UV curing adhesive for electrochemical point-of-use water disinfection. *Chemosphere*, *154*, 537–545. https://doi.org/10.1016/j.chemosphere.2016.04.013

Hong, X., Wen, J., Xiong, X., & Hu, Y. (2016b). Shape effect on the antibacterial activity of silver nanoparticles synthesized via a microwave-assisted method. *Environmental Science and Pollution Research*, *23*(5), 4489–4497. https://doi.org/10.1007/s11356-015-5668-z

Hossain, F., Perales-Perez, O. J., Hwang, S., & Román, F. (2014). Antimicrobial nanomaterials as water disinfectant: Applications, limitations and future perspectives. *Science of the Total Environment*, *466–467*, 1047–1059. https://doi.org/10.1016/j.scitotenv.2013.08.009

Jain, P., & Pradeep, T. (2005). Potential of silver nanoparticle-coated polyurethane foam as an antibacterial water filter. *Biotechnology and Bioengineering*, *90*(1), 59–63. https://doi.org/10.1002/bit.20368

Jiang, J., Zhang, C., Zeng, G. M., Gong, J. L., Chang, Y. N., Song, B., … Liu, H. Y.

(2016). The disinfection performance and mechanisms of Ag/lysozyme nanoparticles supported with montmorillonite clay. *Journal of Hazardous Materials*, *317*, 416–429. https://doi.org/10.1016/j.jhazmat.2016.05.089

Jiang, S., & Teng, C. P. (2017). Fabrication of silver nanowires-loaded polydimethylsiloxane film with antimicrobial activities and cell compatibility. *Materials Science and Engineering C*, *70*, 1011–1017. https://doi.org/10.1016/j.msec.2016.04.094

Johnston, K. A., Stabryla, L. M., Smith, A. M., Gan, X. Y., Gilbertson, L. M., & Millstone, J. E. (2018). Impacts of broth chemistry on silver ion release, surface chemistry composition, and bacterial cytotoxicity of silver nanoparticles. *Environmental Science: Nano*, *5*(2), 304–312. https://doi.org/10.1039/c7en00974g

Jones, R., Draheim, R., & Roldo, M. (2018). Silver Nanowires: Synthesis, Antibacterial Activity and Biomedical Applications. *Applied Sciences*, *8*(5), 673. https://doi.org/10.3390/app8050673

Jung, W. K., Koo, H. C., Kim, K. W., Shin, S., Kim, S. H., & Park, Y. H. (2008). Antibacterial Activity and Mechanism of Action of the Silver Ion in Staphylococcus aureus and Escherichia coli. *Applied and Environmental Microbiology*, *74*(7), 2171–2178. https://doi.org/10.1128/AEM.02001-07

Kahler, D. M., Koermer, N. T., Reichl, A. R., Samie, A., & Smith, J. A. (2016). Performance and acceptance of novel silver-impregnated ceramic cubes for drinking water treatment in two field sites: Limpopo province, South Africa and Dodoma Region, Tanzania. *Water (Switzerland)*, *8*(3). https://doi.org/10.3390/w8030095

Kalakonda, P. (2016). Synthesis of silver nanowires for highly conductive and transparent films. *Nanomaterials and Nanotechnology*, *6*, 1–6. https://doi.org/10.1177/1847980416663672

Kallman, E., Smith, J. A., & Oyanedel-Craver, V. (2009). Ceramic Water Filters Impregnated with Silver Nanoparticles for Point-of-Use Water Treatment in Rural Guatemala. *Proceedings of the Water Environment Federation*, *2009*(1), 19–30. https://doi.org/10.2175/193864709793848158

Karumuri, A. K., Oswal, D. P., Hostetler, H. A., & Mukhopadhyay, S. M. (2013). Silver nanoparticles attached to porous carbon substrates: Robust materials for chemical-free water disinfection. *Materials Letters*, *109*, 83–87. https://doi.org/10.1016/j.matlet.2013.07.021

Kayembe, J. M., Thevenon, F., La, A., Sivalingam, P., Ngelinkoto, P., Mulaji, C. K.,

… Pote, J. (2018). High levels of faecal contamination in drinking groundwater and recreational water due to poor sanitation , in the sub-rural neighbourhoods of Kinshasa , Democratic Republic of the Congo. *International Journal of Hygiene and Environmental Health*, *221*, 400–408. https://doi.org/10.1016/j.ijheh.2018.01.003

Khodashenas, B., & Ghorbani, H. R. (2015). Synthesis of silver nanoparticles with different shapes. *Arabian Journal of Chemistry*. https://doi.org/10.1016/j.arabjc.2014.12.014

Kholoud, M. M., El-Nour, A., Eftaiha, A., Al-Warthan, A., & Ammar, R. A. A. (2010). Synthesis and applications of silver nanoparticles. *Arabian Journal of Chemistry*, *3*(3), 135–140. https://doi.org/10.1016/j.arabjc.2010.04.008

Koizhaiganova, M., Yaşa, I., & Gülümser, G. (2016). *Characterization and Antimicrobial Activity of Silver Doped Hydroxyapatite Obtained by the Microwave Method. 22*(3), 2–7.

Lalley, J., Dionysiou, D. D., Varma, R. S., Shankara, S., Yang, D. J., & Nadagouda, M. N. (2014). Silver-based antibacterial surfaces for drinking water disinfection - An overview. *Current Opinion in Chemical Engineering*, *3*, 25–29. https://doi.org/10.1016/j.coche.2013.09.004

Le Ouay, B., & Stellacci, F. (2015). Antibacterial activity of silver nanoparticles: A surface science insight. *Nano Today*, *10*(3), 339–354. https://doi.org/10.1016/j.nantod.2015.04.002

Lee, E. J., Chang, M. H., Kim, Y. S., & Kim, J. Y. (2013). High-pressure polyol synthesis of ultrathin silver nanowires: Electrical and optical properties. *APL Materials*, *1*(4). https://doi.org/10.1063/1.4826154

Lee, O. M., Kim, H. Y., Park, W., Kim, T. H., & Yu, S. (2015). A comparative study of disinfection efficiency and regrowth control of microorganism in secondary wastewater effluent using UV, ozone, and ionizing irradiation process. *Journal of Hazardous Materials*, *295*, 201–208. https://doi.org/10.1016/j.jhazmat.2015.04.016

Li, J., Xie, S., Ahmed, S., Wang, F., Gu, Y., Zhang, C., … Cheng, G. (2017). Antimicrobial activity and resistance: Influencing factors. *Frontiers in Pharmacology*, *8*(JUN), 1–11. https://doi.org/10.3389/fphar.2017.00364

Li, Q., Mahendra, S., Lyon, D. Y., Brunet, L., Liga, M. V., Li, D., & Alvarez, P. J. J. (2008). Antimicrobial nanomaterials for water disinfection and microbial control: Potential applications and implications. *Water Research*, *42*(18), 4591–4602. https://doi.org/10.1016/j.watres.2008.08.015

Li, Y., Yuan, X., Yang, H., Chao, Y., Guo, S., & Wang, C. (2019). One-step synthesis of silver nanowires with ultra-long length and thin diameter to make flexible transparent conductive films. *Materials*, *12*(3). https://doi.org/10.3390/ma12030401

Lilje, J., & Mosler, H. (2018). Effects of a behavior change campaign on household drinking water disinfection in the Lake Chad basin using the RANAS approach. *Science of the Total Environment*, *619–620*, 1599–1607. https://doi.org/10.1016/j.scitotenv.2017.10.142

Lin, S., Huang, R., Cheng, Y., Liu, J., Lau, B. L. T., & Wiesner, M. R. (2013). Silver nanoparticle-alginate composite beads for point-of-use drinking water disinfection. *Water Research*, *47*(12), 3959–3965. https://doi.org/10.1016/j.watres.2012.09.005

Liu, B., Yan, H., Chen, S., Guan, Y., Wu, G., Jin, R., & Li, L. (2017). Stable and Controllable Synthesis of Silver Nanowires for Transparent Conducting Film. *Nanoscale Research Letters*, *12*(1), 4–9. https://doi.org/10.1186/s11671-017-1963-6

Liu, C., Xie, X., Zhao, W., Liu, N., Maraccini, P. A., Sassoubre, L. M., … Cui, Y. (2013). Conducting nanosponge electroporation for affordable and high-efficiency disinfection of bacteria and viruses in water. *Nano Letters*, *13*(9), 4288–4293. https://doi.org/10.1021/nl402053z

Liu, J., Sonshine, D. a, Shervani, S., & Hurt, R. H. (2010). Controlled Release of Biologically Active Silver from Nanosilver Surfaces. *ACS Nano*, *4*(11), 6903–6913. https://doi.org/10.1021/nn102272n

Lkhagvajav, N., Koizhaiganova, M., Yasa, I., Çelik, E., & Sari, Ö. (2015). *Characterization and antimicrobial performance of nano silver coatings on leather materials*. *48*, 41–48.

Luu, Q. N., Doorn, J. M., Berry, M. T., Jiang, C., Lin, C., & May, P. S. (2011). Preparation and optical properties of silver nanowires and silver-nanowire thin films. *Journal of Colloid and Interface Science*, *356*(1), 151–158. https://doi.org/10.1016/j.jcis.2010.12.077

Madigan, M. T., Martiko, J. M., Stahl, D. A., & Clark, D. P. (2012). *Brock Biology of Microorganisms* (Thirteenth). https://doi.org/10.1093/nq/s3-XII.310.469-a

Maillard, J. Y., & Hartemann, P. (2013). Silver as an antimicrobial: facts and gaps in knowledge. *Critical Reviews in Microbiology*, *39*(4), 373–383. https://doi.org/10.3109/1040841X.2012.713323

Martinez-Gutierrez, F., Olive, P. L., Banuelos, A., Orrantia, E., Nino, N., Sanchez, E. M., … Av-Gay, Y. (2010). Synthesis, characterization, and evaluation of antimicrobial and cytotoxic effect of silver and titanium nanoparticles. *Nanomedicine: Nanotechnology, Biology, and Medicine*, *6*(5), 681–688. https://doi.org/10.1016/j.nano.2010.02.001

Mikelonis, A. M., Lawler, D. F., & Passalacqua, P. (2016). Multilevel modeling of retention and disinfection efficacy of silver nanoparticles on ceramic water filters. *Science of the Total Environment*, *566–567*, 368–377. https://doi.org/10.1016/j.scitotenv.2016.05.076

Mollahosseini, A., Rahimpour, A., Jahamshahi, M., Peyravi, M., & Khavarpour, M. (2012). The effect of silver nanoparticle size on performance and antibacteriality of polysulfone ultrafiltration membrane. *Desalination*, *306*, 41–50. https://doi.org/10.1016/j.desal.2012.08.035

Morones, J. R., Elechiguerra, J. L., Camacho, A., Holt, K., Kouri, J. B., Ram, J. T., & Yacaman, M. J. (2005). The bactericidal effect of silver nanoparticles. *Nanotechnology*, *16*, 2346–2353. https://doi.org/10.1088/0957-4484/16/10/059

Mpenyana-Monyatsi, L., Mthombeni, N. H., Onyango, M. S., & Momba, M. N. B. (2012). Cost-effective filter materials coated with silver nanoparticles for the removal of pathogenic bacteria in groundwater. *International Journal of Environmental Research and Public Health*, *9*(1), 244–271. https://doi.org/10.3390/ijerph9010244

Mthombeni, N. H., Mpenyana-Monyatsi, L., Onyango, M. S., & Momba, M. N. B. (2012). Breakthrough analysis for water disinfection using silver nanoparticles coated resin beads in fixed-bed column. *Journal of Hazardous Materials*, *217–218*, 133–140. https://doi.org/10.1016/j.jhazmat.2012.03.004

Mukherji, S., Mukherji, S., & Mukherji, S. (2017). Disinfection of water in a batch reactor using chloridized silver surfaces. *Journal of Water Process Engineering*, *16*, 41–49. https://doi.org/10.1016/j.jwpe.2016.12.009

Nair, K. G., Jayaseelan, D., & Biji, P. (2015). Direct-writing of circuit interconnects on cellulose paper using ultra-long, silver nanowires based conducting ink. *RSC Advances*, *5*(93), 76092–76100. https://doi.org/10.1039/c5ra10837c

Nangmenyi, G., & Economy, J. (2009). Nanometallic Particles for Oligodynamic Microbial Disinfection. In *Nanotechnology Applications for Clean Water: Solutions for Improving Water Quality: Second Edition* (pp. 3–15). https://doi.org/10.1016/B978-1-4557-3116-9.00018-4

Nangmenyi, G., Li, X., Mehrabi, S., Mintz, E., & Economy, J. (2011). Silver-modified

iron oxide nanoparticle impregnated fiberglass for disinfection of bacteria and viruses in water. *Materials Letters*, *65*(8), 1191–1193. https://doi.org/10.1016/j.matlet.2011.01.042

Nangmenyi, G., Xao, W., Mehrabi, S., Mintz, E., & Economy, J. (2009). Bactericidal activity of Ag nanoparticle-impregnated fibreglass for water disinfection. *Journal of Water and Health*, *7*(4), 657–663. https://doi.org/10.2166/wh.2009.107

Nateghi, M. R., & Shateri-Khalilabad, M. (2015). Silver nanowire-functionalized cotton fabric. *Carbohydrate Polymers*, *117*, 160–168. https://doi.org/10.1016/j.carbpol.2014.09.057

Nawaz, M., Han, M. Y., Kim, T. il, Manzoor, U., & Amin, M. T. (2012). Silver disinfection of Pseudomonas aeruginosa and E. coli in rooftop harvested rainwater for potable purposes. *Science of the Total Environment*, *431*, 20–25. https://doi.org/10.1016/j.scitotenv.2012.05.022

Nguyen, K. C., Seligy, V. L., Massarsky, A., Moon, T. W., Rippstein, P., Tan, J., & Tayabali, A. F. (2013). Comparison of toxicity of uncoated and coated silver nanoparticles. *Journal of Physics: Conference Series*, *429*(1). https://doi.org/10.1088/1742-6596/429/1/012025

Okafor, N. (2011). *Environmental Microbiology of Aquatic and Waste Systems*. Springer.

Pal, S., Tak, Y. K., & Song, J. M. (2007). Does the antibacterial activity of silver nanoparticles depend on the shape of the nanoparticle? A study of the gram-negative bacterium Escherichia coli. *Applied and Environmental Microbiology*, *73*(6), 1712–1720. https://doi.org/10.1128/AEM.02218-06

Panáček, A., Kvítek, L., Smékalová, M., Večeřová, R., Kolář, M., Röderová, M., … Zbořil, R. (2018). Bacterial resistance to silver nanoparticles and how to overcome it. *Nature Nanotechnology*, *13*(1), 65–71. https://doi.org/10.1038/s41565-017-0013-y

Parandhaman, T., Das, A., Ramalingam, B., Samanta, D., Sastry, T. P., Mandal, A. B., & Das, S. K. (2015). Antimicrobial behavior of biosynthesized silica-silver nanocomposite for water disinfection: A mechanistic perspective. *Journal of Hazardous Materials*, *290*, 117–126. https://doi.org/10.1016/j.jhazmat.2015.02.061

Park, S. J., Park, H. H., Ko, Y. S., Lee, S. J., Le, T. S., Woo, K., & Ko, G. P. (2017). Disinfection of various bacterial pathogens using novel silver nanoparticle-decorated magnetic hybrid colloids. *Science of the Total Environment*, *609*, 289–

296. https://doi.org/10.1016/j.scitotenv.2017.07.071

Pepper, I. L., Gerba, C. P., & Gentry, T. J. (2015). *Environmental Microbiology* (Third Ed.). Elsevier.

Percival, S. L., Yates, M. V., Williams, D. W., Chalmers, R. M., & Gray, N. F. (2013). Microbiology of Waterborne Diseases: Microbiological Aspects and Risks: Second Edition. In *Microbiology of Waterborne Diseases: Microbiological Aspects and Risks: Second Edition* (2nd Ed.). https://doi.org/10.1016/C2010-0-67101-X

Perk, C. (2016). *Detection of Antimicrobial Effect of Silver Nanowires Embedded in Poly Lactic Acid (PLA) and Filter Paper on Pathogenic Bacteria*. Middle East Technical University.

Phong, N. T. P., Thanh, N. V. K., & Phuong, P. H. (2009). Fabrication of antibacterial water filter by coating silver nanoparticles on flexible polyurethane foams. *Journal of Physics: Conference Series*, *187*, 012079. https://doi.org/10.1088/1742-6596/187/1/012079

Praveena, S. M., & Aris, A. Z. (2015). Application of Low-Cost Materials Coated with Silver Nanoparticle as Water Filter in Escherichia coli Removal. *Water Quality, Exposure and Health*, *7*(4), 617–625. https://doi.org/10.1007/s12403-015-0167-5

Praveena, S. M., Han, L. S., Than, L. T. L., & Aris, A. Z. (2016). Preparation and characterisation of silver nanoparticle coated on cellulose paper: evaluation of their potential as antibacterial water filter. *Journal of Experimental Nanoscience*, *11*(17), 1307–1319. https://doi.org/10.1080/17458080.2016.1209790

Quang, D. V., Sarawade, P. B., Jeon, S. J., Kim, S. H., Kim, J. K., Chai, Y. G., & Kim, H. T. (2013). Effective water disinfection using silver nanoparticle containing silica beads. *Applied Surface Science*, *266*, 280–287. https://doi.org/10.1016/j.apsusc.2012.11.168

Quinteros, M. A., Cano Aristizábal, V., Dalmasso, P. R., Paraje, M. G., & Páez, P. L. (2016). Oxidative stress generation of silver nanoparticles in three bacterial genera and its relationship with the antimicrobial activity. *Toxicology in Vitro*, *36*, 216–223. https://doi.org/10.1016/j.tiv.2016.08.007

Rai, M., Yadav, A., & Gade, A. (2009). Silver nanoparticles as a new generation of antimicrobials. *Biotechnology Advances*, *27*(1), 76–83. https://doi.org/10.1016/j.biotechadv.2008.09.002

Ramasamy, P., Seo, D. M., Kim, S. H., & Kim, J. (2012). Effects of TiO 2 shells on

optical and thermal properties of silver nanowires. *Journal of Materials Chemistry*, *22*(23), 11651–11657. https://doi.org/10.1039/c2jm00010e

Randall, C. P., Gupta, A., Jackson, N., Busse, D., & O'Neill, A. J. (2014). Silver resistance in Gram-negative bacteria: A dissection of endogenous and exogenous mechanisms. *Journal of Antimicrobial Chemotherapy*, *70*(4), 1037–1046. https://doi.org/10.1093/jac/dku523

Rao, G., Brastad, K. S., Zhang, Q., Robinson, R., He, Z., & Li, Y. (2016). Enhanced disinfection of Escherichia coli and bacteriophage MS2 in water using a copper and silver loaded titanium dioxide nanowire membrane. *Frontiers of Environmental Science and Engineering*, *10*(4). https://doi.org/10.1007/s11783-016-0854-x

Ribeiro, F., Gallego-Urrea, J. A., Jurkschat, K., Crossley, A., Hassellöv, M., Taylor, C., … Loureiro, S. (2014). Silver nanoparticles and silver nitrate induce high toxicity to Pseudokirchneriella subcapitata, Daphnia magna and Danio rerio. *Science of the Total Environment*. https://doi.org/10.1016/j.scitotenv.2013.06.101

Rizzello, L., & Pompa, P. P. (2014). Nanosilver-based antibacterial drugs and devices: Mechanisms, methodological drawbacks, and guidelines. *Chem. Soc. Rev.*, *43*(5), 1501–1518. https://doi.org/10.1039/C3CS60218D

Rosa, L. R., Rosa, R. D., & Da Veiga, M. A. M. S. (2016). Colloidal silver and silver nanoparticles bioaccessibility in drinking water filters. *Journal of Environmental Chemical Engineering*, *4*(3), 3451–3458. https://doi.org/10.1016/j.jece.2016.07.017

Roy, A., Butola, B. S., & Joshi, M. (2017). Synthesis, characterization and antibacterial properties of novel nano-silver loaded acid activated montmorillonite. *Applied Clay Science*, *146*(June), 278–285. https://doi.org/10.1016/j.clay.2017.05.043

Ruparelia, J. P., Chatterjee, A. K., Duttagupta, S. P., & Mukherji, S. (2008). Strain specificity in antimicrobial activity of silver and copper nanoparticles. *Acta Biomaterialia*, *4*(3), 707–716. https://doi.org/10.1016/j.actbio.2007.11.006

Sawada, I., Fachrul, R., Ito, T., Ohmukai, Y., Maruyama, T., & Matsuyama, H. (2012). Development of a hydrophilic polymer membrane containing silver nanoparticles with both organic antifouling and antibacterial properties. *Journal of Membrane Science*, *387–388*(1), 1–6. https://doi.org/10.1016/j.memsci.2011.06.020

Scanlan, L. D., Reed, R. B., Loguinov, A. V., Antczak, P., Tagmount, A., Aloni, S., … Gilbert, B. (2013). Silver nanowire exposure results in internalization and

toxicity to daphnia magna. *ACS Nano*, *7*(12), 10681–10694. https://doi.org/10.1021/nn4034103

Schoen, D. T., Schoen, A. P., Hu, L., Kim, H. S., Heilshorn, S. C., & Cui, Y. (2010). High speed water sterilization using one-dimensional nanostructures. *Nano Letters*, *10*(9), 3628–3632. https://doi.org/10.1021/nl101944e

Shameli, K., Ahmad, M. Bin, Jazayeri, S. D., Shabanzadeh, P., Sangpour, P., Jahangirian, H., & Gharayebi, Y. (2012). Investigation of antibacterial properties silver nanoparticles prepared via green method. *Chemistry Central Journal*, *6*(1), 469. https://doi.org/10.1186/1752-153X-6-73

Shameli, K., Mansor Bin Ahmad, M., Mohsen, Z., Yunis, W. Z., Ibrahim, N. A., & Rustaiyan, A. (2011). Synthesis of silver nanoparticles in montmorillonite and their antibacterial behavior. *International Journal of Nanomedicine*, (June 2014), 581. https://doi.org/10.2147/ijn.s17112

Silvestry-Rodriques, N., Sicairos-Ruelas, E., Gerba, C., & Bright, K. (2007). Silver as a Disinfectant. *Reviews of Environmental Contamination and Toxicology*, *191*, 23–45. https://doi.org/10.1007/978-3-319-20013-2

Son, W. K., Youk, J. H., Lee, T. S., & Park, W. H. (2004). Preparation of antimicrobial ultrafine cellulose acetate fibers with silver nanoparticles. *Macromolecular Rapid Communications*, *25*(18), 1632–1637. https://doi.org/10.1002/marc.200400323

Sondi, I., & Salopek-Sondi, B. (2004). Silver nanoparticles as antimicrobial agent: A case study on E. coli as a model for Gram-negative bacteria. *Journal of Colloid and Interface Science*, *275*(1), 177–182. https://doi.org/10.1016/j.jcis.2004.02.012

Song, B., Zhang, C., Zeng, G., Gong, J., Chang, Y., & Jiang, Y. (2016). Antibacterial properties and mechanism of graphene oxide-silver nanocomposites as bactericidal agents for water disinfection. *Archives of Biochemistry and Biophysics*, *604*, 167–176. https://doi.org/10.1016/j.abb.2016.04.018

Stabryla, L. M., Johnston, K. A., Millstone, J. E., & Gilbertson, L. M. (2018). Emerging investigator series: It's not all about the ion: Support for particle-specific contributions to silver nanoparticle antimicrobial activity. *Environmental Science: Nano*, *5*(9), 2047–2068. https://doi.org/10.1039/c8en00429c

Suthar, S., Chhimpa, V., & Singh, S. (2008). Bacterial contamination in drinking water: a case study in rural areas of northern Rajasthan, India. *Environmental Monitoring and Assessment*, 1–6. https://doi.org/10.1007/s10661-008-0611-0

Tan, X., Chen, C., Hu, Y., Wen, J., Qin, Y., Cheng, J., & Chen, Y. (2018). Novel AgNW-PAN/TPU membrane for point-of-use drinking water electrochemical disinfection. *Science of the Total Environment*, *637–638*, 408–417. https://doi.org/10.1016/j.scitotenv.2018.05.012

Tartanson, M. A., Soussan, L., Rivallin, M., Chis, C., Penaranda, D., Lapergue, R., … Faur, C. (2014). A new silver based composite material for SPA water disinfection. *Water Research*, *63*, 135–146. https://doi.org/10.1016/j.watres.2014.06.019

Taurozzi, J. S., Arul, H., Bosak, V. Z., Burban, A. F., Voice, T. C., Bruening, M. L., & Tarabara, V. V. (2008). Effect of filler incorporation route on the properties of polysulfone-silver nanocomposite membranes of different porosities. *Journal of Membrane Science*, *325*(1), 58–68. https://doi.org/10.1016/j.memsci.2008.07.010

Tendencia, E. A. (2004). Disk diffusion method. In *In Laboratory manual of standardized methods for antimicrobial sensitivity tests for bacteria isolated from aquatic animals and environment* (pp. 13–29). https://doi.org/10.1007/978-1-4419-6247-8_13582

The Environmental Protection Agency. (2011). *Water Treatment Manual : Disinfection*. Wexford, Ireland.

Tiwari, D. K., Behari, J., & Sen, P. (2008). Application of Nanoparticles in Waste Water Treatment. *Carbon Nanotubes*, *3*(3), 417–433. https://doi.org/10.1016/j.matchemphys.2009.10.034

Toker, R. D., & Kahraman, M. V. (2013). UV-curable nano-silver containing polyurethane based organic – inorganic hybrid coatings. *Progress in Organic Coatings*, *76*(9), 1243–1250. https://doi.org/10.1016/j.porgcoat.2013.03.023

Tolaymat, T. M., El Badawy, A. M., Genaidy, A., Scheckel, K. G., Luxton, T. P., & Suidan, M. (2010). An evidence-based environmental perspective of manufactured silver nanoparticle in syntheses and applications: A systematic review and critical appraisal of peer-reviewed scientific papers. *Science of the Total Environment*, *408*(5), 999–1006. https://doi.org/10.1016/j.scitotenv.2009.11.003

Tortora, G. J., Funke, B. R., & Case, C. I. (2013). *Microbiology: An Introduction* (Eleventh E). Edinburgh: Pearson Education Inc.

Udekwu, K. I., Parrish, N., Ankomah, P., Baquero, F., & Levin, B. R. (2009). Functional relationship between bacterial cell density and the efficacy of antibiotics. *The Journal of Antimicrobial Chemotherapy*, *63*(4), 745–757.

https://doi.org/10.1093/jac/dkn554

USEPA. (2018). 2018 Edition of the Drinking Water Standards and Health Advisories. In *United States Environmental Protection Agency*. https://doi.org/EPA 822-S-12-001

Wang, J., Jiu, J., Araki, T., Nogi, M., Sugahara, T., Nagao, S., … Suganuma, K. (2015). Silver nanowire electrodes: Conductivity improvement without post-treatment and application in capacitive pressure sensors. *Nano-Micro Letters*, *7*(1), 51–58. https://doi.org/10.1007/s40820-014-0018-0

Wei, L., Lu, J., Xu, H., Chen, Z.-S., & Chen, G. (2015). Silver nanoparticles: synthesis, properties, and therapeutic applications. *Drug Discovery Today*, *20*(5), 595–601. https://doi.org/10.1016/j.drudis.2014.11.014

Wen, J., Tan, X., Hu, Y., Guo, Q., & Hong, X. (2017). Filtration and Electrochemical Disinfection Performance of PAN/PANI/AgNW-CC Composite Nanofiber Membrane. *Environmental Science and Technology*, *51*(11), 6395–6403. https://doi.org/10.1021/acs.est.6b06290

WHO. (2011). *Guidelines for drinking water quality* (Forth Ed.). https://doi.org/10.1016/S1462-0758(00)00006-6

WHO. (2018a). Drinking-water. Retrieved from https://www.who.int/news-room/fact-sheets/detail/drinking-water

WHO. (2018b). The top 10 causes of death. Retrieved from https://www.who.int/news-room/fact-sheets/detail/the-top-10-causes-of-death

Wong, K. K. Y., & Liu, X. (2010). Silver nanoparticles - The real "silver bullet" in clinical medicine? *MedChemComm*, *1*(2), 125–131. https://doi.org/10.1039/c0md00069h

Xiu, Z., Zhang, Q., Puppala, H., Colvin, L., & Alvarez, P. (2012). Negligible particle-specific antibacterial activity of silver nanoparticles. *Nano Letters*, *12*, 4271–4275.

Yang, W. H., Tsai, T. Y., Wu, C. C., Hu, T. L., & Kan, C. C. (2012). A Novel Disinfection Material-Nano Ag Particle Impregnated Media. *Advanced Materials Research*, *560–561*, 732–736. https://doi.org/10.4028/www.scientific.net/AMR.560-561.732

Yang, X., Chu, X., Hu, J., & Ong, S. (2014). Disinfection performance of nanosilver and impacts of environmental conditions on viral inactivation by nanosilver. *Water Science and Technology*, *14.1*, 150–157. https://doi.org/10.2166/ws.2013.183

You, J., Zhang, Y., & Hu, Z. (2011). Bacteria and bacteriophage inactivation by silver and zinc oxide nanoparticles. *Colloids and Surfaces B: Biointerfaces*, *85*(2), 161–167. https://doi.org/10.1016/j.colsurfb.2011.02.023

Zain, N. M., Stapley, A. G. F., & Shama, G. (2014). Green synthesis of silver and copper nanoparticles using ascorbic acid and chitosan for antimicrobial applications. *Carbohydrate Polymers*, *112*, 195–202. https://doi.org/10.1016/j.carbpol.2014.05.081

Zaporojtchenko, V., Podschun, R., Schürmann, U., Kulkarni, A., & Faupel, F. (2006). Physico-chemical and antimicrobial properties of co-sputtered Ag–Au/PTFE nanocomposite coatings. *Nanotechnology*, *17*(19), 4904–4908. https://doi.org/10.1088/0957-4484/17/19/020

Zhang, C., Hu, Z., & Deng, B. (2016). Silver nanoparticles in aquatic environments: Physiochemical behavior and antimicrobial mechanisms. *Water Research*, *88*, 403–427. https://doi.org/10.1016/j.watres.2015.10.025

Zhang, H. (2013). *Application of silver nanoparticles in drinking water purification* (University of Rhode Island). Retrieved from http://digitalcommons.uri.edu/cgi/viewcontent.cgi?article=1033&context=oa_diss#page=124

Zhang, H., Smith, J. A., & Oyanedel-Craver, V. (2012). The effect of natural water conditions on the anti-bacterial performance and stability of silver nanoparticles capped with different polymers. *Water Research*, *46*(3), 691–699. https://doi.org/10.1016/j.watres.2011.11.037

Zhang, H. Z., Zhang, C., Zeng, G. M., Gong, J. L., Ou, X. M., & Huan, S. Y. (2016). Easily separated silver nanoparticle-decorated magnetic graphene oxide: Synthesis and high antibacterial activity. *Journal of Colloid and Interface Science*, *471*, 94–102. https://doi.org/10.1016/j.jcis.2016.03.015

Zhang, P., Wyman, I., Hu, J., Lin, S., Zhong, Z., Tu, Y., … Wei, Y. (2017). Silver nanowires: Synthesis technologies, growth mechanism and multifunctional applications. *Materials Science and Engineering B: Solid-State Materials for Advanced Technology*, *223*, 1–23. https://doi.org/10.1016/j.mseb.2017.05.002

Zhao, T., Fan, J. B., Cui, J., Liu, J. H., Xu, X. B., & Zhu, M. Q. (2011). Microwave-controlled ultrafast synthesis of uniform silver nanocubes and nanowires. *Chemical Physics Letters*, *501*(4–6), 414–418. https://doi.org/10.1016/j.cplett.2010.11.031

Zhu, Z., Su, M., Ma, L., Ma, L., Liu, D., & Wang, Z. (2013). Preparation of graphene oxide-silver nanoparticle nanohybrids with highly antibacterial capability.

Talanta, *117*, 449–455. https://doi.org/10.1016/j.talanta.2013.09.017

Zodrow, K., Brunet, L., Mahendra, S., Li, D., Zhang, A., Li, Q., & Alvarez, P. J. J. (2009). Polysulfone ultrafiltration membranes impregnated with silver nanoparticles show improved biofouling resistance and virus removal. *Water Research*, *43*(3), 715–723. https://doi.org/10.1016/j.watres.2008.11.014

APPENDICES

A. Fabrication of Stand-Alone AgNW Foils

AgNW were synthesized by polyol method as explained Materials and Methods Section (Section 3.2.1). In order to fabricate silver nanowire based foils, vacuum filtration method was used. Teflon based hydrophilic 47 mm. filter papers were used. Following vacuum filtration process, 40 mm-width silver nanowire based foils were obtained. Figure A1 shows a photo of a stand-alone AgNW foil and SEM image of stand-alone AgNW foil with higher magnification. As it can be seen from SEM image, foils do not have packed structure but they have porous-like structure.
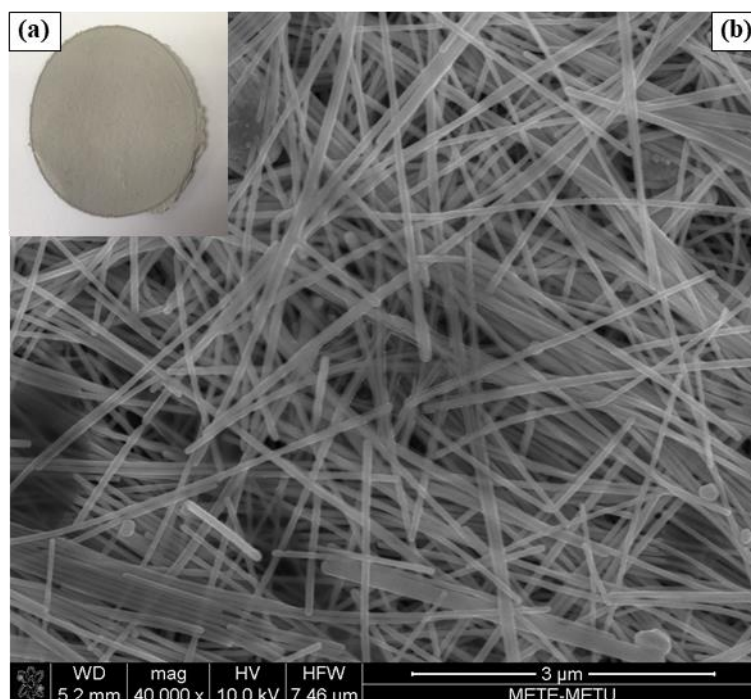

Figure A1. A photo of stand-alone AgNW foil (a) and SEM image of stand-alone AgNW foil (b).
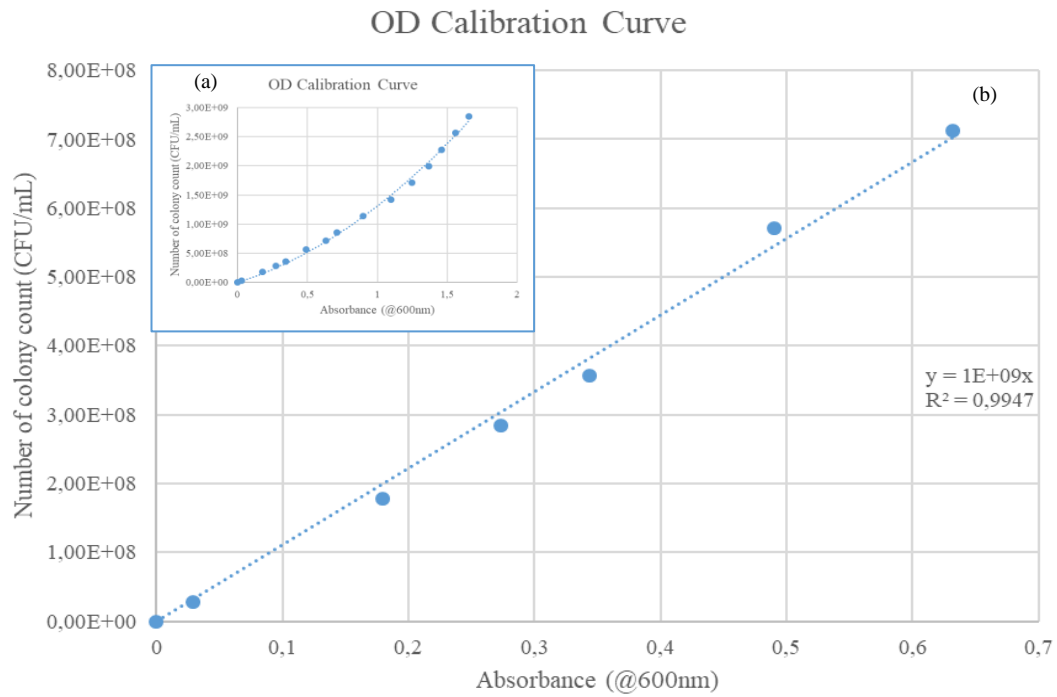
B. OD Calibration Curve

Figure B1. OD Calibration Curve (a) and linear part of the calibration curve (b)

Table B1. Data table for OD calibration curve

Dilution ratio	Absorbance (@600nm)	Number of Colony Count (CFU/mL)
0	0	0,00E+00
0,01	0,029	2,85E+07
0,06	0,18	1,78E+08
0,10	0,273	2,85E+08
0,13	0,344	3,56E+08
0,20	0,49	5,70E+08
0,25	0,632	7,13E+08
0,30	0,712	8,55E+08
0,40	0,898	1,14E+09
0,50	1,096	1,43E+09
0,60	1,246	1,71E+09
0,70	1,367	2,00E+09
0,80	1,46	2,28E+09
0,90	1,558	2,57E+09
1,00	1,655	2,85E+09

C. Preliminary Results
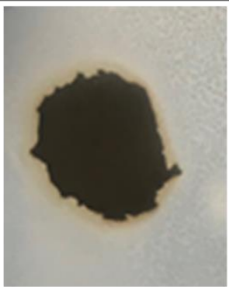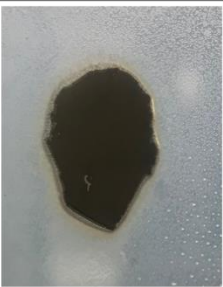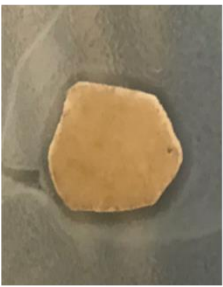
	10^{10} CFU/ml	10^8 CFU/ml	10^6 CFU/ml
Stand-alone AgNW foil			
AgNW-GF filter			

Figure C1. Comparison of inhibition zones of stand-alone AgNW foil and AgNW-GF filter in disk diffusion test.
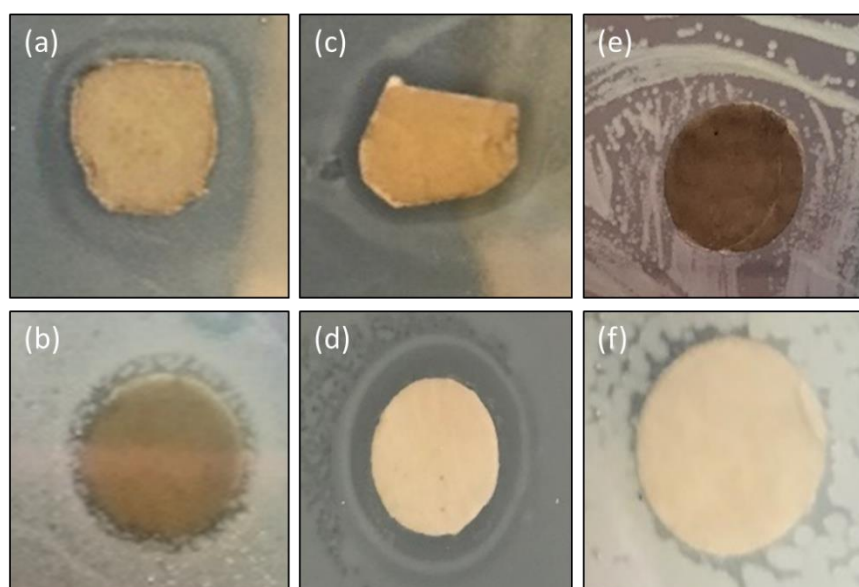
Figure C2. Results (fuzzy zones (a, b, c, d) or no inhibition zone (e, f)) obtained from preliminary disk diffusion tests.

132

D. Disk Diffusion Test Results

Table D1. Disk diffusion test results of Group X AgNWs-GF filters

E. coli concentration (CFU/ml)	Inhibition zone diameters (cm)					
	Control	X1 21.74 mg/g	X2 17.13 mg/g	X3 16.77 mg/g	X4 11.32 mg/g	X5 5.81 mg/g
4.98E+09	Not observed	1.1	1.1	1.2	1.1	1.1
4.98E+07	Not observed	1.3	1.25	1.25	1.2	1.15
4.98E+05	Not observed	1.4	1.35	1.3	1.25	1.2

Table D2. Disk diffusion test results of Group Y AgNWs-GF filters

E. coli concentration (CFU/ml)	Inhibition zone diameters (cm)				
	Control	Y1 0.95 mg/g	Y2 4.49 mg/g	Y3 4.8 mg/g	Y4 9.9 mg/g
2.61E+09	Not observed	1.2	1.15	1.2	1.17
2.61E+07	Not observed	1.3	1.2	1.25	1.25
2.61E+05	Not observed	1.35	1.25	1.3	1.3

E. Flow Test Results of Group Y AgNW-GF Filters

Table E1. Flow test results conducted in order to investigate the effect of flow rate on *E. coli* removal efficiency

Experiment No.	Filter Type	Flow Rate (mL/min)	Influent *E.coli* concentration (CFU/ml)	Effluent *E.coli* concentration (CFU/ml)	Removal efficiency (%)	Removal efficiency (Log-removal)	Silver Release (ppb)
A1.1	Y2 AgNWs-GF	1	2.63E+08	1.01E+08	61.7	0.42	43
A1.2	Y2 AgNWs-GF	1	6.30E+09	1.55E+08	97.5	1.61	51
A2.1	Y2 AgNWs-GF	2.5	8.00E+08	4.00E+08	50.0	0.30	43
A2.2	Y2 AgNWs-GF	2.5	4.00E+08	1.50E+08	62.5	0.43	42
A3.1	Y2 AgNWs-GF	5	6.00E+08	2.00E+08	66.7	0.48	40
A3.2	Y2 AgNWs-GF	5	2.88E+08	1.81E+08	37.1	0.20	46
A4.1	Control GF	1	3.46E+08	2.70E+08	22.0	0.11	-
A4.2	Control GF	1	3.05E+08	2.05E+08	32.8	0.17	-
A5.1	Control GF	2.5	5.84E+08	4.28E+08	26.7	0.13	-
A5.2	Control GF	2.5	3.18E+08	2.39E+08	24.9	0.12	-
A6.1	Control GF	5	5.00E+08	4.00E+08	20.0	0.10	-
A6.2	Control GF	5	4.50E+08	3.52E+08	21.8	0.11	-

Table E2. Flow test results conducted in order to investigate the effect of AgNWs loading on *E. coli* removal efficiency

Experiment No.	Filter Type	Flow rate (ml/min)	AgNWs loading (mg/g)	Influent *E.coli* concentration (CFU/ml)	Effluent *E.coli* concentration (CFU/ml)	Removal efficiency (%)	Removal efficiency (Log-removal)	Silver Release (ppb)
B1.1	Control GF	1	0.0	3.05E+08	2.05E+08	32.8	0.17	-
B1.2	ControlGF	1	0.0	3.46E+08	2.70E+08	22.0	0.11	-
B2.1	Y1 AgNWs-GF	1	1.0	3.69E+08	2.07E+08	44.0	0.25	23
B2.2	Y1 AgNWs-GF	1	1.0	3.98E+08	3.00E+08	24.5	0.12	30
B3.1	Y3 AgNWs-GF	1	4.8	2.62E+08	9.00E+07	65.6	0.46	38
B3.2	Y3 AgNWs-GF	1	4.8	8.00E+08	1.00E+08	87.5	0.90	31
B4.1	Y4 AgNWs-GF	1	9.9	5.25E+08	7.00E+07	86.7	0.88	58
B4.2	Y4 AgNWs-GF	1	9.9	3.75E+08	3.25E+07	91.3	1.06	67

135

Table E3. Flow test results conducted in order to investigate the effect of influent *E. coli* concentration on *E. coli* removal efficiency

Experiment No.	Filter Type	Flow rate (ml/min)	Influent *E.coli* Concentration (Order of magnitude)	Influent *E.coli* concentration (CFU/ml)	Effluent *E.coli* concentration (CFU/ml)	Removal efficiency (%)	Removal efficiency (Log-removal)	Silver Release (ppb)
C1.1	Y4 AgNWs-GF	1	1.00E+03	1.24E+03	1.50E+01	98.8	1.92	21
C1.2	Y4 AgNWs-GF	1	1.00E+03	3.60E+03	3.00E+01	99.2	2.08	14
C2.1	Y4 AgNWs-GF	1	1.00E+05	2.14E+05	1.10E+04	94.9	1.29	15
C2.2	Y4 AgNWs-GF	1	1.00E+05	1.58E+05	1.00E+04	93.7	1.20	18
C3.1	Y4 AgNWs-GF	1	1.00E+08	5.25E+08	7.00E+07	86.7	0.88	58
C3.2	Y4 AgNWs-GF	1	1.00E+08	3.75E+08	3.25E+07	91.3	1.06	67
C4	Control GF	1	1.00E+03	4.00E+03	1.54E+03	61.5	0.41	-
C5	Control GF	1	1.00E+05	2.90E+05	1.30E+05	55.3	0.35	-
C6.1	Control GF	1	1.00E+08	3.05E+08	2.05E+08	32.8	0.17	-
C6.2	Control GF	1	1.00E+08	3.46E+08	2.70E+08	22.0	0.11	-

Table E4. Flow test results conducted in two-stage serial filtering application

Experiment No.	Filter Type	Stage	Flow rate (ml/min)	Influent *E.coli* concentration (CFU/ml)	Effluent *E.coli* concentration (CFU/ml)	Removal efficiency (%)	Removal efficiency (Log-removal)	Silver Release (ppb)
D1	Control GF	1st stage	1	4.00E+03	1.54E+03	61.5	0.41	-
D2	Control GF	2nd stage	1	1.54E+03	5.28E+02	65.7	0.47	-
D3	Y4 AgNWs-GF	1st stage	1	5.30E+03	4.45E+02	91.6	1.08	13
D4	Y4 AgNWs-GF	2nd stage	1	4.45E+02	4.00E+01	91.0	1.05	22

137